View metadata, citation and similar papers at core.ac.uk

brought to you by CORE

provided by DigitalCommons@University of Nebraska

University of Nebraska - Lincoln

DigitalCommons@University of Nebraska - Lincoln

Architectural Engineering -- Faculty Publications

Architectural Engineering and Construction, Durham School of

2003

"Predictive Optimal Control of Active and Passive Building Thermal Storage Inventory"

Gregor P. Henze
University of Nebraska - Lincoln

Moncef Krarti
University of Colorado at Boulder

Follow this and additional works at: https://digitalcommons.unl.edu/archengfacpub

 Part of the Architectural Engineering Commons

Henze, Gregor P. and Krarti, Moncef, ""Predictive Optimal Control of Active and Passive Building Thermal Storage Inventory"" (2003). *Architectural Engineering -- Faculty Publications*. 1.
https://digitalcommons.unl.edu/archengfacpub/1

This Article is brought to you for free and open access by the Architectural Engineering and Construction, Durham School of at DigitalCommons@University of Nebraska - Lincoln. It has been accepted for inclusion in Architectural Engineering -- Faculty Publications by an authorized administrator of DigitalCommons@University of Nebraska - Lincoln.

"Predictive Optimal Control of Active and Passive Building Thermal Storage Inventory"

Topical Report

Reporting Period Start Date: September 20 2001

Reporting Period End Date: January 1, 2003

Principal Authors:

Principal Investigator:

Gregor P. Henze, Ph.D., P.E.
Assistant Professor of Architectural Engineering
University of Nebraska – Lincoln
College of Engineering and Technology
Omaha, Nebraska 68182-0681

Co-Principal Investigator:

Moncef Krarti, Ph.D., P.E.
Associate Professor of Architectural Engineering
University of Colorado at Boulder
College of Engineering
Boulder, Colorado 80309-0428

Date Report was Issued: April 2003

DOE Award Number:

DE-FC-26-01NT41255

Name and Address of Submitting Organization:

Primary Organization:

University of Nebraska – Lincoln
303 Canfield Administration Building
Lincoln, Nebraska 68588-0430

Subcontractor:

The Regents of the University of Colorado
University of Colorado at Boulder
Boulder, Colorado 80309-0428

Disclaimer

"This report was prepared as an account of work sponsored by an agency of the United States Government. Neither the United States Government nor any agency thereof, nor any of their employees, makes any warranty, express or implied, or assumes any legal liability or responsibility for the accuracy, completeness, or usefulness of any information, apparatus, product, or process disclosed, or represents that its use would not infringe on privately owned rights. Reference herein to any specific commercial product, process, or service by trade name, trademark, manufacturer, or otherwise does not necessarily constitute or imply its endorsement, recommendation, or favoring by the United States Government or any agency thereof. The views and opinions of authors expressed herein do not necessarily state or reflect those of the United States Government or any agency thereof."

Abstract

Cooling of commercial buildings contributes significantly to the peak demand placed on an electrical utility grid. Time-of-use electricity rates encourage shifting of electrical loads to off-peak periods at night and weekends. Buildings can respond to these pricing signals by shifting cooling-related thermal loads either by precooling the building's massive structure or the use of active thermal energy storage systems such as ice storage. While these two thermal batteries have been engaged separately in the past, this project investigates the merits of harnessing both storage media concurrently in the context of predictive optimal control.

The analysis, modeling, and simulation research presented in this topical report covers the first of three project phases. Based on the new dynamic building simulation program EnergyPlus, we added a utility rate module, two thermal energy storage models, and incorporated a sequential optimization approach to the cost minimization problem using direct search, gradient-based, and dynamic programming methods. The objective function is the total utility bill including the cost of heating and a time-of-use electricity rate with demand charges. The evaluation of the combined optimal control assumes perfect weather prediction and match between the building model and the actual building counterpart.

The analysis shows that the combined utilization leads to cost savings that is significantly greater than either storage but less than the sum of the individual savings. The findings reveal that the cooling-related on-peak electrical demand of commercial buildings can be drastically reduced and justify the development of a predictive optimal controller that accounts for uncertainty in predicted variables and modeling mismatch in real time.

Table of Contents

1 Introduction

1.1 Problem Definition and Motivation

This topical final report describes the accomplishments achieved in the first of three phases of a research project aiming to develop a software-based supervisory building controller for commercial buildings that utilizes the combined capacity of building thermal mass and thermal energy storage systems. This controller will optimize cooling and ventilation equipment operation under real-time pricing and conventional electricity rates and will cooperate with the building automation system to minimize energy consumption and operating cost while ensuring human comfort. Due to the uncertain nature of future climate conditions, thermal loads, non-cooling electricity consumption and system performance, the approach is based on stochastic optimization. This load-management technology holds the promise of innovation in building automation and represents a unique approach to the control of building thermal storage.

The project is undertaken as a joint effort lead by the University of Nebraska – Lincoln, with support from the University of Colorado and Johnson Controls as the industrial partner.

The overriding **research goal** of this project is to transform a novel concept of supervisory building control into a load management and optimization system that operates in conjunction with a building's energy management and control system to optimize cooling and ventilation operation under dynamic and conventional electricity rates. To achieve this goal, we pursued these **research objectives**:

- Develop **physical models** for the building's energy systems and its dynamic thermal response.
- Conduct a **parametric study** to identify the preferred set of conditions under which the merits of the new technology is maximized and to isolate the key aspects affecting controller performance.
- Perform **model-based analysis** to identify a supervisory optimal control strategy capable of handling uncertainty in future variables and models while ensuring safe and comfortable operation.

Now, that these objectives are completed, we plan to

- **Design, implement, and validate the supervisory controller** in a full-scale HVAC laboratory
- **Field-test the optimization system** in a suitable location (low humidity with large diurnal temperature swings) and equipped with a thermal energy storage system as well as a modern building automation system.

Commercial building electricity consumption is enormous. Commercial buildings contribute a substantial 13% or 12.1 out of 96.6 quadrillion Btu ("quads") to the total U.S. primary energy consumption.[1,2] Aggravated primarily by an immense surge in the use of office equipment combined with the associated demand for cooling energy, electricity is responsible for 80% of the end-use primary energy consumption in commercial buildings, more than 150 million metric tons of carbon emissions per year, and $60 billion of utility cost.[2] Harnessing the efficiency potential in current and future construction will be instrumental in attenuating the growth of energy consumption and demand as well as the nation's dependency on an uninterrupted supply of fossil fuels. This constitutes the motivation for this research.

The equipment and systems providing thermal comfort and indoor air quality for commercial buildings consume 42% of the total energy used in buildings. Energy use and utility cost can be reduced significantly by increasing the efficiency of this equipment, by distributing thermal energy more efficiently and by more closely meeting the needs of building occupants. The energy efficiency of system components for heating, ventilating, and air-conditioning (HVAC) has improved considerably over the past 20 years. For example, shipment-weighted energy efficiency ratios of unitary air conditioners in the United States have increased by 54%.[3] The average efficiency of centrifugal chillers improved by 36% and the efficiency of the best chillers increased by 50%.[4] With similar improvements in the efficiencies of boilers, motors, fans, and pumps, outstanding opportunities exist for reducing energy use and cost in commercial sites. Yet, these opportunities depend on effective building operations: e.g., a building with coincident heating and cooling due to inferior control loop parameters wastes energy regardless of boiler and chiller efficiency.

In contrast to energy conversion equipment, less improvement has been achieved in thermal energy distribution, storage and control systems in terms of energy efficiency and peak load reduction potential. Advancements are also needed to improve thermal storage systems, improve control systems and improve

systems integration from a whole building perspective while meeting occupant comfort and performance requirements.[5] This research project is charged with developing those advancements.

This project tackles the novel concept of **combined optimal control** of both "passive" building thermal capacitance and "active" thermal energy storage systems, e.g., chilled-water or ice storage systems, to minimize an objective function of choice including total energy consumption, energy cost, occupant discomfort, or a combination of these. The controller will eventually be implemented in real-time in an actual commercial building. Instead of merely meeting instantaneous building cooling requirements, both active and passive storage inventories will be effectively harnessed in the framework of supervisory control:

a) To exploit the performance benefits of cooler ambient conditions during nighttime for central chilled water plants, allowing for optimal scheduling of chillers, cooling towers, fans and pumps;
b) To shape the next day's cooling load profile by pre-cooling the building's massive structure at night;
c) To make best possible use of the cost savings potential offered by dynamic utility rate structures, including real-time pricing options that are offered by an increasing number of utilities.

Several investigators have identified promising savings potentials when building operation has been optimized in buildings *without* storage.[6–9, 35] Moreover, recent analyses suggest significant performance merits from *either* active[10–18] *or* passive[19–23] thermal storage inventory under optimal control.

The *combined* use of both storage media under optimal control has been investigated for a 24-hour deterministic simulation study which revealed that significant operating cost savings (~18%) and electrical demand reduction can be achieved.[24] Optimal building control proved most effective in dry climates with large diurnal temperature swings, in the presence of utility rates strongly encouraging load-shifting, and when cool storage systems allow more effective load-shifting than building pre-cooling alone. These results in conjunction with personal experience in optimal control applied to building systems,[10–13, 25–27] encouraged me to develop this idea into a predictive supervisory controller suitable for implementation in commercial buildings with dynamic utility rates.

1.2 Description of the Technology

1.2.1 Summary Description of Technology

Research and development of a predictive optimal controller for active and passive thermal storage inventory and subsequent implementation in laboratory and field settings appears particularly attractive and promising. The project's load management and optimization technology will more effectively account for complex electric rate structures resulting from the deregulation of utilities than traditional control heuristics. In addition, the controller will unlock the potential of building thermal capacitance for the reduction of operating cost, electricity consumption and electricity demand.

This approach will be built into a software package that will operate in conjunction with a building's energy management and control system to optimize cooling and ventilation equipment operation under real-time pricing and conventional electricity rates. In the definition of this project report, 'active' denotes that thermal storage systems, such as ice storage, require an additional fluid loop to charge and discharge the storage tank or to deliver cooling to the existing chilled water loop. Building thermal capacitance is 'passive' since it requires no additional heat exchange fluid in addition to the conditioned air stream.

1.2.2 Constituent Elements of this Technology

1.2.2.1 Active Thermal Storage Inventory

Background – Thermal energy storage (TES) is an electrical load management and building equipment utilization strategy, which can reduce utility electricity demand and equipment first-costs. Typical applications of TES systems include medium-size to large office buildings, hotels, and retail stores. TES systems are designed to avoid high utility demand charges from cooling during the summer and level a building's electrical demand profile. Electrical demand and time-of-use rates have been tailored to reflect the significance of peak energy use periods. TES systems have gained acceptance to reduce peak electrical consumption and installed chiller capacity. Compared to conventional HVAC systems, those designed with TES can provide colder supply water temperatures and permit innovative design on the airside of the cooling system achieving substantial capital and operating cost savings.[42, 43] Moreover, TES systems are used to boost the capacity of gas turbines during hot weather by pre-cooling the inlet airflow.

The basic operating strategy of a TES system is to run electrical chillers during times of low electrical demand and energy prices to charge a storage medium. Either ice is melted or a chilled-water tank is discharged to provide cooling and reduce the use of mechanical cooling. Control of TES systems describes the process of shifting the cooling load from daytime to nighttime by charging and discharging storage.

The ability of a TES system to remove heat is a function of several parameters such as the inventory, ambient conditions, and building load.[28] If inappropriately designed, thermal storage systems may not be able to meet the building cooling load late in the day since only a reduced discharge rate can be achieved from a near empty storage tank.[37–41] The knowledge of thermal storage system performance is crucial for successful design, installation, operation, and maintenance of TES systems.[29, 30]

Experience with TES Systems – A field survey of 37 TES systems indicated that several are not reliably delivering the expected load shifting.[31] Another cold storage field test study showed that the reliance on manual fine-tuning resulted in suboptimal performance for six out of the eight investigated chilled-water systems.[32] Previous experience also shows that while TES systems save varying amounts of operating cost, they tend to consume more energy than a conventional system meeting all the loads by direct cooling.[33] Furthermore, field surveys of existing installations revealed several problems that contributed to the tarnished image of TES technology including poor system design, inadequate equipment selection and integration, and inappropriate commissioning procedures.

Yet, the major obstacle that hinders the acceptance of TES technology is the lack of understanding among facility owners, HVAC designers and HVAC contractors of the proper operation and control that improve the cost-effectiveness of TES systems.[31, 32, 34]

With no sophisticated control available, investments are ineffectively utilized and the full potential of cool storage is not exploited. As a result, cost savings of all TES systems combined are less than ideal and their cumulative energy consumption is higher than necessary. Consequently, a strong need exists for the development of an advanced controller for active thermal inventory addressing these shortcomings.

1.2.2.2 Optimal Control of Active Thermal Storage Inventory

Absence of Uncertainty – The principal investigator and co-investigators have carried out extensive research in the field of advanced control for active TES systems. Driven by the need for a better understanding of the behavior of thermal energy storage systems, we developed a comprehensive simulation environment to evaluate a wide range of key parameters influencing the system's performance.[10] This approach, part of a research project funded by the American Society of Heating, Refrigerating, and Air-Conditioning Engineers (ASHRAE), allowed me to evaluate the *full theoretical potential* of TES systems in reducing operating cost.[25] Within this environment, the optimal control strategy that minimizes the total electricity cost combining energy and demand charges was developed and validated.

In addition to the rate of TES charging and discharging rate as the primary control variable, a set of *plant parameters* governs the operation of the HVAC equipment. These parameters include temperature setpoints such as the chilled water supply and supply air temperatures. These values are adjusted in a separate optimization routine (plant optimization), which is embedded in the cost optimization so that the instantaneous power consumption for the current set of external parameters is minimized.[25] Only the simultaneous cost and plant optimization allow for an optimal control trajectory in which each charging/discharging control is associated with the minimal attainable cooling plant power consumption.

Based on building cooling loads and weather data, the optimal control strategy properly accounts for the effects of all environmental variables including utility rate structure and cooling plant performance characteristics. Existing control strategies were compared to this optimal strategy, and three of these conventional strategies were modeled: chiller-priority, constant-proportion, and storage-priority control.[10]

We found that under favorable conditions, such as strong utility load-shifting incentives or a small energy penalty for operating the chiller in icemaking mode, a TES system with conventional controls can indeed provide considerable cost savings of up to 20%. However, except for these conditions, only optimal control will yield cost savings. In fact, optimal control succeeded in reducing cost, even under the most adverse conditions. Typically, optimal control saved 10–20% more energy cost than the conventional controls.

Excess Energy Use – We also confirmed the reputation that TES systems consume more energy than central cooling systems without storage. A competitive central cooling system must be energy efficient. A major strength of optimal control comes into play here: by tailoring the objective function underlying the optimization, optimal control has the potential of making TES economically attractive *and* ecologically sound.

The desire to save energy consumption is simply expressed as an additional term in the objective function of the optimization. While beforehand only energy cost was minimized, the optimization environment now determines the optimum to an objective function that includes both operating cost [$] and energy consumption [kWh].[12] Introducing a weighting factor *w*, the cost function can accommodate arbitrary impacts of the two components of the cost function. Figure 1 shows the results for a particular configuration. By increasing the weighting factor, more emphasis is placed on operating cost, and optimal control yields higher operating cost savings, but at the price of increasing energy consumptions. The performance shown is relative to the performance of a conventional system. At $w \approx 0.70$, optimal control obtains 20% cost savings without energy penalty.

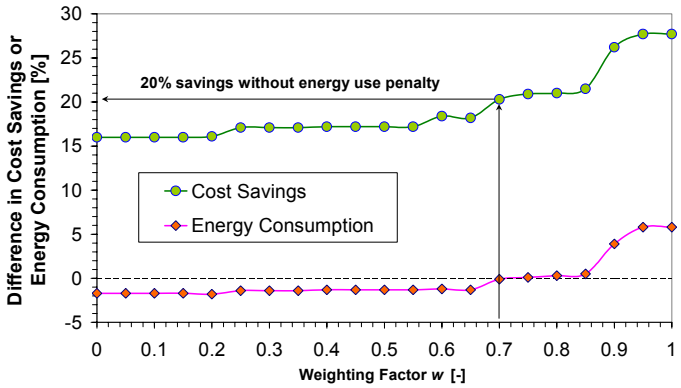

Figure 1: Cost savings and energy consumption of optimal control as a function of the weighting factor w relative to a conventional system without active storage inventory.

Presence of Uncertainty – During a subsequent investigation phase, we determined the extent of the merits of optimal control that can be retained when the optimal controller is subject to uncertainty in the external variables driving the physical process, such as future weather variables and cooling loads.[11]

The predictive optimal strategy is based on closed-loop optimization, i.e., an optimal storage charging and discharging strategy is developed at every time step over a marching planning horizon utilizing updated forecasts. The prediction of climate conditions, utility rates and cooling loads is updated at the beginning of each time step over the optimization period, and a new optimal strategy is computed. Only the control action of the first hour is executed at each time step. Short horizons (≈21 hours) were found to be only marginally suboptimal relative to a strategy that is optimal over the entire simulation horizon (e.g., one month). Thus, there is no point in predicting further into the future than 24 hours.

1.2.2.3 Dynamic Utility Rates

Utilities have been experimenting with and implementing real-time pricing (RTP) of electrical energy. These electric rates vary hourly based upon the utility delivery cost of generation (or purchases from other utilities) and are transmitted electronically to the building through various methods; the two major approaches are (a) 24-hour-ahead pricing and (b) 1-hour-at-a-time rate signals. For the first method, the utility must forecast its costs for the day and sometimes make multi-hour revisions. In the second method, hourly rates are transmitted at the beginning of each hour. In the latter case, a control system that attempts to optimize the performance of a thermal storage system must create a forecast of the electricity rates for the day in order to determine appropriate charging and discharging of storage.

There is ample evidence that customers respond to changing hourly prices, particularly very high prices. Georgia Power's RTP program serves customers with an aggregated demand of 5,000 MW; these customers have reduced load 400-750 MW on moderate- to high-priced days. A subset of very responsive customers reduced load by 60% when prices exceeded $1.00/kWh.[91]

Dynamic pricing can and has been implemented in a number of ways: pure hourly rates, spot prices or "super peak" prices that are limited to a small number of critical hours per year, and a variety of interruptible-load programs.[92,93] For example, Southern California Edison's I-6 interruptible rate is triggered by a reduction in capacity margin as signaled by the Independent System Operator; the rate assesses a very

substantial surcharge for power purchased during the designated hours, in return for reduced energy and demand charges during normal periods.

More widespread use of rates such as these is considered to be an appropriate mechanism for ameliorating power crises such as the one in 2000 in California, which can be characterized by power shortages and near bankruptcy of the two largest investor-owned utilities. Many retail customers pay a fixed amount for electricity and have no incentive to reduce load, while the two largest investor-owned utilities have been required to buy very expensive power from the wholesale spot market. Passing on market prices would give customers the economic signal to adopt control strategies such as optimal use of thermal storage systems and the thermal capacity of building materials. As a further benefit, even modest reduction in load can substantially reduce spot prices, by a ratio as much as 10:1.[94]

As communications and controls equipment becomes less expensive and more powerful, more regions of the country will introduce variable rates. Today, interruptible load programs have been implemented by the PJM Interconnection, the ISO New England, and such utilities as Portland General Electric, GPU Energy, and Wisconsin Electric.[94]

We compared the predictive optimal controller to three conventional control heuristics. In the presence of complex rate structures, the optimal controller was found to have a vast performance benefit (saving 40%) over conventional controls while requiring only simple predictors.[11] Interestingly, these general findings did not change when there was considerable model mismatch, i.e., uncertainty with respect to the behavior of the actual cooling plant. Recent investigations regarding forecasting uncertainty determined that this controller is robust and does not require high accuracy in predicting loads and utility rates.[13]

In summary, dynamic rate structures including RTP could make thermal energy storage systems more economically attractive while TES systems may increase the applicability of dynamic rates. We employ both the active *and* passive thermal storage capacity of a commercial building under optimal supervisory control using dynamic utility rates. Our past work serves as the foundation for the predictive optimal control of the active thermal storage inventory and will be united with the predictive optimal control of the passive thermal storage inventory described in the next section.

1.2.2.4 Passive Thermal Storage Inventory

Background – Building zone conditions are usually controlled to maintain constant temperature humidity setpoints that ensure acceptable comfort during occupancy. When unoccupied, the building energy equipment is turned off and the zone temperature is allowed to float. This strategy is coined *night setup control*. However, in many commercial buildings, building structural mass embodies a substantial thermal storage medium that can be harnessed to reduce operating costs.

Modeling Results – Several simulation studies have shown that proper pre-cooling and discharge of building thermal storage inventory can attain considerable reductions of operating costs in buildings. These savings result from both utility rate incentives (time-of-use and demand charges) and improvements in operating efficiency due to nighttime free cooling and improved chiller performance (lower ambient temperatures and more even loading). Ranges of 10% to 50% in energy cost savings and 10% to 35% in peak power reductions over night setup control were documented in a comprehensive simulation study.[19] The savings were highest when cool ambient temperatures allowed for free cooling. Other modeling studies yielded similar results.[21–22, 44–47] Common to these studies is that the level of savings and the superior control strategy strongly depend on the investigated HVAC system and on the climate.

Experimental Results – Two experiments on building pre-cooling were conducted on an office building in Florida without optimizing the storage.[49] An experimental facility at the National Institute of Standards and Technology (NIST) was used to study the use of building thermal mass to shift cooling load.[48] Several heuristic strategies were evaluated in the facility that was designed to represent a zone in a common commercial office building. A more recent set of experiments performed at NIST validated the potential for load shifting and peak cooling load reduction associated with optimal control.[21] Here, a model of the test facility was developed and validated that included detailed models of the building structure, cooling system, and human comfort. Optimization techniques were applied to the simulation model to determine control strategies used in the two separate tests. The first control strategy was designed to minimize total energy costs and resulted in the shifting of 51% of the total cooling load to the off peak hours. The second control strategy was designed to minimize the peak electrical demand and resulted in a 40% reduction in peak cooling load. Thermal comfort was maintained throughout both experiments.

Optimal Control of Passive Thermal Storage Inventory – A simplified method was developed based on simulation that defines the optimal zone temperature setpoints to minimize daily energy costs over a 24-hour period and subsequently reduced this problem to the determination of only two variables.[22] Calculation of the energy costs did not include utility demand charges. Thus, dynamic utility rates, which typically only have an energy cost component, are covered. The simplified method compared favorably with a more detailed benchmark approach[21] that involves the optimization of 24 variables for each zone (the zone temperatures for each hour of the day). The simplified procedure provides a global optimum for any application and will be investigated for use as an on-line, adaptive algorithm for controlling building thermal storage under dynamic utility rates. Energy cost savings between 22% and 42% were achieved dependent on the average ambient temperature; higher fractional savings can be achieved with pre-cooling on cooler days.

1.2.3 Expected Merits of Research Activities

The investigated technology addresses need for improved thermal storage systems, improved control systems, reduced system auxiliary and parasitic energy use as well as improved whole building systems integration.[5] Specifically, the expected merits of the technology are

1. **Energy and carbon emission savings**: Improved system efficiency will reduce energy consumption in commercial buildings and the associated carbon emissions. The operation of the building energy systems will be orchestrated to minimize their aggregate power consumption and thereby reduce parasitic and auxiliary energy use. Assuming only 15% overall efficiency improvement, a primary energy consumption reduction of 0.113 quads will be attained for the following equipment: electrical chillers, supply, return, condenser, and cooling tower fans as well as chilled and condenser water pumps.[2] The corresponding cut in carbon emissions is substantial: 0.113 quads • 15.67 kg_C/MMBtu = 1.77 million metric tons of carbon per year.
2. **Superior cost savings for the building owner**: Utility cost savings will be vastly superior to existing control strategies. Based on a total electricity bill of $60 billion/a, the annual dollar savings may be estimated to be proportional to the energy savings: 0.113/9.65 • $60 billion = $700 million.[1]
3. **Attractive market potential**: According to a recent study on the market potential of optimization systems for active building storage inventory, economical application of this technology can be assumed for large commercial buildings as long as the incremental capital cost is kept below $0.10/ft^2 and the corresponding incremental operation and maintenance cost below $0.05/ft^2/a.[50]
4. **Utility deregulation**: Dynamic pricing models such as real-time pricing can easily be accommodated, and savings from optimal control will exceed those from conventional control strategies by an even larger margin since the latter are designed for conventional time-of-use rate structures. Optimal control inherently makes best possible use of whatever load-shifting incentive may exist. Consequently, utility deregulation is an outstanding opportunity for operating cost savings.
5. **Customizable operational strategy**: Energy savings can be facilitated *concurrently* with utility cost savings by properly designing the optimization objective function. In fact, the combined thermal storage inventory can be controlled to exclusively minimize building energy use.

The scientific task tackled is one of stochastic optimization—caused by the uncertain nature of future climate conditions, thermal loads, non-cooling electricity consumption and system performance—applied to the control of commercial buildings. We believe that this approach holds the promise of innovation in the domain of building automation and offers answers to problems associated with the control of building thermal storage.

2 Experimental

2.1 Work Plan Overview

Our research plan is divided into three consecutive phases: Phase I covered a 14-month budget period, while Phases II and III will extend over 10 and 9 months, respectively. Total project duration is 33 months. Based on a project start date of September 20, 2001, the project will be completed by the end of June 2004. This final report documents the work accomplished in the context of Phase I.

Phase I was applied research (Technology Maturation Stage 2) and confirmed the conceptual approach of the technology through **analysis, modeling, and simulation**, while Phase II is exploratory development (Technology Maturation Stage 3) and involves **laboratory testing**. Phase III is advanced development (Technology Maturation Stage 4) and will identify one suitable site for **field-testing**. This site will be equipped with the necessary instrumentation and controls equipment. During the cooling season of Phase III, the predictive optimal controller will be used to govern the operation of the air-handling units and chilled water plants of the selected site. The performance will be compared to basecase control strategies by alternating between optimal and conventional control periodically.

Phase I:	Phase II:	Phase III:
Analysis, Modeling, and Simulation (14 months)	Laboratory Testing (10 months)	Implementation in Field Setting (9 mts.)

Pending the successful completion of the three research phases and industry demand, we expect that the prototype will be turned into a tangible commercial product by subsequent engineering development.

2.2 Phase I: Analysis, Modeling, and Simulation

In Phase I, individual models were developed for the building structure's thermal response, the building energy equipment including the active TES systems, and human thermal comfort. We integrated these models into a simulation environment that allows for the systematic analysis of optimal and conventional control strategies with respect to energy consumption and demand, electrical utility cost, and comfort. Figure 2 illustrates the interaction of the model components.

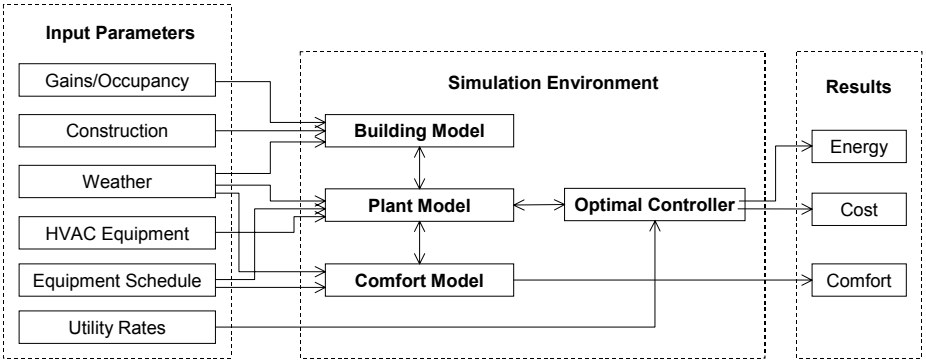

Figure 2: Block diagram of components developed in Phase I

2.3 Task 1: Building Dynamic Thermal Response Model

Task Purpose: The first task in the simulation phase entailed the development of a **building model** that effectively models the dynamic response of a commercial building. Based on a typical floor plan, the hourly cooling and heating (sensible) loads for the chosen facility are determined using the heat balance approach for a given location and weather region. The heat balance method allows for the instantaneous sensible heating and/or cooling load to be determined on the space air mass. To formulate heat balance equations, a space within the building is considered enclosed by surfaces (walls, floors, windows, and ceiling). Assuming each of the surfaces to be at a uniform temperature for a given time, the heat flow into the surface is balanced by the conductive flux leaving the surface to penetrate the solid.[51] Transient conduction in the multi-layered walls is determined by the transfer function method using a time history of air temperatures and heat fluxes.[52]

Task Summary: EnergyPlus modules for the calculation of building heating and cooling loads have been evaluated and tested. Figure 3 shows a flow chart of the EnergyPlus modules for estimating building dynamic thermal response. A sensitivity analysis was carried out to determine the effect of the time step on the accuracy and the CPU time for calculating the building loads. Figure 4 shows the results of the sensitivity analysis. A linearly proportional relationship was found. The time step will remain an adjustable variable to allow for the greatest flexibility in developing the optimal controller. This task is considered to be complete.

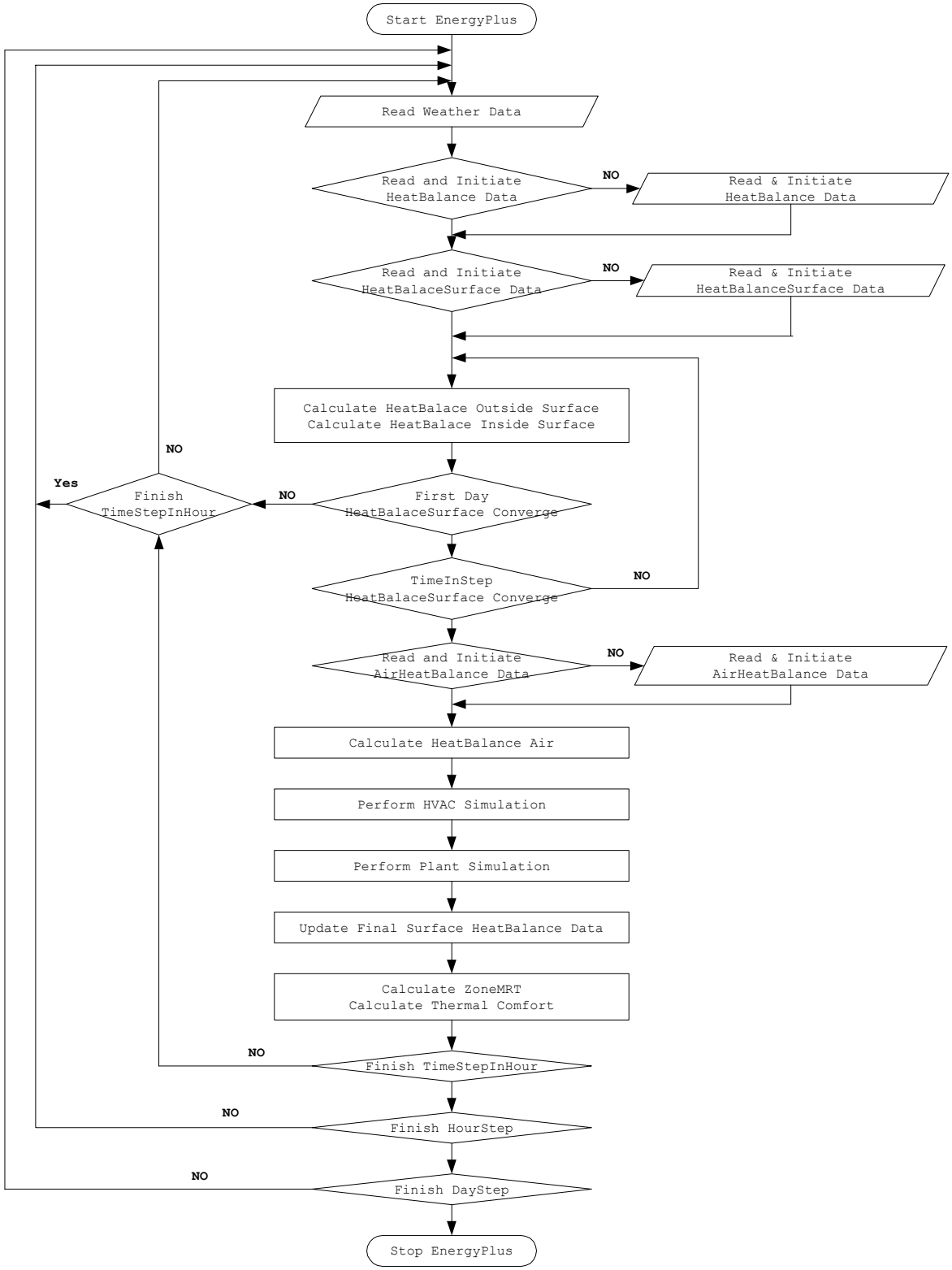

Figure 3: Flow Chart of EnergyPlus for Calculating Building Heating/Cooling Loads

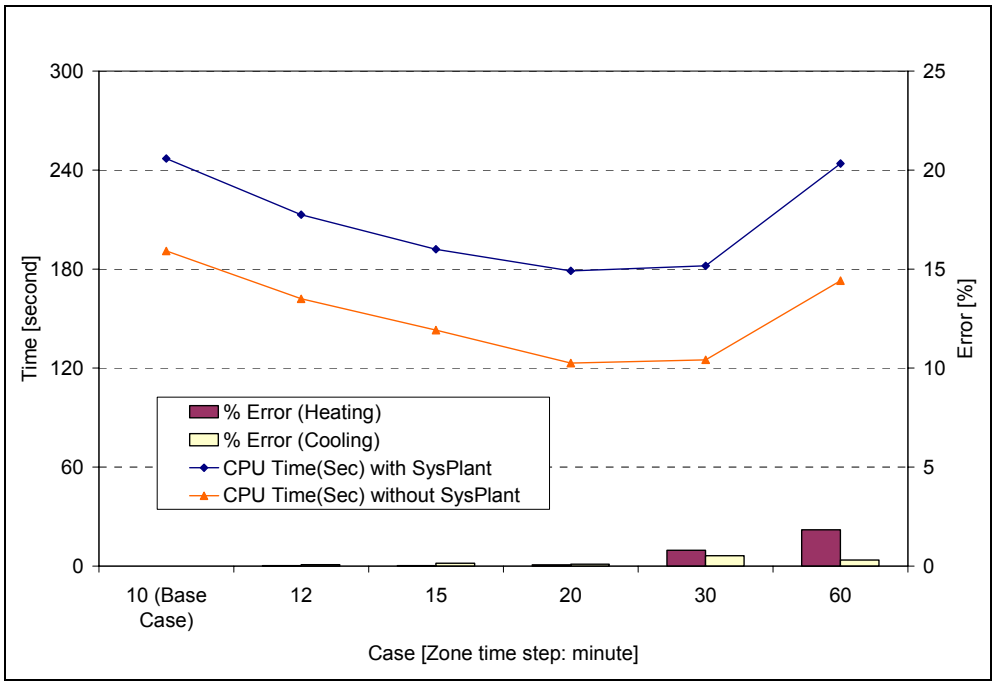

Figure 4: Effect of Time Step on Accuracy and CPU time for Calculating Building Loads

2.4 Task 2: Building Energy Systems Model

Task Purpose: A steady-state building energy systems model (**plant model**) will be developed to evaluate optimal control of active and passive thermal storage inventory. The model will calculate the power consumption of the air-handling units, chiller, cooling tower, pumps, and fans under an arbitrarily variable range of operating conditions. Given external parameters, the model will implicitly calculate the total instantaneous power consumption of all affected building energy systems. Embedded in the optimal control routine, the sequence of control variables that minimizes the objective function can be found. A similar approach has been successfully developed and applied to the evaluation of ice storage control strategies.[1,11] Routines and algorithms adapted from the BLAST and DOE-2 energy modeling programs and their successor EnergyPlus are employed.[95] Ice storage and chilled-water system models will be integrated in the simulation environment.

Task Summary: EnergyPlus has been selected as the development environment for this project. Unlike simulation tools such as DOE-2 and BLAST, EnergyPlus uses a "nested" approach in which the secondary systems performance is allowed to affect the generation of zone loads. Though more realistic, this nested approach makes it harder to develop linear sequential code to suit the project tasks at hand. The development of two ***Ice Thermal Energy Storage System*** modules for EnergyPlus is finished. A ***Utility Cost*** module for time-of-use electrical utility rates has been successfully developed and is used in the optimization analyses.

2.4.1 Development of Ice Thermal Energy Storage System Modules for EnergyPlus

A thermal energy storage (TES) plant model has been developed for EnergyPlus based on the steady-state plant model of King and Potter (1998)[98]. Their model was designed to meet the building cooling load directly and was used in evaluating optimal control of ice thermal energy storage systems. The TES model was developed as a complete system consisting of air-handling unit, chiller, pump, and cooling tower. However, the model cannot be directly used for EnergyPlus due to the optimal control methodology employed and the air-handling unit system which is already contained in EnergyPlus. The purpose of the newly developed TES plant model is to work as one of EnergyPlus plant equipment modules within its environment and to accommodate the entire continuum of states-of charge/discharge rate given user input data of charging/discharging rate and chiller outlet water temperature.

2.4.1.1 Methodology of ice thermal energy storage plant

Figure 5 describes the connection of EnergyPlus with the TES and other existing plant models in the EnergyPlus environment. The *PlantLoopSupplySideManager* calculates the demand on the plant loop, selects the equipment that is available to meet the demand based on the plant operation scheme, and calls the equipment simulation modules to operate each piece of equipment on the loop. The main subroutine *ManagePlantSupplySides* in *PlantLoopSupplySideManager* is the driver routine for the plant equipment simulation. Its main function is to determine which pieces of plant equipment are operating and to call the appropriate equipment simulation managers. Then, each element of plant equipment is simulated with the priority set by a user-defined building load range. After each plant simulation is completed, the loop properties such as mass flow rate, inlet water and outlet water temperatures are reported as node properties in EnergyPlus.

When modeling the TES plant, the additional icemaking equipment such as chiller, pump, and cooling tower are integrated into the TES model. Due to the plant loop definition of EnergyPlus, it is difficult to create additional plant loops in EnergyPlus. However, a dedicated chiller that only makes ice for the TES is commonly used. When TES is selected for the operating plant, the plant operates under one of three modes depending on the input data for *u*, the charging/discharging rate. The initial state-of-charge *x* of the thermal energy storage tank is set to 0. The detailed calculation procedure for the TES plant model can be found in King and Potter (1998)[98].

1. Dormant process: *u* is zero (0) value
2. Charging process: *u* is positive (+) value
3. Discharging process: *u* is negative (-) value

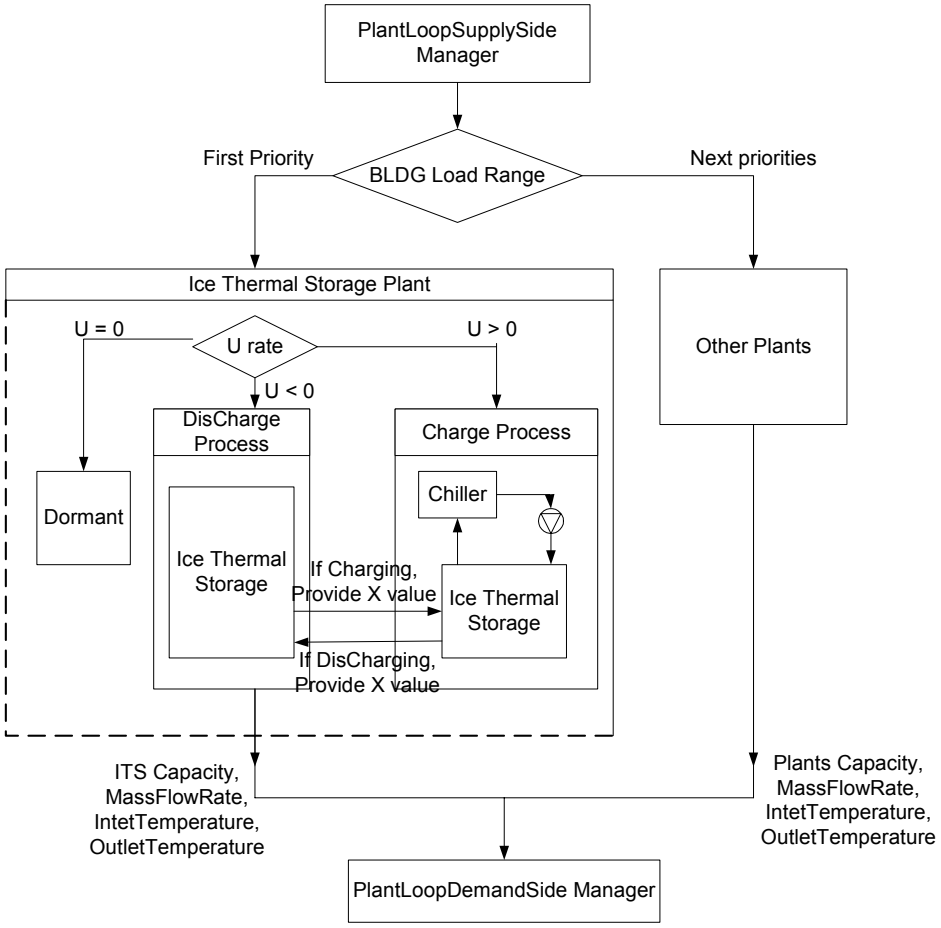

Figure 5: Flow Chart for the Implementation of the Ice Thermal Storage Model in EnergyPlus

Dormant process

When the *u* value is 0 in the hourly schedule, the TES plant provides the property of water such that TES mass flow rate is 0, and the outlet water temperature is the same as the inlet water temperature. There is no capacity available to handle building cooling load and to make ice for TES plant.

Charging process

During charging, the dedicated chiller integrated into the TES model produces ice at a rate of *u* (+), provided sufficient chiller ice-making capacity is available. In this case, the cooling capacity delivered to EnergyPlus is set to 0, and *x* is increased according to Eq. (1). Only when the charge rate *u* can be physically realized, i.e., given sufficient capacity, will the storage level increase.

$$\begin{aligned} & x_t = u\Delta t + x_{t-\Delta t} \\ & x_t \quad : \text{current charging level} \\ & x_{t-\Delta t} : \text{previous charging level} \\ & \Delta t \quad : \text{simulation time interval [}\textit{fraction of hour}\text{]} \end{aligned} \tag{1}$$

Similar to the dormant process, the TES mass flow rate is 0, and the outlet water temperature is the same as the inlet water temperature inside of EnergyPlus. However, inside of the TES model, the chiller inlet water temperature is calculated with the chiller outlet water temperature provided in an hourly schedule. Once the inlet water temperature is calculated given the icemaking load and outlet water temperature, the electricity consumption of the icemaking equipment is calculated.

Discharging process

The TES plant provides cooling capacity to meet the cooling demand on the supply side in EnergyPlus based on the discharge rate *u* (-) rate provided in an hourly schedule. The mass flow rate through TES is calculated using the TES cooling load and the temperature difference between inlet water temperature and supply loop water setpoint temperature in Eq. 2. Outlet water is provided at the supply loop water outlet setpoint temperature. The ice level of TES plant is also calculated with Eq. (1).

$$\begin{aligned} & \dot{m}_{ice} = \frac{\dot{Q}_{ice}}{c_{p,water}(T_{inlet} - T_{LoopSetpoint})} \\ & \dot{m}_{ice} \quad : \text{TES water mass flow rate [}\textit{kg/s}\text{]} \\ & \dot{Q}_{ice} \quad : \text{TES cooling load [}\textit{W}\text{]} \\ & c_{p,water} \quad : \text{Specific heat of water [} {}^{J}\!/_{kg\,^\circ C}\text{]} \\ & T_{inlet} \quad : \text{Inlet water temperature from EnergyPlus[}^\circ C\text{]} \\ & T_{LoopSetpoint} : \text{Supply loop setpoint water temperature[}^\circ C\text{]} \end{aligned} \tag{2}$$

2.4.1.2 Module Modifications

In order to implement the TES model, three modules are modified, *Energy+.idd*, *DataPlant.f90*, and *PlantLoopSupplySideManager.f90*, as well as the new module for TES plant modeling, *PlantIceThermalStorage.f90*, is added to EnergyPlus. The added or modified section can be found with "*! by PI*" keyword.

Energy+.idd

These can be placed under the group of *Plant-Condenser Equipment* section.

```
ICESTORAGE:REFINED,
    \memo Chiller Model is from King and Potter
  A1, \field ITS Name
  A2, \field ITS Type
    \type choice
```

```
        \key IOC Internal
        \key IOC External
        \key Ice Harvester
    A3, \field ITS Urate Schedule
        \type object-list
        \object-list ScheduleNames
    N1, \field ITS Capacity
        \units W_hour
        \type real
    A4, \field Plant_Loop_Inlet_Node
    A5, \field Plant_Loop_Outlet_Node
    A6, \field ITSChiller Type
        \type choice
        \key Centrifugal
        \key Reciprocating
        \key Screw
    A7, \field ITSChillerOutletTemp Schedule
        \type object-list
        \object-list ScheduleNames
    N2, \field ITSChiller Nominal Capacity
        \units W
        \type real
    N3, \field ITSChillerNom OutletWaterTemp
        \units degF
        \type real
    N4, \field ITSChillerNom InletWaterTemp
        \units degF
        \type real
    N5, \field ITSPumpNom HeadLoss
        \type real
    N6; \field ITSPump Efficiency
        \units fraction
        \type real
```

DataPlant.f90

The added variables are specified for status information of TES plant in EnergyPlus such as simulation state and equipment location within all supply side plants.

```
  TYPE ITSSetCapData
    LOGICAL :: ITSFlag = .FALSE.
    INTEGER :: LoopNum
    INTEGER :: BranchNum
    INTEGER :: CompNum
  END TYPE ITSSetCapData
  TYPE (ITSSetCapData) :: ITSSetCap
```

PlantLoopSupplySideManager.f90

Using the additional variables listed in *DataPlant.f90*, the capacity of the TES plant is calculated at each hour or timestep in EnergyPlus, unlike other plant equipment whose capacities are assigned only once. The capacity needs to be recalculated when the TES plant is called in EnergyPlus because the TES plant is subject to variable charge/discharge rates *u* and the chilled water outlet temperature profile changes according to an hourly schedule.

PlantIceThermalStorage.f90

The algorithm for implementing TES plant is explained briefly above. King and Potter (1998)[98] and the comments in the source code of *PlantIceThermalStorage.f90* provide a more detailed description of the plant.

Input and Output

Input data

Most input data for defining the TES plant is similar to other plant equipment in EnergyPlus. The performance coefficients for TES and integrated chiller are already built into the TES plant module. Three common kinds of ice-based TES and chiller types can be selected by user. All information should be entered in SI units.

Output results

Ice level and *u* rate in all processes

- *Ice Thermal Storage Starting Fraction [fraction]*
  Ice level of TES plant at the beginning of the hour or simulation time.
- *Ice Thermal Storage Dis(-)/Charge(+) U Input Hour [fraction]*
  Repeated input value of *u* rate in schedule profile.
- *Ice Thermal Storage Dis(-)/Charge(+) U Current Hour [fraction]*
  Calculating suitable *u* rate based on input *u* and TES and chiller capacities [fraction].

TES information in discharging process

- *Ice Thermal Storage ITS Water mass flow rate [kg/s]*
- *Ice Thermal Storage ITS Water Inlet Temp [°C]*
- *Ice Thermal Storage ITS Water Outlet Temp [°C]*
- *Ice Thermal Storage ITS Cooling Rate [W]*
- *Ice Thermal Storage ITS Cooling Energy [J]*

Built-in plant equipment in TES plant in charging mode

- *Ice Thermal Storage CHILLER Water mass flow rate [kg/s]*
- *Ice Thermal Storage CHILLER Water Inlet Temp [°C]*
  Chilled water inlet temperature from TES to built-in chiller.
- *Ice Thermal Storage CHILLER Water Outlet Temp [°C]*
  Chilled water outlet temperature in hourly schedule from chiller to TES.
- *Ice Thermal Storage CHILLER Pump Power [W]*
- *Ice Thermal Storage CHILLER Chiller Power [W]*
- *Ice Thermal Storage CHILLER Tower Power [W]*
- *Ice Thermal Storage CHILLER Total Power [W]*
- *Ice Thermal Storage CHILLER Total Power Consumption [J]*
  Total energy consumption for built-in TES equipment (chiller, pump, and cooling tower)

2.4.2 Development of a Utility Cost Module for EnergyPlus

To be able to calculate the operating cost of the HVAC system, a utility cost calculation module was developed and implemented in EnergyPlus. This module computes the electricity consumption of the whole building and the total HVAC system electricity use, and a time-of-use (TOU) utility rate is applied. This section provides a description and summarizes the functionality of the new utility cost module added into EnergyPlus, explains how to use the new module and where to find the results.

2.4.2.1 Methodology and module organization

The utility cost module summarizes the electricity consumption of all the components in the simulation including cooling and non-cooling loads by tracking the hourly meter values provided by EnergyPlus. The total cost of operation includes both energy and demand portions. A new object called ***Utility*** is set up to input the hourly energy and demand rates. The hourly value of the energy charge is calculated by multiplying the hourly electricity consumption with the corresponding energy rate, and then at the end of the simulation, the total energy cost is the sum of the hourly energy charges. For the demand charge portion, the maximum demand charge in each rate period (on-peak, mid-peak, off-peak …) is tracked, multiplied by the corresponding rate, and stored in an array. At the end of the simulation, the sum of the array elements is the total demand charge. But we have to consider that the simulation period is usually not one month, and the demand charge is a monthly charge. Thus, we may want to apply a runtime factor, which may be the ratio of the number of hours in the simulation divided by the average number of hours in a month, i.e., 8760/12 = 730 hours. This ensures that the demand charge is reasonable for any simulation period. The procedures of the calculation are summarized in the following formulas:

Hourly energy charge:

$$C_{energy,i} = r_{energy} E$$

Where:

r_{energy} is the energy rate [$/kWh]

E is the electricity consumption [kWh]

Total energy charge:

$$C_{energy,sum} = \sum_{i=1}^{n} C_{energy,i}$$

n is the number of total simulation hours

Demand charge of certain time period

$$C_{demand,i} = r_{demand,i} \max(P_1, P_2 .... P_m)$$

where:

P_i is the electricity demand at certain hour [kW]

$r_{demand,i}$ is the demand rate in this time period

Total demand charge for the runtime period

$$C_{demand,sum} = f_{RT}(\sum_{i=1}^{n} C_{demand,i})$$

where, f_{RT} is the runtime factor

$$f_{RT} = \frac{\text{Number of hours in simulation}}{\text{730 (average hours in one month)}}$$

Total cost of the operation cost

$$C_{total} = C_{energy,sum} + C_{demand,sum}$$

2.4.2.2 Module organization

New object:

***Utility*:**

A1, \Utilityname
A2, \Name of EnergyRateSchedule
A3, \Name of DemandRateSchedule

New module:

UtilityCost.f90

It has the following functionalities:

1. This module reads the object ***Utility*** from the input file.
2. Identifies the hourly energy and demand rates by reading the value from the corresponding schedule.
3. Calculates the energy cost for each hour.
4. Sets up an array to store the maximum demand charge for each utility rate period, which is used later to determine the final demand charge.
5. Updates the sum of hourly energy costs, which will be the final value of the energy cost portion of the total cost at the end of simulation.
6. Update the sum of array of demand charges, which will be the final value of the demand cost portion of the total cost at the end of simulation.

Modified Modules:

Three modules were modified, but the integrity of EnergyPlus is not changed. And these modifications can be kept with updates of EnergyPlus itself since all modifications are marked with "*! Added by Simeng Liu*".

a. DataGlobals.f90

Additional variables are declared which are called:

TotalElecCurrentHour

The total electricity consumption hourly, including cooling portion and non-cooling portion, [J]

BldgElecCurrentHour

The hourly non-cooling electricity consumption [J]

CoolingElecCurrentHour

The hourly cooling electricity consumption [J]

OutputFileEconomic

Unit number for economic file, which summarizes the hourly cost

FirstHour

Logical variable which is set true which the simulation is in first hour, used by initialization of the demand charge array

TotalEnergyCostSum

The total (not hourly) energy cost portion for the whole building and HVAC system, including cooling and non-cooling portion components [$]

CoolingEnergyCostSum

The total (not hourly) energy cost portion for the HVAC system [$]

NonCoolingEnergyCostSum

The total (NOT hourly) energy cost portion for the non-cooling portion [$]

TotalDemandCost

The total demand cost [$]

Money

The total cost of the simulation, which equals the sum of *TotalEnergyCostSum* and *TotalDemandCost*

b. OutputProcessor.f90

Modification is made in the subroutine ***UpdateMeters,*** where the meter values are tracked hourly, and the ***UtilityCost*** function is called.

c. SimulationManager.f90

Modifications are made in the subroutine ***OpenOutputFiles*** and ***CloseOutputFiles***, to open and close the output files, and specify the format of the results.

2.4.2.3 Input and Output

To use the utility cost module with EnergyPlus, a new Energy+.idd file is required which includes the definition of the new object *Utility*. The input file should have a *Utility* object, which includes the name of the *Utility* object and one schedule for the energy rate, the other schedule for the demand rate. The users

have the flexibility to define the rate structures hour by hour, week by week and month by month. Holidays and other special occasions can be reflected as well.

The result of the economic calculation is summarized in an output file with the extension *.eco, which includes the detailed report of the energy cost portion and the final values for demand cost, energy cost and total cost. The final values is also available in the standard EnergyPlus output file *.eso.

The new module and the modified modules are included with the new IDD file. One can compile them with the other modules of EnergyPlus, and run in the CVF (Compaq Visual Fortran) environment, or use the new executable file *.exe to replace the old one in the EnergyPlus directory, by running it with new IDD file.

Note: If you run the new EXE file, the *.eco report file will always be generated in the directory of EnergyPlus, but not where the input file (IDF file) located.

2.4.2.4 Validation of Utility Cost module

1. Validation

   Validation of the economic module is completed by comparing EnergyPlus output with MS Excel calculations. Different cases were studied to validate the accuracy of the model.

   a) Basecase

      The basecase used during the validation is as follows:

      Runtime Period = June 28 (one day);

      Time Step = 1 hour;

      On-peak hours = 9:00-18:00, the rests are off-peak hours;

      On-peak energy rate = 0.12 $/kWh, off-peak 0.05 $/kWh;

      On-peak demand rate = 20 $/kW, off-peak 5 $/kW;

      Meter report frequency = Hourly;

   b) Run period: Three run period were studied, i.e., June 28 (one day), June 22 to June 28 (one week), June 1 to 30 (one month). The results are summarized in the table below. Table 1 shows that the utility cost module and MS Excel give the same outputs.

Table 1: Summary of Runtime Period Comparison

	One Month Period		One Week Period		One Day Period	
	EXCEL Output	Eco. Model Output	EXCEL Output	Eco. Model Output	EXCEL Output	Eco. Model Output
Total Energy Cost ($)	625.703	625.703	145.158	145.158	23.517	23.51704
Total Demand Cost ($)	383.606	383.606	89.219	89.219	12.734	12.73424
Total Elec. Cost ($)	1009.309	1009.309	234.377	234.377	36.251	36.25128

   c) Time steps: Two time steps were studied, 1 hour, and 10 min. The results are summarized in Table 2 below.

Table 2: Summary of Timestep Comparison

	One Hour TimeStep		10 Min TimeStep	
	EXCEL Output	Eco. Model Output	EXCEL Output	Eco. Model Output
Total Energy Cost ($)	23.517	23.520	23.554	23.550
Total Demand Cost ($)	12.734	12.730	12.750	12.750
Total Elec. Cost ($)	36.251	36.250	36.303	36.300

   Table 2 shows again that the utility cost module and MS Excel computes the same results. The difference of output between one hour time step and 10 min time step is caused by EnergyPlus convergence.

Another issue related to the timestep is the choice of meter reporting frequency to be per time step instead of per hour. The utility cost module gives slightly different results as shown in Table 3, which is due to floating point performance.

Table 3: Summary of Meter Report Frequency Comparison

	Eco. Model Output (10 min Timestep)	
	Meter Report Hourly	Meter Report per TimeStep
Total Energy Cost ($)	23.550	23.55421
Total Demand Cost ($)	12.750	12.7495
Total Elec. Cost ($)	36.300	36.30372

d) Rate structure

Since the effect of energy rate structure is straightforward, the effect of demand rate structure is studied. A flat demand rate of 5$/kW is used to test the model. Table 4 shows that the output from the utility cost module matches that from Excel very well.

Table 4: Summary of Demand Rate Structure Comparison

	Base Case Demand Rate		Flat Demand Rate	
	EXCEL Output	Eco. Model Output	EXCEL Output	Eco. Model Output
Total Energy Cost ($)	23.517	23.520	23.517	23.517
Total Demand Cost ($)	12.734	12.730	2.557	2.557
Total Elec. Cost ($)	36.251	36.250	26.074	26.074

2. Conclusions

By comparing the output of the utility cost module and that of MS Excel, it is safe to say that the utility cost module gives the intended results according to the numerical model of utility calculation. The utility cost module represents the utility cost calculations accurately.

2.5 Task 3: Building Thermal Comfort Model

Task Purpose: Comfort-based control instead of thermostatic control will investigated. The use of comfort-based control, though uncommon in practice, has been investigated and documented.[71–74] Comfort indices will be calculated from predicted mean vote (PMV) correlations developed by Fanger (1972).[70] The inputs to the **comfort model** will be air temperature, relative humidity, mean radiant temperature, occupant activity level, and occupant clothing. When the building control is expressed as a zone PMV setpoint, the zone temperature setpoints are adjusted to produce a desired PMV value for the space. Simpler, alternative comfort indices will also be investigated.[83]

Task Summary: Three comfort models (Fanger, Pierce, and KSU) have been evaluated using EnergyPlus. The predictions of EnergyPlus are generally in good agreement with calculated and measured results reported in the literature for three thermal comfort models. The use of the Fanger model is recommended since it is most commonly used for assessing thermal comfort within buildings.

Task Details: Analysis of EnergyPlus Thermal Comfort Module

The thermal comfort module for EnergyPlus is based on three comfort models (Fanger, Pierce, and KSU). Selected results are presented in the following sections to compare the predictions of EnergyPlus with those reported in the literature.

2.5.1 Results for Fanger Model

First, the predictions of the Fanger model as implemented in EnergyPlus are compared with published results from Fanger (1972).[70] The results of the comparative analysis are summarized in Table 5. The results indicate that the predictions from EnergyPlus module are very close to those provided by Fanger (1972) with an average error of 3%.

Table 5: Comparison between Predictions of EnergyPlus Fanger Module and Results by Fanger (1972)

FANGER MODEL COMPARISION TABLE Met = 1, Tr = Ta, 50% RH										
Clothing (clo)	Ta (C)	Vel = 0.1m/s			Vel = 0.2 m/s			Vel = 0.4 m/s		
		PMV	PMV_fanger	error = PMV - PMV fanger	PMV	PMV_fanger	error = PMV - PMV fanger	PMV	PMV_fanger	error = PMV - PMV fanger
0	26	-1.6	-1.62	*0.02*	-2.34	-2.34	*0.00*	-3.50	-	-
	28	-0.39	-0.42	*0.03*	-1.00	-1.05	*0.05*	-1.87	-	-
	30	0.75	0.68	*0.07*	0.34	0.26	*0.08*	-0.23	-	-
0.5	24	-0.73	-0.73	*0.00*	-1.10	-1.10	*0.00*	-1.53	-1.53	*0.00*
	26	0.00	-0.01	*0.01*	-0.28	-0.31	*0.03*	-0.63	-0.66	*0.03*
	28	0.76	0.72	*0.04*	0.54	0.49	*0.05*	0.28	0.23	*0.05*
1	22	-0.33	-0.33	*0.00*	-0.54	-0.55	*0.01*	-0.78	-0.80	*0.02*
	24	0.22	0.20	*0.02*	0.04	0.02	*0.02*	-0.16	-0.18	*0.02*
	26	0.77	0.75	*0.02*	0.63	0.60	*0.03*	0.47	0.44	*0.03*

2.5.2 Results for Pierce Model

Figure 6 compares the calculations of the PMVET (i.e., Predicted Mean Value under Effective Temperature as defined in the Pierce model) performed by EnergyPlus module and those reported in Gagge et al. (1997).[96] The results of Figure 6 show that the PMVET calculated by EnergyPlus are nearly identical to those reported by Gagge et al. (1997). Good agreement between the calculations of EnergyPlus and reported results by Gagge et al. (1997) for DISC values are illustrated in Figure 7.

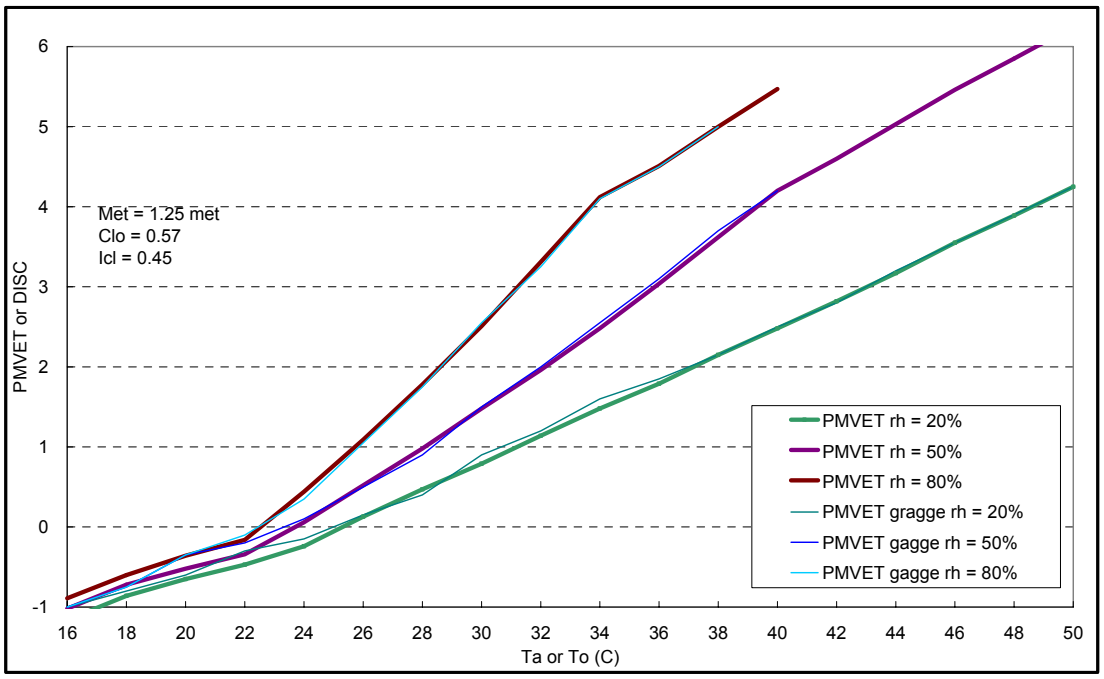

Figure 6: Comparison of predictions of EnergyPlus Pierce module and those reported by Gagge et al. (1997) for PMVET values.

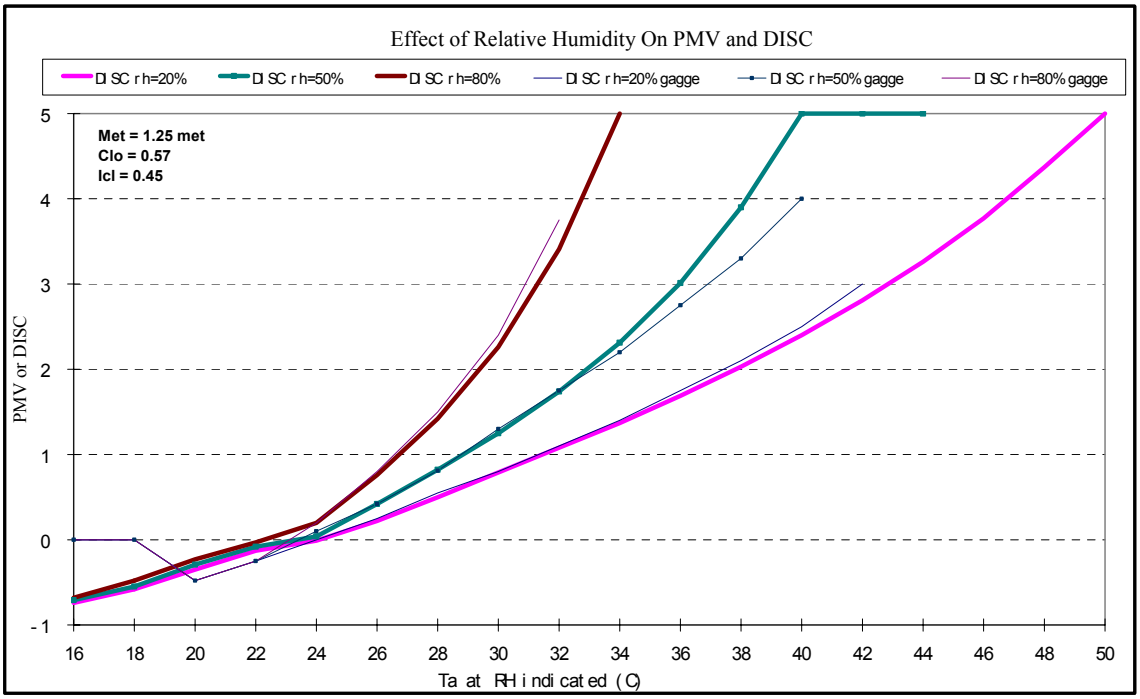

Figure 7: Comparison of the predictions of the EnergyPlus Pierce module and those reported by Gagge et al. (1997) for DISC values.

2.5.3 Results for KSU Model

The results of a comparative analysis between EnergyPlus predictions and laboratory measured data (Berglund, 1978)[97] and calculation by a program developed by Gagge et al. (1997) for Thermal Sensation Prediction values showed that EnergyPlus accurately calculates KSU Thermal Sensation Prediction for cold conditions. However, EnergyPlus predicts about 0.5-0.7 vote higher than the result for warmer conditions. However, the difference between EnergyPlus predictions and reported results by Gagge et al. (1997) is still within an acceptable range.

2.6 Task 4: Model Integration

Task Purpose: Once all of the necessary models for building thermal response, energy systems, and human comfort had been created, they were integrated into a comprehensive simulation environment. Figure 8 depicts the interaction of the components.

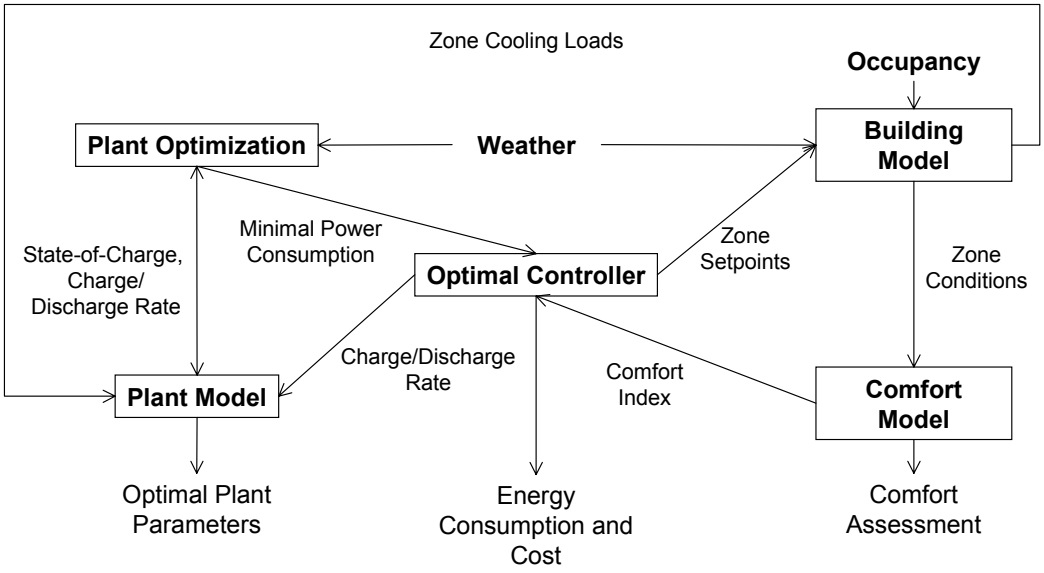

Figure 8: Flow of information within the simulation environment

For each considered point in the optimization space, the optimal controller generates the zone setpoints for the building model and the charge/discharge rates for the active TES system in the plant model. The building model uses its control input in conjunction with ambient weather conditions to calculate the sensible and latent cooling requirement. Subsequently, the zone cooling loads are used by the plant model to calculate the total cooling related power consumption, which is required to maintain the zone setpoints. The plant optimization subroutine determines those plant parameters that minimize the instantaneous power consumption for the given cooling load, weather condition, TES state-of-charge and charge/discharge rate. The comfort model uses the zone conditions to ascertain occupant comfort based on the PMV scale.

Task Summary: The integration rests on the EnergyPlus program architecture and is complete, including the availability of the ice-based and idealized TES modules.

2.6.1 Analysis of EnergyPlus Convergence

As part of the integration of an optimization routine within EnergyPlus, it was found that the cooling loads and indoor temperatures fluctuate significantly depending on the time step and the initial conditions (determined by a 3-day "warm-up" period). A simple test was then performed to determine the cooling load predictions of EnergyPlus for a sample input file (i.e., a 3-zone low-rise building as indicated in Figure 9) as a function of the time step during a large sequence of identical days. For each day of the sequence both the indoor and outdoor conditions are maintained identical.

Figure 10 shows the predictions of EnergyPlus for six time steps (ranging from 1 hour to 10 minutes). It is clear that EnergyPlus does not provide consistent predictions when using a simulation timestep of 20 minutes. The reason for this problem is not apparent at this point. It is hoped the developers of EnergyPlus can help solve this problem. Even for the other timesteps, the same conditions do not lead to identical cooling loads. These prediction problems are attributed to the convergence criteria and the warm-up period of EnergyPlus.

Stricter convergence criteria for cooling loads and peak cooling loads as well as longer warm-up periods were implemented in EnergyPlus in an attempt to obtain more consistent cooling load predictions from EnergyPlus. Figure 11 illustrates the impact of the stricter convergence criteria on the predictions of EnergyPlus using a time step of one-hour using the same building used in Figure 9. The additional convergence criteria appear to improve the prediction consistency of EnergyPlus.

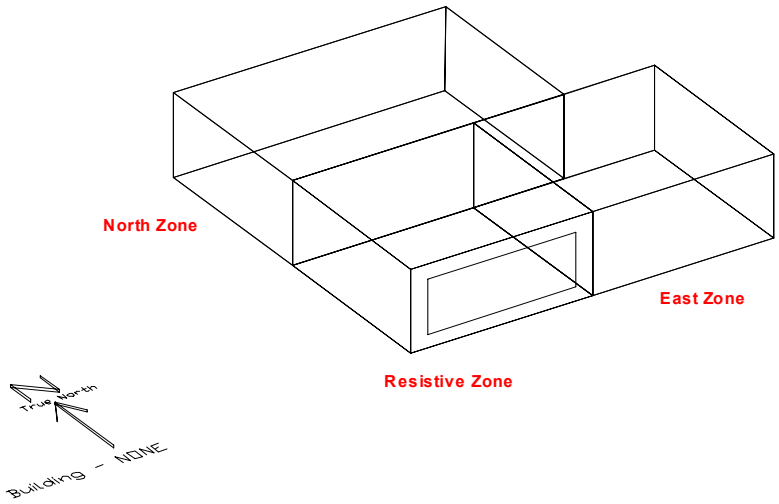

Figure 9: 3-zone building with slab-on-grade floor foundation.

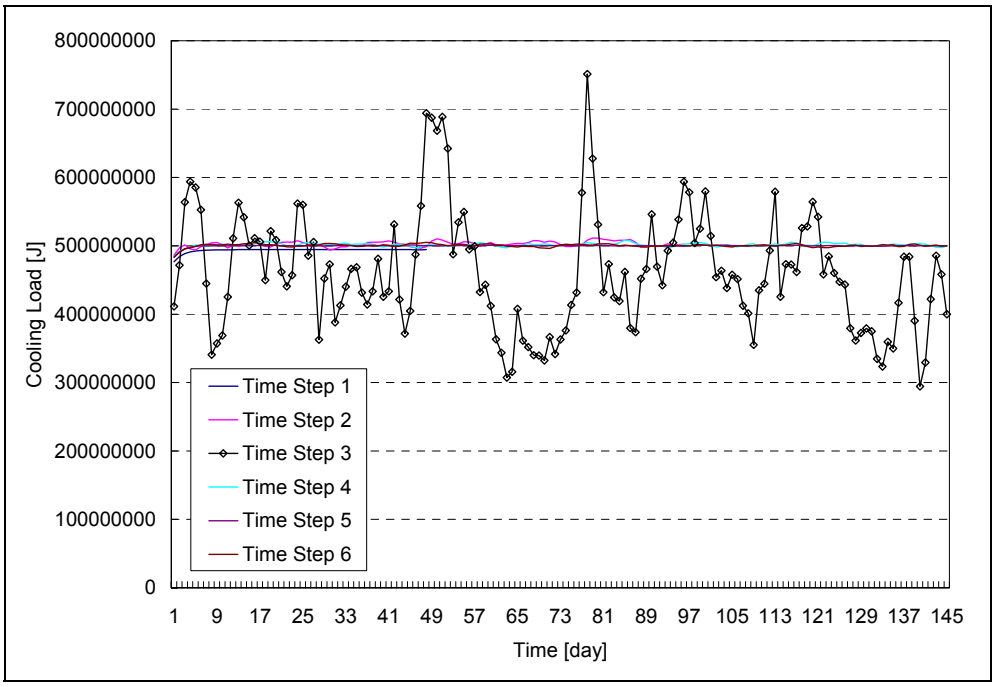

Figure 10: Predictions of EnergyPlus for cooling loads for a sequence of identical days using various time steps.

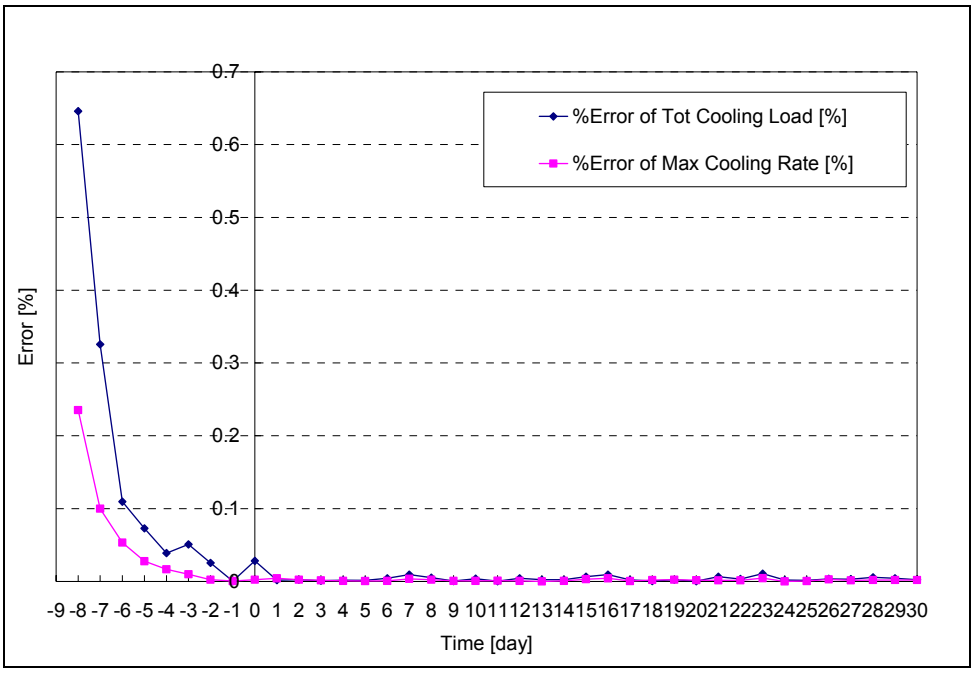

Figure 11: Impact of stricter convergence criteria on the predictions of EnergyPlus for cooling loads for a sequence of identical days using one-hour time step.

2.6.2 Analysis of Integration of Optimization Modules within EnergyPlus

Using a 3-zone low-rise building as sketched in Figure 9, testing of an optimization module incorporated within EnergyPlus has been carried out. The building structure is medium thermal mass with about 60 lb/ft^2. The optimizer module is extracted from the IMSL library and is based on the Nelder-Mead Simplex method. The optimization module in EnergyPlus is used to determine the optimal precooling strategies that minimize a well defined cost function under various rate structures. Three rate structures, with varying degree of load shifting incentives, are considered as defined in Table 6. Three cost functions are considered:

- Energy charges excluding any demand charges
- Demand charges excluding any energy charges
- Total Cost including both energy and demand charges

Most of the results presented in this report are obtained for a typical day in summer month (July 15) using Chicago, IL weather data.

Table 6: Characteristics of the electricity rates used in the parametric analysis

On-Peak Period	Hour 10 to 16		
	Rate 1	Rate 2	Rate 3
On-Peak Energy Charge	$0.10	$0.10	$0.10
Off-Peak Energy Charge	$0.05	$0.05	$0.05
On-Peak Demand Charge	$1	$5	$10
Off-peak Demand Charge	$1	$1	$1

2.6.2.1 Selection of Tolerance Value for Optimization Module

Various parametric analyses have been conducted to explore the impact of selected features of the optimization module. In particular, the convergence criterion of the optimization module has been investigated. Figure 12 summarizes the effect of decreasing the value of the convergence tolerance on the optimal value and the CPU time required to run the optimizer/EnergyPlus program when the cost function accounts for total charges (including energy and demand charges) using Rate 2 for electricity rate structure. A stricter tolerance value of 10^{-4} has been considered but the required CPU time is excessively long (almost 24 hours were needed to run EnergyPlus/Optimizer program).

Table 7 provides more details on the impact of the tolerance value selection for the optimization module. It is clear the selection of a tolerance value of 10^{-2} is acceptable without large computational penalties to obtain relatively accurate estimates of the optimal values for the cost function. A tolerance value of 10^{-2} is selected for the remainder of the analyses.

Table 7: Impact of the tolerance value on the optimal cost function values (demand and energy charges)

		Optimal Cost Function Values		
Tolerance	CPU Time [s]	Energy [J]	Peak Energy Rate [W]	Cost [$]
1.0E-1	1074	668,198,784	13,077	91.01
1.0E-2	3623	725,000,000	12,397	88.00
1.0E-3	6731	714,195,456	12,186	84.60
1.0E-4	20813	713,367,040	12,162	84.51

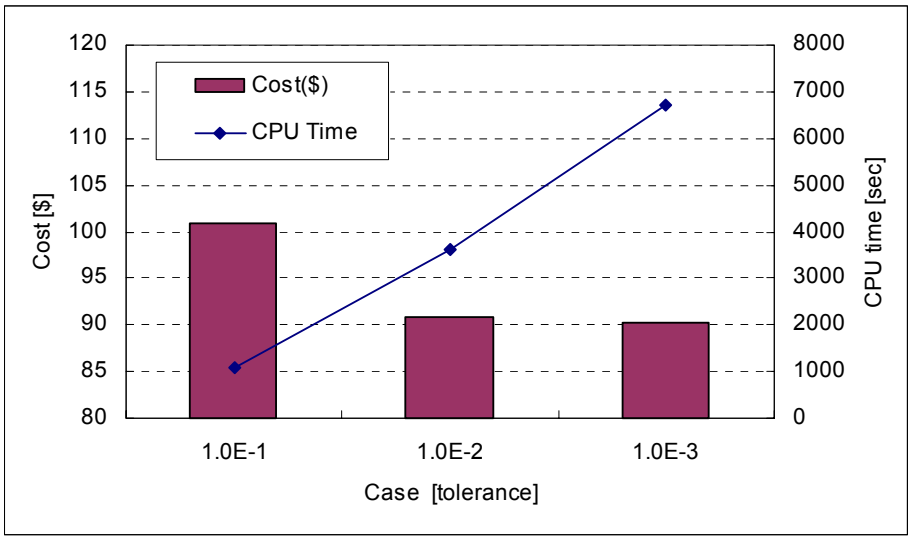

Figure 12: Effect of tolerance value on the optimal cost value and CPU time.

2.6.2.2 Impact of Cost Function and Utility Rates

The optimizer/EnergyPlus program has been used to determine the optimal solutions for precooling the building thermal mass in order to reduce the cost function under the three rate structures defined in Table 6. Table 8 summarizes the results of this investigation. Significant savings can be achieved when the peak demand is shaved off. Figures 13, 14 and 15 show the temperatures setpoints and cooling loads profiles for both conventional and optimized precooling control strategies to minimize respectively, demand charges, energy charges, and total charges using Rate 2.

When the demand or the total charges are minimized, the building mass is precooled for most of the un-occupied hours as indicated in Figures 13(a) and 15(a). This nearly continuous precooling ensures that the peak demand is reduced during the occupied period as shown in Figures 13(b) and 15(b).

When energy charges are minimized, precooling is called for only for few hours before occupied period as indicated in Figure 14(a). The small amount of precooling results in a reduction of the cooling load during the entire occupied period as shown in Figure 14(b).

The comparison of the outdoor temperature variation with the optimal temperature setpoint schedules for all cases indicates that there is potential to use economizer cycle to precool the building mass without operating the chiller as indicated in Figures 13(c), 14(c), and 15(c).

Table 8: Cost savings due optimal precooling of building for various cost functions and rate structures.

Cost Function(Rate)	No Optimization [$]	With Optimization [$]	Savings [%]
Energy (Rate 1, 2, or 3)	12.05	11.76	2
Demand (Rate 1)	32.83	24.27	26
Demand (Rate 2)	98.96	73.87	25
Demand (Rate 3)	181.62	136.04	25
Total (Rate 1)	44.88	37.32	17
Total (Rate 2)	111.01	87.21	21
Total (Rate 3)	193.67	149.34	23

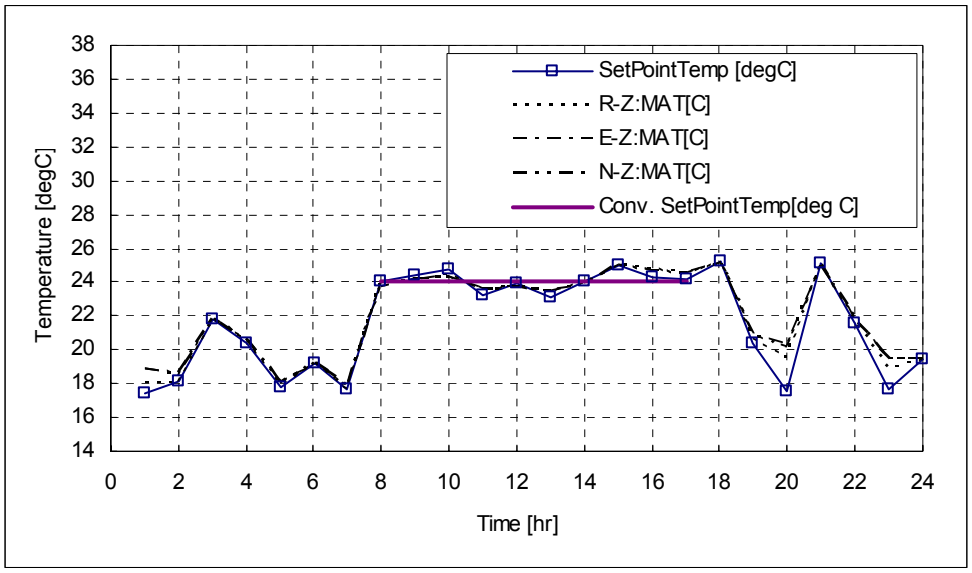

Figure 13(a): Indoor temperatures set-point schedules for both conventional and optimal pre-cooling controls set for the 3-zone building when **demand charges** are minimized using rate 2.

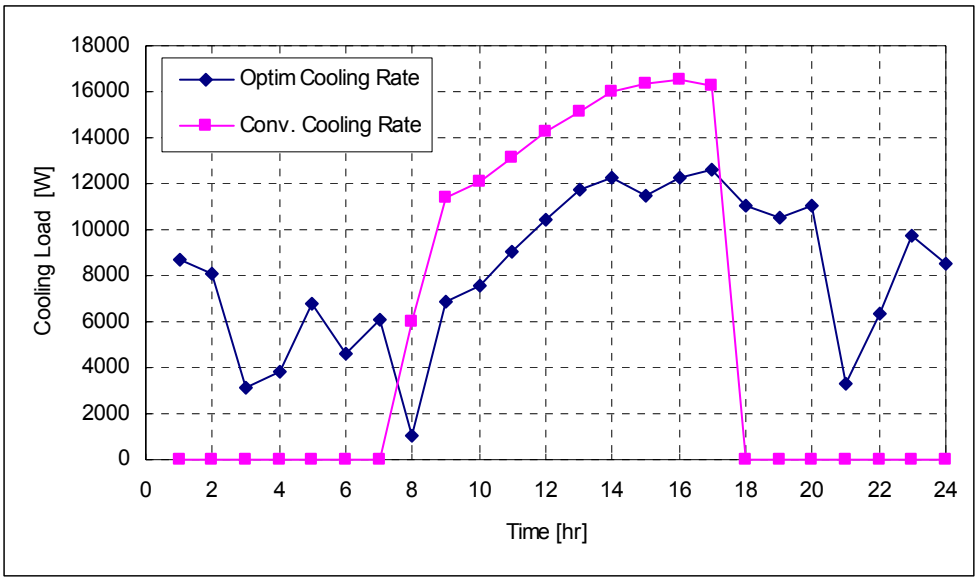

Figure 13(b): Cooling load profiles for both conventional and pre-cooling controls obtained for the 3-zone building when **demand charges** are minimized using rate 2.

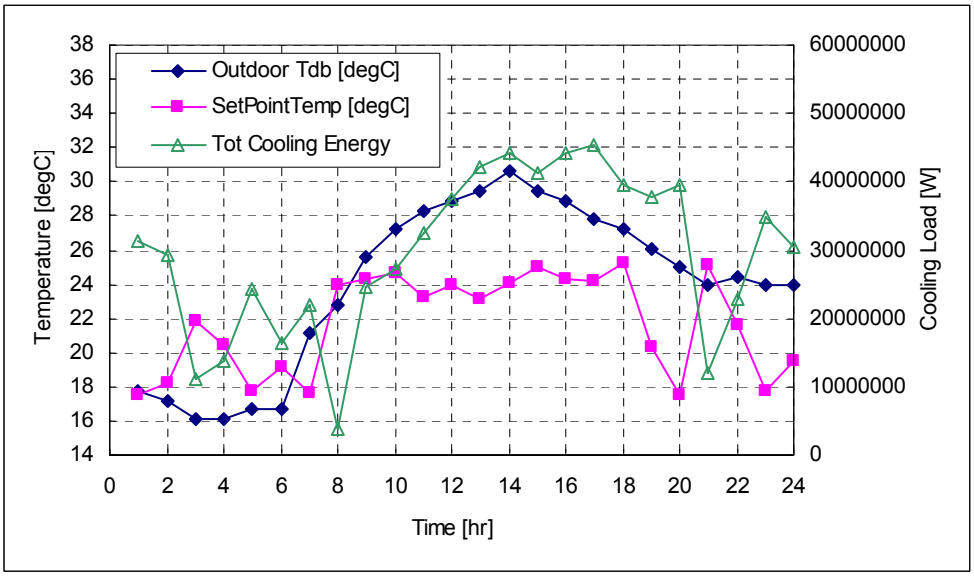

Figure 13(c): Outdoor temperature, optimal indoor set-point, and cooling load profiles for the 3-zone building when **demand charges** are minimized using rate 2.

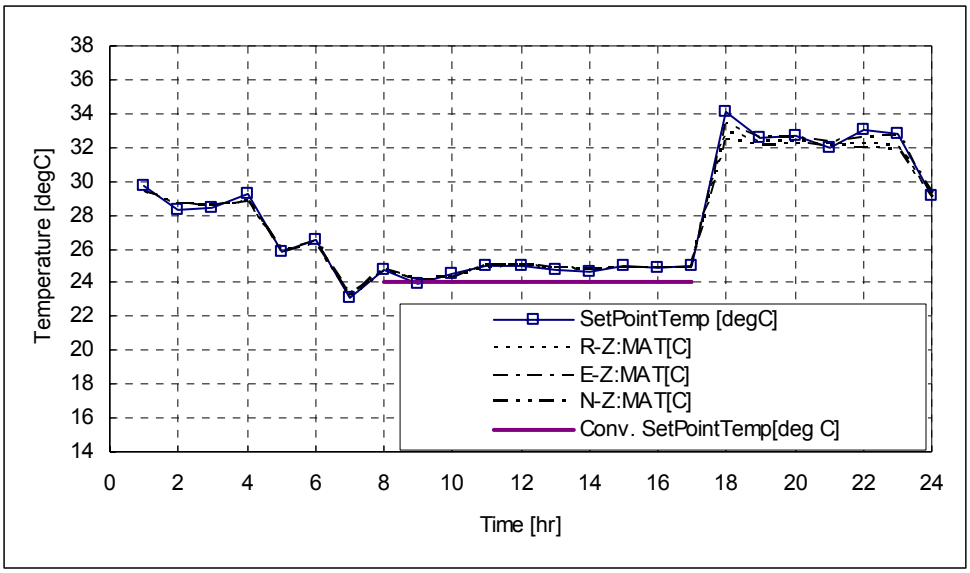

Figure 14(a): Indoor temperatures set-point schedules for both conventional and optimal precooling controls set for the 3-zone building when **energy charges** are minimized using any of the three rates.

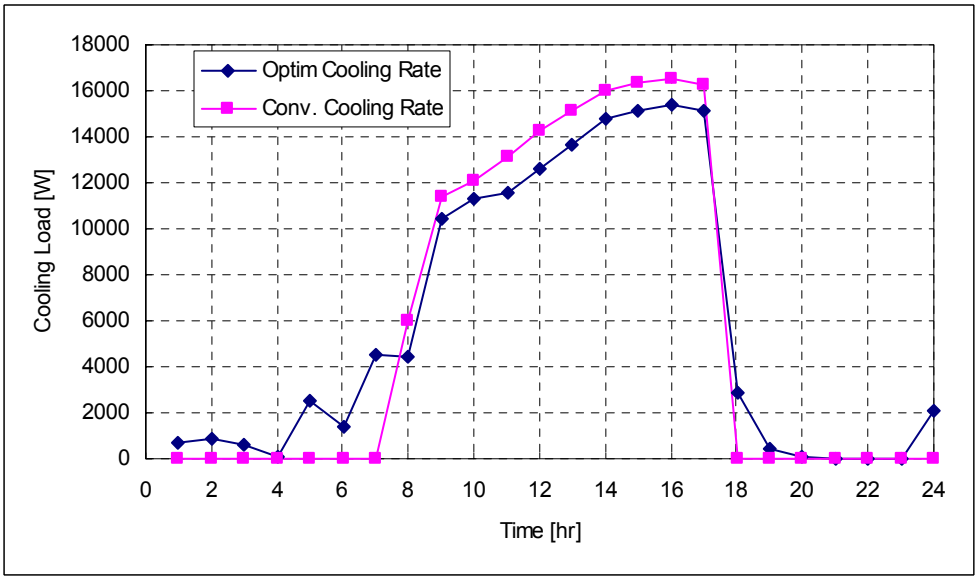

Figure 14(b): Cooling load profiles for both conventional and pre-cooling controls obtained for the 3-zone building when **energy charges** are minimized using any of the three rates.

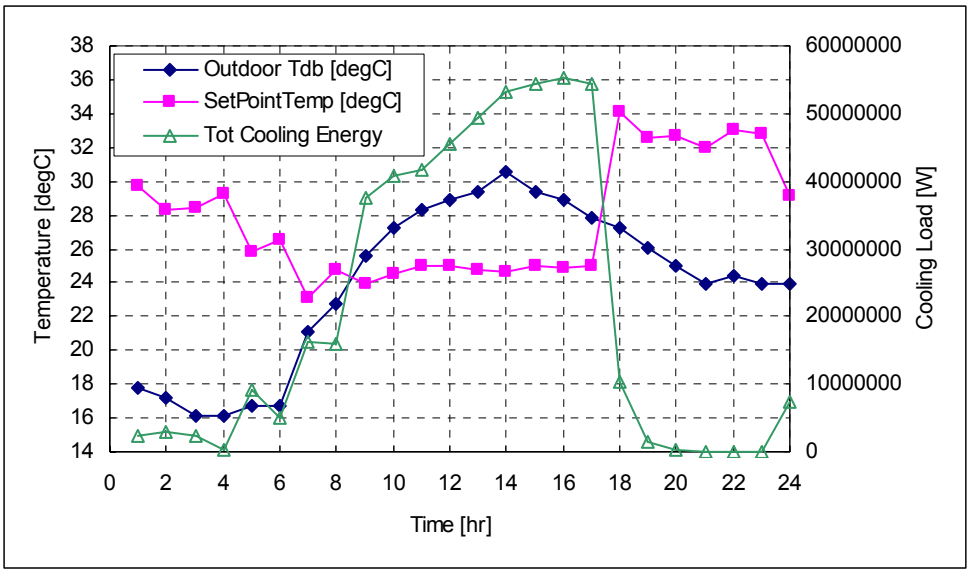

Figure 14(c): Outdoor temperature, optimal indoor setpoint, and cooling load profiles for the 3-zone building when **energy charges** are minimized using any of the three rates.

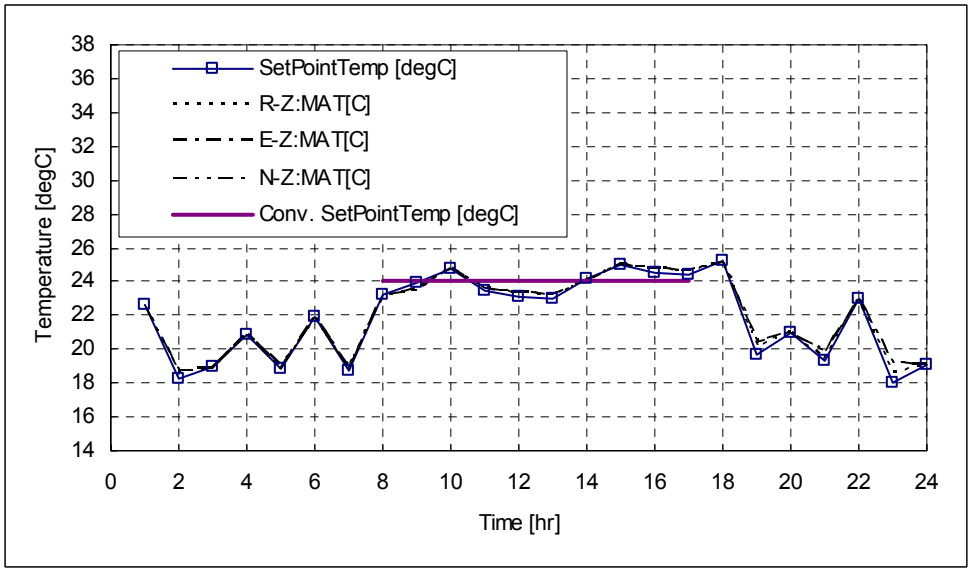

Figure 15(a): Indoor temperatures set-point schedules for both conventional and optimal pre-cooling controls set for the 3-zone building when **total charges** are minimized using rate 2.

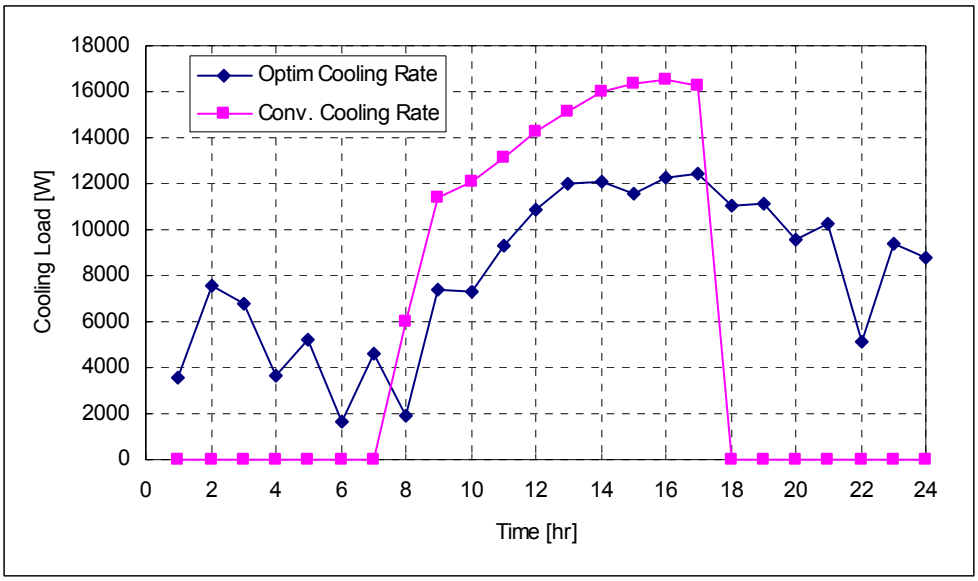

Figure 15(b): Cooling load profiles for both conventional and pre-cooling controls obtained for the 3-zone building when **total charges** are minimized using rate 2.

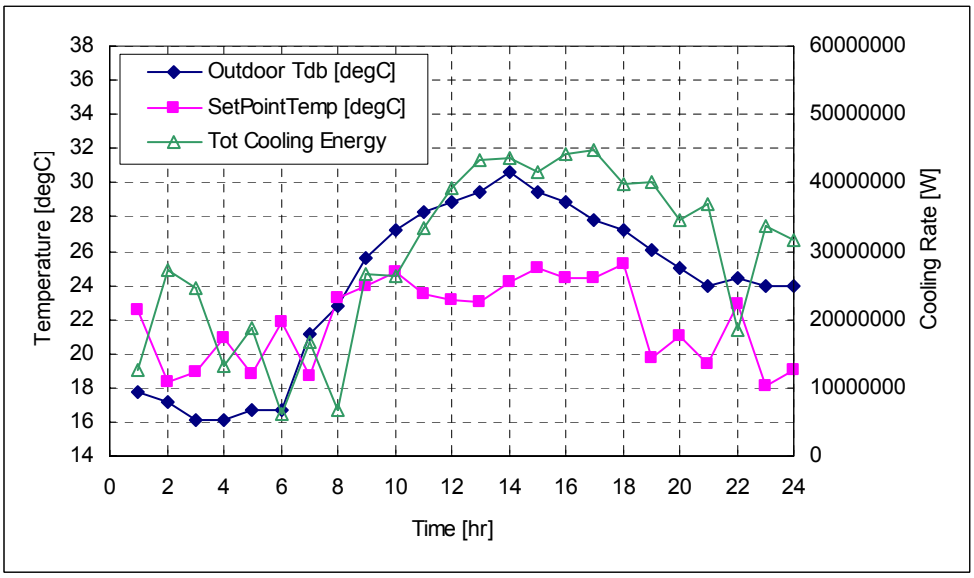

Figure 15(c): Outdoor temperature, optimal indoor setpoint, and cooling load profiles for the 3-zone building when **total charges** are minimized using rate 2.

2.6.2.3 Impact of "Smoothing" Optimal Setpoint Schedules

As shown in Figures 13, 14, or 15, the optimal precooling schedules are generally not smooth and thus are potentially difficult to implement in real buildings. The "alpine" optimal schedules result in rather sudden changes in the cooling loads that the chiller has to meet. To avoid this operational problem, smoothing procedures of the optimal precooling schedules were investigated. Two smoothing procedures were considered:

- Smoothing Procedure 1 uses a relatively large rate of change or gradient based on the highest and lowest temperatures setting
- Smoothing Procedure 2 uses a smaller rate of change or gradient based on temperature settings for two hours.

The results of two smoothing procedures are illustrated in Figure 16 for the three cases considered in Figures 13, 14, and 15. In general, the smoothing procedure 2 provides less abrupt changes in the pre-cooling temperature setpoint schedules. The results of the smoothing of the optimal precooling setpoints are summarized in Table 9 using smoothing procedure 2. In general, the smoothed optimal precooling schedules reduce only slightly the potential cost savings for most cases.

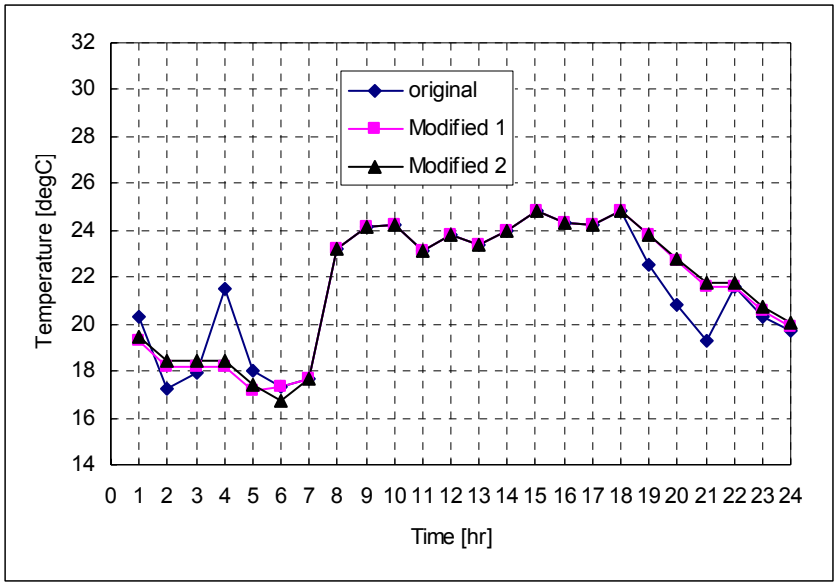

Figure 16(a): Smoothed and original optimal precooling setpoint schedules for the 3-zone building when demand charges are minimized using rate 2.

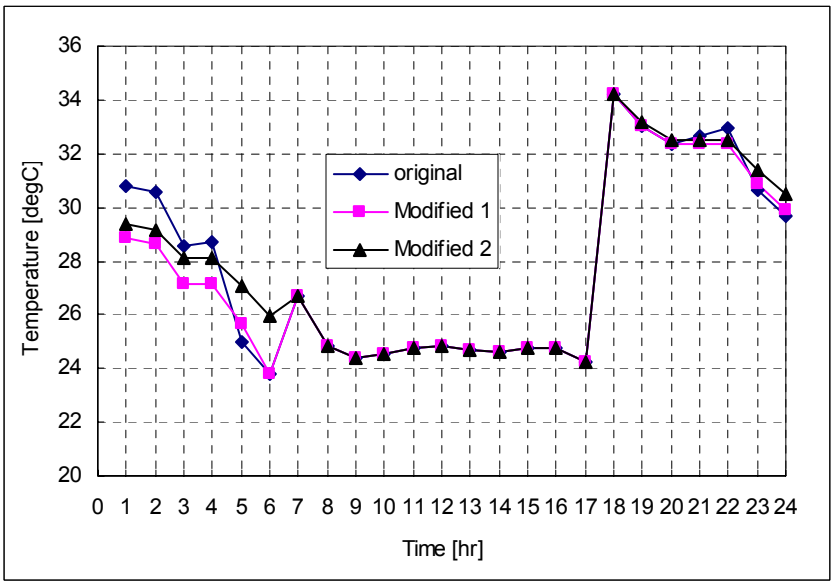

Figure 16(b): Smoothed and original optimal precooling setpoint schedules for the 3-zone building when energy charges are minimized using any of the three rates.

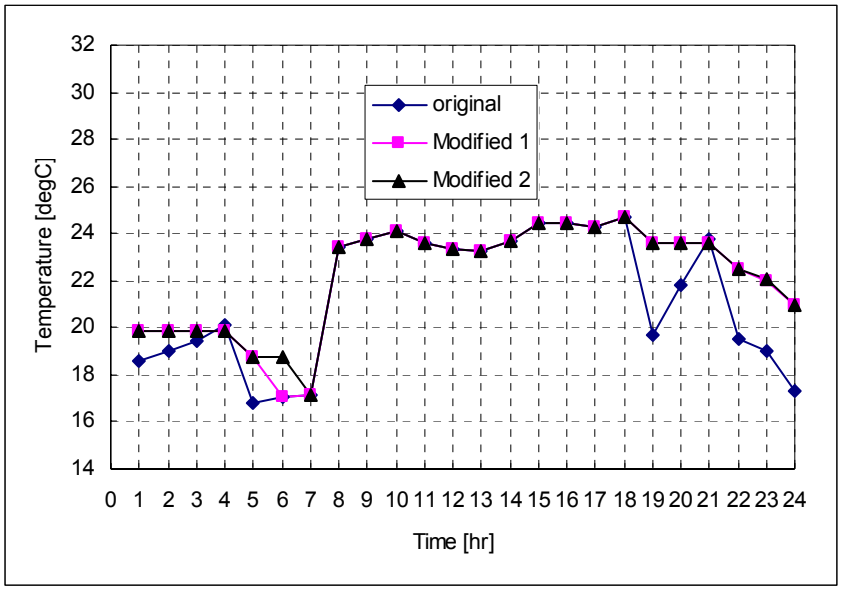

Figure 16(c): Smoothed and original optimal precooling setpoint schedules for the 3-zone building when total charges are minimized using rate 2.

Table 9: Effect of smoothed optimal precooling temperature schedules on cost function values for various rate structures using smoothing procedure 2.

Cost Function (Rate)	No Optimization [$]	Original Optimization [$]	Smoothed Optimization [$]
Energy (Rate 1, 2, or 3)	12.05	11.76	11.80
Demand (Rate 1)	32.83	24.27	25.30
Demand (Rate 2)	98.96	73.87	74.01
Demand (Rate 3)	181.62	136.04	148.87
Total (Rate 1)	44.88	37.32	39.02
Total (Rate 2)	111.01	87.21	90.80
Total (Rate 3)	193.67	149.34	154.12

2.7 Task 5: Analysis of Optimal and Conventional Control

Task Purpose: The theoretical minimum of the objective function, which will likely be the building's electrical utility bill, will be found by determining the sequence of **optimal control** actions over the time horizon of interest, which may likely be an infinite horizon. Because of the focus on dynamic rate structures such as real-time pricing without demand charges, minimizing the cost over the next 24 hours will suffice. Time-of-use utility rate structures including demand rates are more difficult to deal with, since it is not known when the optimal demand occurs. However, an approach to dealing with TOU rates has been developed and is discussed below. Most of the results discussed include a demand charge portion.

Once the optimal solution is found, *basecase scenarios* will be defined for comparison and a parametric study will identify the performance merits of optimal control relative to conventional control basecases, the preferred set of conditions under which the merits of the novel technology is maximized, and the key as-

pects affecting controller performance. The results will be the foundation for the development of a predictive optimal controller.

Task Summary: Efforts have been focused on identifying a suitable optimization framework. It is considered to either a) call EnergyPlus from an *external optimization engine* such as GenOpt, or b) *integrate optimization algorithms into EnergyPlus* such as the ones offered by the IMSL/Math Library to accommodate our optimization functionality. It has been decided to proceed with both approaches in parallel and both approaches have successfully optimized medium-scale optimization problems. The detailed results of a parametric analysis are discussed in Section 3.

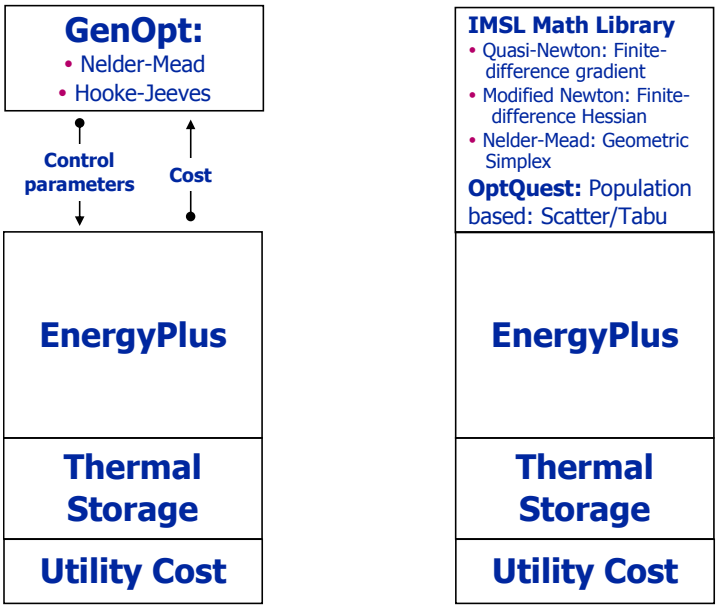

Figure 17: Schematic of External (left) and Integrated Optimization (right)

Different optimization methods were integrated into EnergyPlus and their performances compared. These optimization methods include: the Nelder-Mead simplex method (IMSL BCPOL routine), quasi-Newton method (IMSL BCONF routine), a population-based scatter search method (OptQuest), simulated annealing, Box's complex method, line search method, and dynamic programming (for active thermal storage inventory only). Considering optimization performance, robustness, and efficiencies, the IMSL BCPOL routine was chosen to be used to optimize passive thermal inventories and dynamic programming method is chosen to be used to optimize active thermal inventories.

2.8 Task 6: Predictive Optimal Control Strategy

Task Purpose: Within the simulation environment, extensive model-based analysis will be performed to identify a **robust predictive optimal supervisory controller** capable of handling uncertainty in future variables and models while ensuring economical, healthy, and comfortable operation. The features that the control strategy has to reveal are:

- Robust: When the controller fails, it fails safely to a comfortable, healthy, and economical operation.
- Predictive: Correctly forecast building loads on the basis of occupancy, weather, and zone setpoints.
- Optimal: Over the optimization horizon, the set of control variables minimizes the objective function.
- Supervisory: The optimal controller will dictate optimal setpoints of subordinate plant parameters.

Task Summary: Based on past experience with real-time optimization, certainty-equivalent closed-loop optimization is employed: The predictive optimal controller carries out an optimization over a predefined planning horizon *L* and of the generated optimal strategy only the first action is executed. At the next time

step the process is repeated. The final control strategy of this near-optimal controller over a total simulation horizon of K steps is thus composed of K initial control actions of K optimal strategies of horizon L, where $L < K$. This ensures that newly available, improved forecasts of future variables are always utilized.

Figure 18 illustrates the procedure involved in determining the predictive optimal control policy. By moving the time window of L time steps forward and updating the control strategy after each time step, the newly updated forecast information is introduced and delivers a policy (thick dotted line), which is different from the policy found at k^* (thin dashed line).

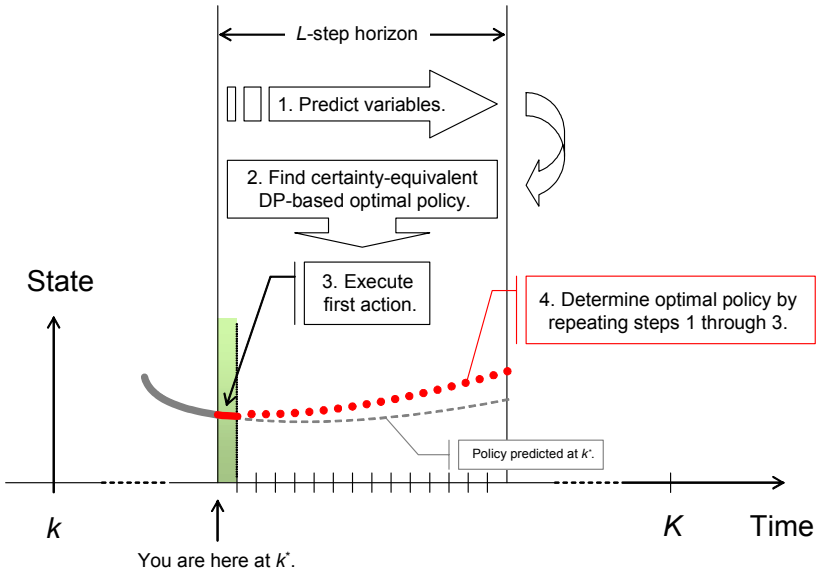

Figure 18: Schematic of the certainty-equivalent, closed-loop, predictive optimal control procedure.

2.8.1 Background

To improve the performances of the selected optimization routines, i.e., to increase their robustness and efficiency, modifications are needed to simplify the problem and to streamline the optimization process. This selection of optimization techniques was carried out in parallel with the selection of appropriate optimization methods.

In the original problem, it is necessary to let optimization routines find hourly setpoints for both passive inventory and active inventory at the same time. If a 24-hour planning horizon is assumed, there will be 2 arrays of 24 variables each to be optimized leading to a 48-dimensional optimization task. Given the capabilities of above available optimization routines, this is a difficult problem to solve. The following two phenomena are observed.

First, the optimization routines tend to ignore the potential of the passive inventory if optimizing passive and active inventory at the same time. This is due to the fact that active thermal inventories have much larger influences on cost function values (electrical bills in our case) than passive thermal inventories do when both changing the setpoints by the same absolute amount. Second, when considering passive thermal inventory only, it is a 24-dimensional problem. This is still a difficult problem for most of the optimization routine to solve especially due to the fact that the building simulation process is highly nonlinear and not differentiable (i.e. to provide gradients to help the optimization routines search in the proper direction). As a result, it was observed that the optimal results are in the shape of "zig-zag", indicating local minima. Finally, due to the complexity of the problem, it takes the optimization routines a long time, i.e., from two to more than twenty hours, to finish a 24-hour optimization, which makes the optimization infeasible.

These problems are solved by introducing the building modes and a sequential optimization technique. The building mode technique groups the setpoints during similar time periods. It reduces the dimension of the problem in a physically reasonable way so that the optimization routines can find the optimum set-

points quicker and almost without affecting the accuracy of the solution. The sequential optimization technique is introduced to help the optimization routine distinguish the effect of different thermal inventories. Instead of optimizing thermal inventories having greater effects on cost functions with those having lower effects on cost functions at the same time, it optimizes different thermal inventories sequentially. Below we will show that using sequential optimization helps the optimization routines find a "near optimum" with results close enough to the global optimum.

2.8.2 Development of an Optimization based on Building Modes and its validation

Purpose: Up to this point, optimizations of building zone setpoint temperatures were based on L = 24 hourly set points. The Nelder-Mead simplex method and OptQuest scatter search optimization approaches were used to conduct the optimization of building total electrical cost. The results show that it takes the Simplex about 30 minutes to 3 hours and OptQuest requires tens of hours to find the solution. This is not feasible in real plant operations. Therefore, while looking for faster optimization techniques, using "building modes" to reduce the size of the optimization problem is a valid approach.

Introduction: According to the plant operation schedule and time-of-use (TOU) electrical rates, buildings can be considered to be operated under distinct modes. One of the most convenient and simplified ways of defining these modes is to divide building operation into the following four modes.

Unoccupied-Offpeak is when the building is not occupied and the electrical rate is off-peak.

Unoccupied-Onpeak is when the building is not occupied but the electrical rate is on-peak.

Occupied-Onpeak is when the building is occupied and electrical rate is on-peak.

Occupied-Offpeak is when the building is occupied but electrical rate is off-peak.

Time periods within a building mode exhibit similar characteristics. For instance, during unoccupied on-peak period, thermal comfort can be neglected and thus the temperatures can be set to higher setpoints to save electricity costs. Therefore, it is possible to take the building mode as an entity and optimize a constant zone temperature setpoint extending over a building mode. It may seem that we sacrifice the accuracy of the optimum setpoints found. However, this sacrifice of accuracy is ameliorated by using the closed-loop optimization feeding fresh high-quality forecasts. Further, since we optimize in a lower dimensional space, the existing optimizers are less likely to get caught in local optima.

During each building mode, the corresponding control variable is kept constant as shown in Figure 19b. Since these few variables describe stepped profiles for each control variable, we denote them as *solution parameters SP*. For the given occupancy and utility rate periods and assuming hourly time steps, the solution space for an L = 24 hour horizon is reduced from 24 dimensions to 5 dimensions. For any horizon L, the number of parameters can increase or decrease depending on how many distinct occupancy and rate periods are covered. Though this simplification causes the solution to become slightly suboptimal compared to the full solution, the problem now becomes computationally tractable.

The active storage (TES) optimization problem is characterized by complex and nonlinear constraints as yet simple state transitions. This class of problem is most readily solved using dynamic programming and yields L solution variables as shown in Figure 19a.

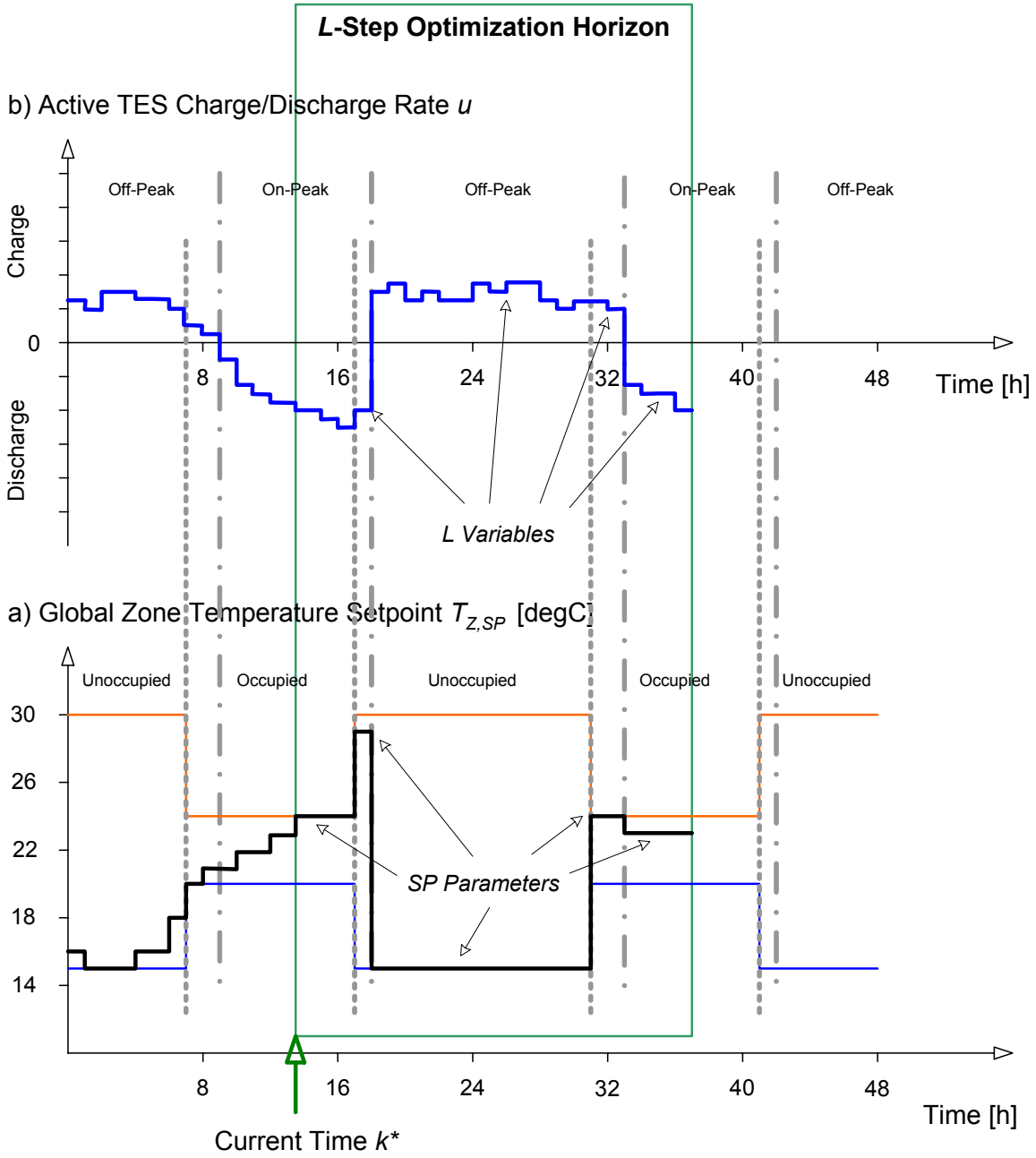

Figure 19: a) Simplified stepped optimization for passive storage and b) active storage optimization

Results and Analysis: The following table offers results comparing the 24 hourly setpoint optimization and the 5 building mode (the Unoccupied-Onpeak modes in the morning and in the night are treated separately) optimization.

The building is a 15-zone 3-story office building occupied from 8:00-17:00. Electrical rate on-peak time is from 9:00-18:00 during which energy rates are 0.20 $/kWh, demand rate is 10 $/kW, and off-peak time is from 19:00-9:00 during which energy rates are 0.05 $/kWh and no demand rates are levied. The five building modes are then:

Unoccupied-Offpeak-1: 1:00-7:00
Occupied-Offpeak: 8:00
Occupied-Onpeak: 9:00-17:00

Unoccupied-Onpeak: 18:00

Unoccupied-Offpeak-2: 19:00-24:00

The comparisons are made for two locations (Phoenix, AZ and Minneapolis, MN) , two seasons (April 1 and July 22), two electrical rates (basic and flat rate) and two building construction types (heavy: 220 lb/ft^2, and light 50 lb/ft^2).

Table 10: Comparison of optimizations based on building modes and 24 hourly setpoints.

		H-1, AZ,July	H-1, MN,April	H-1, MN,July	H-2, AZ,July	H-2, MN,April	H-2, MN,July	L-1, AZ,July	L-1, MN,April	L-1, MN,July
Basecase	Total Cost	788.00	631.00	717.30	815.80	625.80	733.80	903.90	603.50	769.30
Simplex 24 SP	Total Cost	714.00	583.00	672.60	758.00	568.70	691.40	829.50	568.00	716.00
	Runs	*427*	*337*	*270*	*471*	*458*	*476*	*301*	*344*	*266*
	Time	*3:45*	*0:58*	*1:56*	*3:55*	*1:04*	*3:26*	*2:14*	*1:06*	*1:48*
	Saving	-9.39%	-7.61%	-6.23%	-7.09%	-9.12%	-5.78%	-8.23%	-5.88%	-6.93%
Simplex 5 Bldg Mode	Total Cost	704.90	571.00	663.90	764.00	573.00	674.60	819.00	561.00	703.70
	Runs	*35*	*35*	*29*	*51*	*50*	*72*	*33*	*30*	*33*
	Time	*0:05*	*0:01*	*0:03*	*0:07*	*0:02*	*0:08*	*0:05*	*0:02*	*0:04*
	Saving	-10.55%	-9.51%	-7.44%	-6.35%	-8.44%	-8.07%	-9.39%	-7.04%	-8.53%
5 mode Cost Saving		1.15%	1.90%	1.21%	-0.74%	-0.69%	2.29%	1.16%	1.16%	1.60%
5 mode Time Saving		**3:40**	**0:57**	**1:53**	**3:48**	**1:02**	**3:18**	**2:09**	**1:04**	**1:44**
OptQuest 24 SP	Total Cost	712.00	574.00	656.20	723.40	558.70	660.80	804.00	558.00	694.00
	Time	*13:00*	*8:40*	*28:46*	*22:22*	*8:23*	*18:55*	*24:56*	*10:16*	*19:21*
	Saving	-9.64%	-9.03%	-8.52%	-11.33%	-10.72%	-9.95%	-11.05%	-7.54%	-9.79%
OptQuest 5 Bldg Mode	Total Cost	*703.00*	*569.00*	*655.00*	*739.00*	*557.60*	*669.50*	*814.70*	*559.50*	*699.00*
	Time	*12:00*	*3:42*	*10:11*	*12:47*	*3:28*	*9:11*	*13:21*	*4:51*	*10:55*
	Saving	*-10.79%*	*-9.83%*	*-8.69%*	*-9.41%*	*-10.90%*	*-8.76%*	*-9.87%*	*-7.29%*	*-9.14%*
5 mode Cost Saving		1.14%	0.79%	0.17%	-1.91%	0.18%	-1.19%	-1.18%	-0.25%	-0.65%
5 mode Time Saving		**1:00**	**4:58**	**18:35**	**9:35**	**4:55**	**9:44**	**11:35**	**5:25**	**8:26**

H-1 : Heavy-mass building with incentive electrical rate
H-2: Heavy-mass building with flat rate
L-1: Light-mass building with Incentive electrical rate

From Table 10 it can be observed that in terms of cost savings, in some cases the building modes approach saves more than the hourly setpoints approach, while in other cases the reverse is true. The fact that the building modes perform slightly better reveals that the hourly setpoint approach using both Simplex and OptQuest at times gets stuck in local minima. But all the differences are within 0.15-2.3%. In terms of time savings, the advantage of using building modes is obvious. While using hourly setpoints, it takes Nelder-Mead Simplex 1-4 hours or OptQuest 8-29 hours to find the optimum; it takes only 1-5 minutes for Nelder-Mead Simplex and 3-14 hours for OptQuest to find the equally good results.

2.8.3 Dynamic Programming for the Optimization of Active TES Systems

Dynamic programming (DP) has been shown to be an effective method to optimize active thermal storage systems. It is developed and tested with a simple plant model in which the baseload chiller has a constant COP chiller of COP = 4.5, and the thermal storage system is an ice tank with its dedicated chiller with COP = 3.0. The following graphs show the results of using dynamic programming and simplex method to optimize building electrical energy cost.

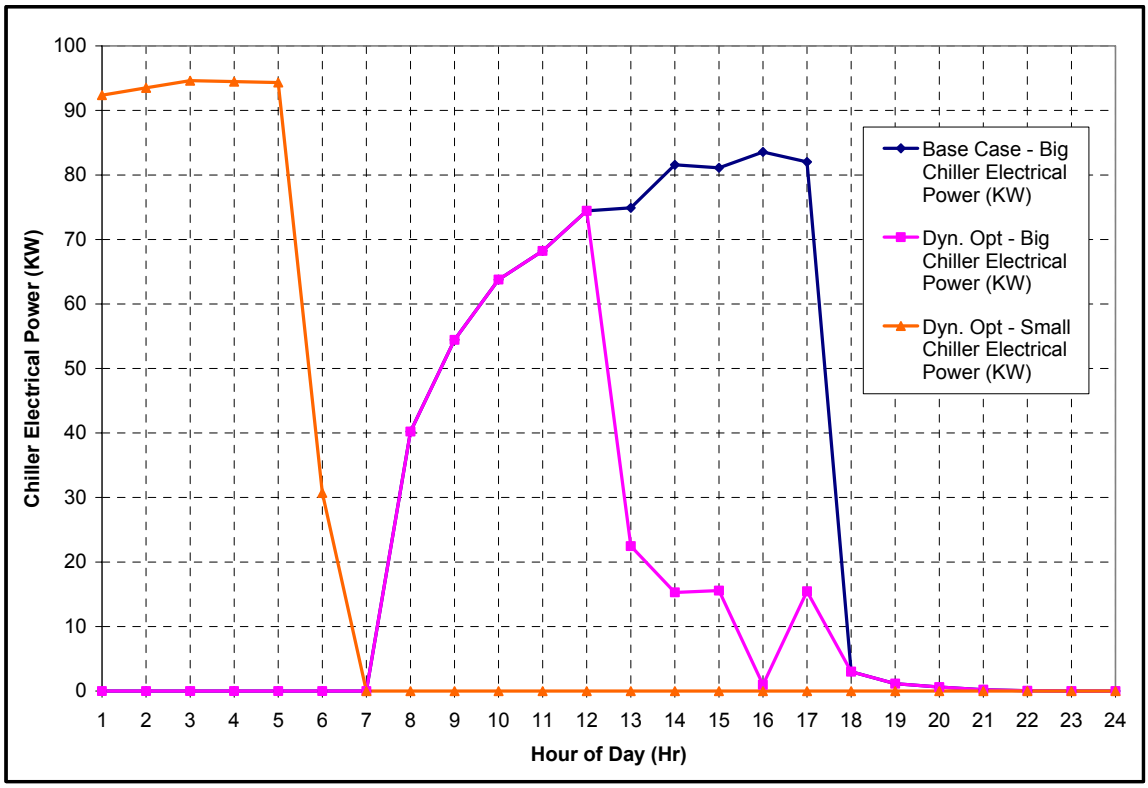

Figure 20: Using dynamic programming to optimize plant energy cost.

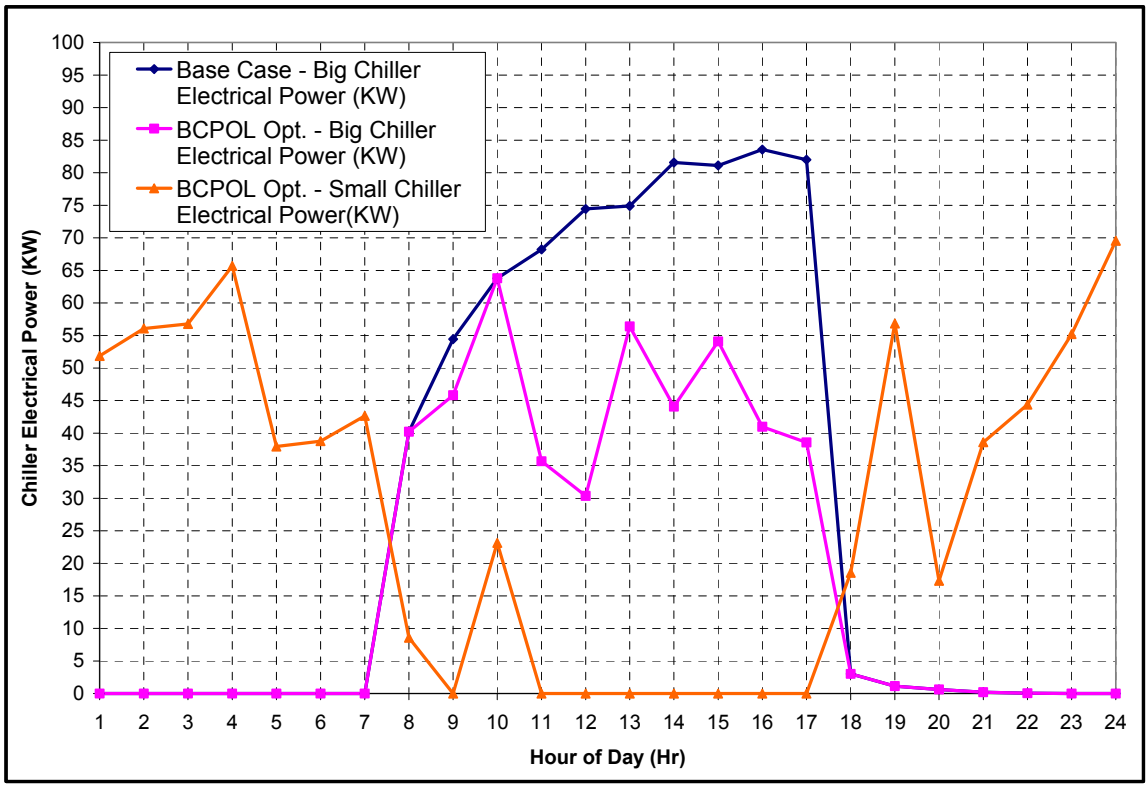

Figure 21: Using Nelder-Mead Simplex method to optimize plant energy cost

While the base case total cost is $135, the DP optimized control gives a cost of $93.8 with a saving of 30.5%. Using the Simplex method, the cost is $129.3 with a saving of only 4.2%.

Another merit of dynamic programming is that by defining terminal state costs, it is convenient to control the final ice inventory level to be the same as initial ice level when initial ice level is nonzero. This is difficult to be accomplished by other optimizers. The following graph shows that with initial ice level being 50%, dynamical programming controls the end ice level to be the same as initial value.

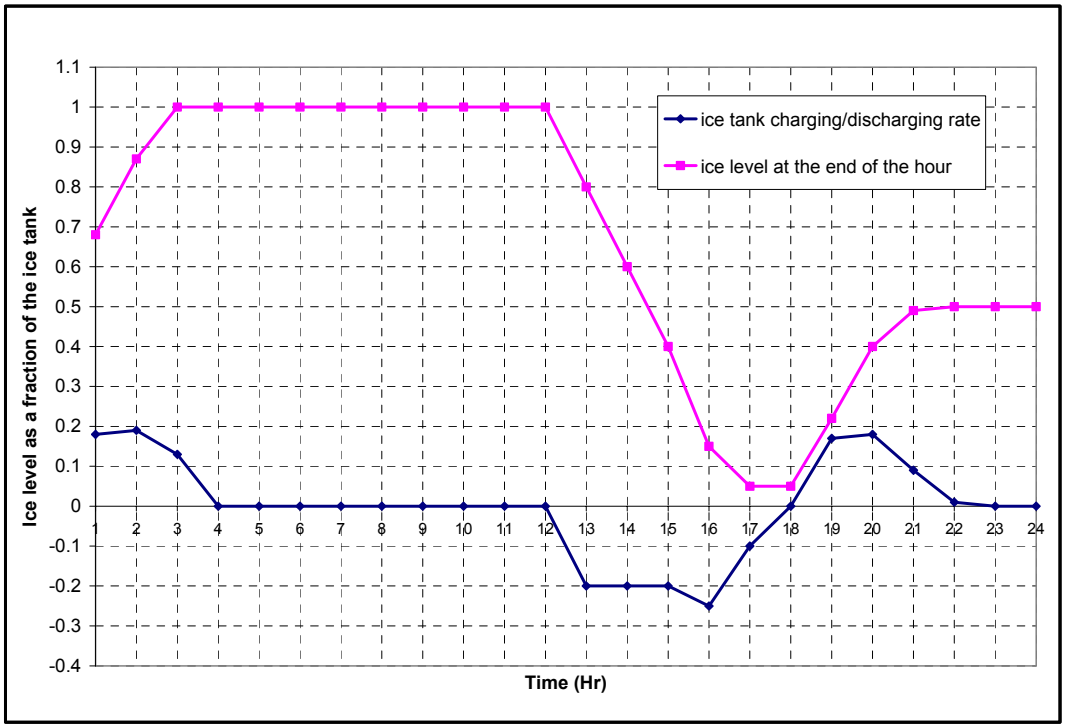

Figure 22: Dynamic programming controls the final state of ice level.

2.8.4 Comparison of simple and refined thermal energy storage system models

Background: At present, a TES model based on a paper by King and Potter[98] is integrated within EnergyPlus. Due to the iterative nature of the heat transfer calculations within the refined model, it takes longer to simulate the TES performance. When the optimization task is added, it takes a considerably longer time and can make it infeasible. By using a simpler model for the TES using a constant-COP chiller, the simulation as well as optimization times can be reduced. Thus, if using a simple plant model offers similar results compared to the refined model, it is recommended to use a simple plant model for the optimization. Thus, a simpler constant-COP TES model was integrated into EnergyPlus, and optimizations based on the refined TES model and the simple TES model are compared.

First, given the same input, the output of electricity consumption of the refined Model and the simple TES model are similar as can be seen in Figure 23.

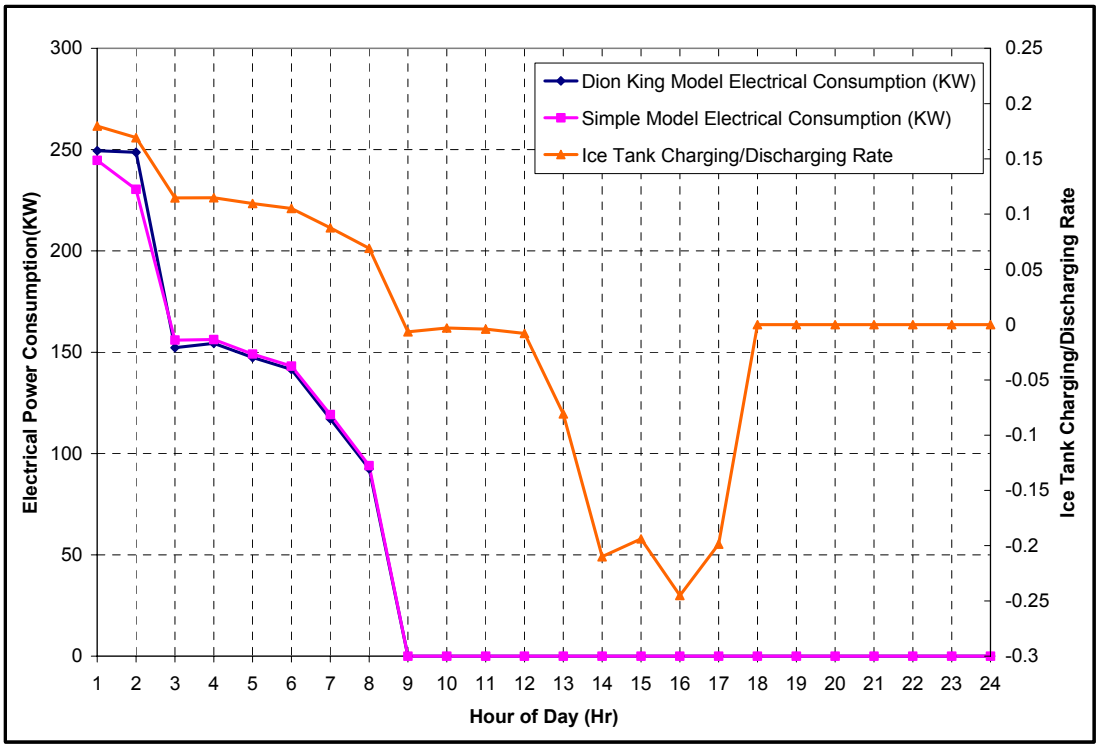

Figure 23: Comparison of Refined TES model and simple TES model

Table 11 shows the results comparing optimization of the RefinedTES model and the simple constant-COP TES model using dynamic programming. The COP of the large base varies from 2.5 to 4.5. Electrical rates vary from 0.25 vs. 0.05 $/kWh (Onpeak vs. Off-peak) to 0.10 vs. 0.05 $/kWh.

Table 11: Comparison of optimizations using refined TES model with simple TES model.

Large Chiller COP		Rate - 1 0.25 : 0.05	Rate - 2 0.20 : 0.05	Rate - 3 0.15 : 0.05
4.5	Basecase	701.33	565.37	429.42
	King & Potter Model Energy Cost	687.26	563.86	429.42
	King & Potter Model Energy Cost Savings.	*-2.01%*	*-0.27%*	*0.00%*
	Simple Model Energy Cost	686.07	565.37	429.42
	Simple Model Energy Cost Savings	*-2.18%*	*0.00%*	*0.00%*
	Model Difference	*-0.17%*	*0.27%*	*0.00%*
4	Basecase	722.44	582.31	442.19
	King & Potter Model Energy Cost	698.91	575.05	442.19
	King & Potter Model Energy Cost Savings.	*-3.26%*	*-1.25%*	*0.00%*
	Simple Model Energy Cost	696.77	575.37	442.19
	Simple Model Energy Cost Savings	*-3.55%*	*-1.19%*	*0.00%*
	Model Difference	*-0.30%*	*0.05%*	*0.00%*
3.5	Basecase	749.58	604.1	458.61
	King & Potter Model Energy Cost	712.97	587.88	458.4
	King & Potter Model Energy Cost Savings.	*-4.88%*	*-2.68%*	*-0.05%*
	Simple Model Energy Cost	710.54	586.46	458.61
	Simple Model Energy Cost Savings	*-5.21%*	*-2.92%*	*0.00%*
	Model Difference	*-0.32%*	*-0.24%*	*0.05%*
3	Basecase	785.77	633.14	480.51
	King & Potter Model Energy Cost	731.95	603.32	473.24
	King & Potter Model Energy Cost Savings.	*-6.85%*	*-4.71%*	*-1.51%*
	Simple Model Energy Cost	728.89	601.23	473.57
	Simple Model Energy Cost Savings	*-7.24%*	*-5.04%*	*-1.44%*
	Model Difference	*-0.39%*	*-0.33%*	*0.07%*
2.5	Basecase	836.44	673.8	511.16
	King & Potter Model Energy Cost	758.37	624.79	491.1
	King & Potter Model Energy Cost Savings.	*-9.33%*	*-7.27%*	*-3.92%*
	Simple Model Energy Cost	754.58	621.9	489.24
	Simple Model Energy Cost Savings	*-9.79%*	*-7.70%*	*-4.29%*
	Model Difference	*-0.45%*	*-0.43%*	*-0.36%*

From Table 11 it can be observed that the differences between the refined TES model and the simple constant-COP TES model less than 0.45%. It takes about 40 seconds for the refined TES model to finish a calculation and 1 second for constant-COP TES model. Considering that a search loop for demand limits is added on top of the energy cost optimization, if 100 searches are necessary, using the refined TES model it is going to take more than 1 hour while using the simple constant-COP model requires less than 2 minutes. The advantage of using the simple TES model is obvious.

2.8.5 Thermal History Variables in EnergyPlus for Building Load Calculation

Summary: A dynamic building energy analysis program such as EnergyPlus requires that historical data be stored to calculate current building thermal performance. Before starting any simulation of building thermal behavior, EnergyPlus uses a pre-simulation process called "warm-up period calculation" in order to estimate and store historical data at the beginning of the simulation period. At each time step during the simulation period, EnergyPlus continues to store historical data used to properly model the dynamic thermal performance of the building. The number of historical data depends on several factors including the construction material, the number of zones, and the type of HVAC system. In order to implement the moving time window closed-loop optimization procedure for passive and active TES systems, it is essential to identify the variables for which EnergyPlus stores thermal historical data. The identification of these variables helps reduce simulation time and thus makes optimization of passive and active TES systems feasible with EnergyPlus.

After giving an introduction on modeling of thermal history, this section provides a list of identified variables that affect building thermal history in EnergyPlus. Results of a verification analysis are also summarized.

2.8.5.1 Modeling of Thermal History

The building structure responds to changes in zone temperature setpoints. The zone temperature T_Z is directly affected only by the net convective heat flux according to the discrete-time energy balance on the zone air

$$C_Z \frac{\Delta T_Z}{\Delta t} = \sum_i \dot{Q}_{conv,i}, \tag{3}$$

where C_Z is the zone thermal capacitance. These convective heat fluxes include contributions from interior wall surfaces, HVAC systems, internal and solar gains, as well as infiltration. Of those, the current interior wall surfaces fluxes depend on a history of past inside and outside air and surface temperatures as well as inside and outside heat fluxes. The transient response of the building envelope is typically modeled by transforming the heat diffusion equation

$$\frac{\partial T_Z}{\partial t} = \alpha \frac{\partial^2 T_Z}{\partial x^2} \tag{4}$$

(where α is the thermal diffusivity) into a conduction transfer function (CTF), where the inside and outside surface heat fluxes are determined with the help of construction-specific CTF coefficients *a, b, c*, and *d*.

$$\begin{aligned} \dot{q}_{s,o} &= \sum_{k=0}^{n_a} a_k T_{s,o,t-k\Delta t} - \sum_{k=0}^{n_b} b_k T_{s,i,t-k\Delta t} - \sum_{k=1}^{n_d} d_k \dot{q}_{s,o,t-k\Delta t} \\ \dot{q}_{s,i} &= \sum_{k=0}^{n_b} b_k T_{s,o,t-k\Delta t} - \sum_{k=0}^{n_c} c_k T_{s,i,t-k\Delta t} - \sum_{k=1}^{n_d} d_k \dot{q}_{s,i,t-k\Delta t} \end{aligned} \tag{5}$$

The zone temperature setpoints can be varied between 15 and 30°C during unoccupied periods and between 20 and 24°C during occupied periods. Building precooling reduces the convective contributions from inside surfaces during occupied periods by depressing the average envelope temperature during unoccupied periods.

In reference to Eq. (5), the "thermal history" of a wall can be abbreviated by

$$\begin{aligned} K_{s,o} &= \sum_{k=1}^{n_a} a_k T_{s,o,t-k\Delta t} - \sum_{k=1}^{n_b} b_k T_{s,i,t-k\Delta t} - \sum_{k=1}^{n_d} d_k \dot{q}_{s,o,t-k\Delta t} \\ K_{s,i} &= \sum_{k=1}^{n_b} b_k T_{s,o,t-k\Delta t} - \sum_{k=1}^{n_c} c_k T_{s,i,t-k\Delta t} - \sum_{k=1}^{n_d} d_k \dot{q}_{s,i,t-k\Delta t} \end{aligned} \tag{6}$$

From the index $k \geq 1$, it is obvious that only and not current past information is used. For the outside surface temperature of an exterior wall, we can balance convective, radiative, and solar source terms

$$\dot{q}_{s,o} = \dot{q}_{s,c,o} + \dot{q}_{s,r,o} + S_{s,o} \tag{7}$$

and yield

$$a_0 T_{s,i} - b_0 T_{s,o} + K_{s,o} = \dot{q}_{s,c,o} + \dot{q}_{s,r,o} + S_{s,o} \tag{8}$$

Since the convective flux can be described by

$$\dot{q}_{s,c,o} = h_{s,c,o} \left(T_{amb} - T_{s,o} \right) \tag{9}$$

we yield the outside surface temperature

$$T_{s,o} = \frac{h_{s,c,o} T_{amb} + h_{s,r,o} T_{sky} + S_{s,o} - K_{s,o} + b_0 T_{s,i}}{h_{s,c,o} + h_{s,r,o} + a_0} \tag{10}$$

By similar arguments for the inside surface of the exterior wall,

$$b_0 T_{s,o} - c_0 T_{s,i} + K_{s,i} = \dot{q}_{s,c,i} + \dot{q}_{s,r,i} - S_{s,i} \tag{11}$$

After defining the convective flux

$$\dot{q}_{s,c,i} = h_{s,c,i}\left(T_{s,i} - T_Z\right) \tag{12}$$

we eliminate $T_{s,o}$ through the use of Eq. (10) and find an expression for the inside surface temperature

$$\begin{aligned} B_i T_{s,i} - h_{s,c,i} T_Z + \sum_{j=1}^{N} h_{s_j,r,i} T_{s_j,i} &= e\left[h_{s,c,o} T_{amb} + h_{s,r,o} T_{sky} + S_{s,o} - K_{s,o}\right] + S_{s,i} + K_{s,i} - \dot{q}_{s,r,i,0} \\ e &= \frac{b_0}{h_{s,c,o} + h_{s,r,o} + a_0} \\ B_i &= h_{s,c,i} + c_0 - b_0 e \end{aligned} \tag{13}$$

Similar approaches can be found for interior walls and windows. With the help of the auxiliary star temperature T_{star} a system of linear equations can be solved:

$$\begin{bmatrix} X_{11} & X_{12} \\ X_{21} & X_{22} \end{bmatrix} \begin{bmatrix} T_Z \\ T_{star} \end{bmatrix} = \begin{bmatrix} Z_1 \\ Z_2 \end{bmatrix} \tag{14}$$

and the zone temperature can be found.

2.8.5.2 Description of Thermal History Variables

Variables that affect thermal history in EnergyPlus are found in five modules namely: *DataHeatBalSurface, DataHeatBalFanSys, DataSurfaces, DataLoopNode,* and *ZoneTempPredictorCorrecto*r module. For each module, the variables are listed and identified below.

A. DataHeatBalSurface Module

THM:	Master temperature history of building construction with zone time step
TH:	Temperature history of building construction with system time step interpolated from THM
QHM:	Master heat flux history of building construction with zone time step
QH:	Heat flux history of building construction with system time step interpolated from QHM
TempSurfIn:	Inside surface temperature for each surface
TempSurfOut:	Outside surface temperature fore each surface

B. DataHeatBalFanSys

XMAT:	Temporary zone temperature to test convergence at current time
XM2T:	Temporary zone temperature to test convergence at one hour ago
XM3T:	Temporary zone temperature to test convergence at two hours ago
XM4T:	Temporary zone temperature to test convergence at three hours ago
ZoneAirHumRat:	Zone air humidity ratio
ZoneAirHumRatOld:	Zone air humidity ration at previous hour
ZT:	Zone air temperature
ZTAV:	Zone air temperature averaged over the system time increment
XZTAV:	Zone air temperature averaged over the system time increment at previous hour
MAT:	Mean air temperature

C. DataSurfaces

SurfaceWindow: Calculated window-related values

D. DataLoopNode

Node: Inlet and outlet condition of each system and plant component containing temperature, flow rate, m aximum allowed (design) flow rate, minimum allowed (design) flow rate, maximum available flow rate, and minimum available flow rate

E. ZoneTempPredictorCorrector

WZoneTimeMinus1:	Humidity ratio history terms for time minus 1 zone time steps
WZoneTimeMinus2:	Humidity ratio history terms for time minus 2 zone time steps

WZoneTimeMinus3:	Humidity ratio history terms for time minus 3 zone time steps
WZoneTimeMinus4:	Humidity ratio history terms for time minus 4 zone time steps
WZoneTimeMinus1Temp:	Temporary zone air humidity ratio at previous time step
WZoneTimeMinus2Temp:	Temporary zone air humidity ratio at time step minus 2
WZoneTimeMinus3Temp:	Temporary zone air humidity ratio at time step minus 3

2.8.5.3 Validation of Thermal History Variables

In this subsection, the results of a validation analysis are summarized. The main objective of this verification analysis is to ensure that thermal history is adequately defined by the variables identified in the previous subsection.

Using a simple three-zone building model, a simulation over a six-month period (January 1st to July 31st) is performed first. During the simulation, the thermal history of the building is stored for January 16 at 7 a.m. (through the variables listed above). Then and immediately after completing the six-month simulation, a second simulation of two days (January 16 and 17) is carried out without a warm-up period (thus, the historical data for the building at the start of the second simulation are based on July 31st results) but with historical data (stored from the first simulation) used starting January 16th at 7 a.m.

Figures 24 through 26 show the hourly variation of respectively, the room air temperature, the heating load, and the cooling load for the 3-zone building model during January 16th. The results obtained from the two simulation runs are presented in Figures 24-26:

- First simulation run: January 1st through July 31st,
- Second simulation run: January 16th through January 17th without the warm-up period but u tilizing the thermal history of January 16th at 7 a.m. obtained from the first simulation run.

At the end of first simulation run, the values of the variables that store building thermal history are calculated based on data obtained at midnight of July 31st (i.e., summer conditions). Therefore, the building behavior is greatly affected by a summer-type thermal history at the start of the second simulation run which is initiated without a warm-up process. This behavior is clearly illustrated in Figures 24-26 for hours between 1 a.m. through 6 a.m. But after 7 a.m., the building thermal behavior obtained by the two simulation runs coincides perfectly. Indeed, the two simulation runs utilize the same thermal history starting from 7 a.m. Consequently, the variables defined in above fully describe the thermal history of the building.

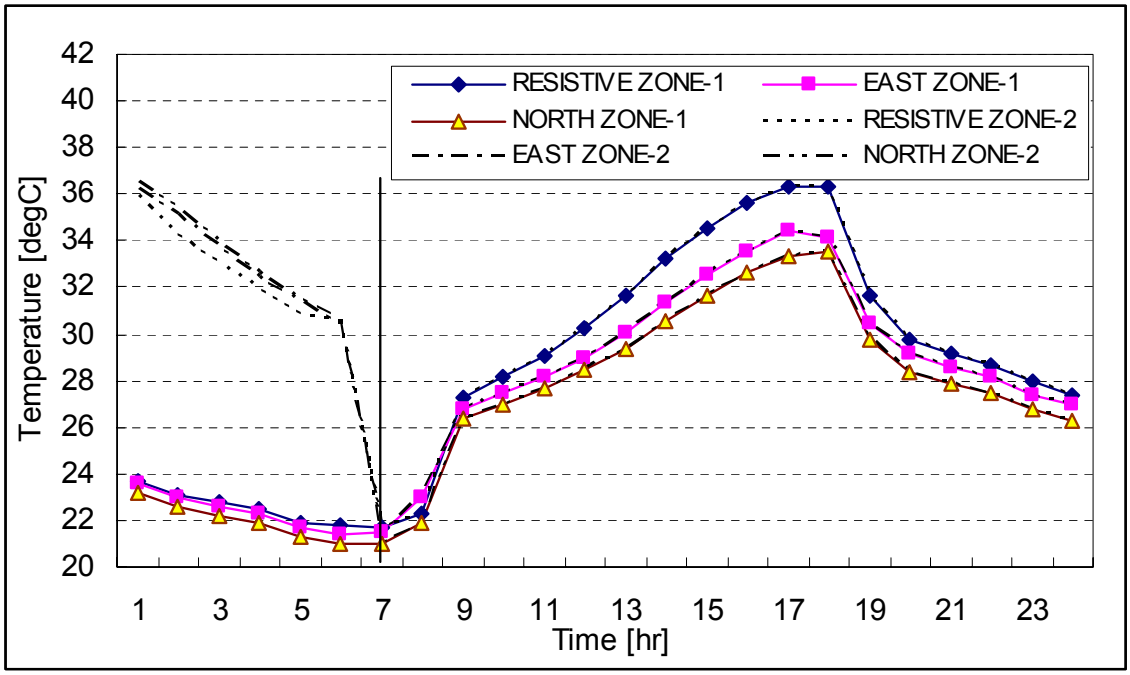

Figure 24: Room air temperature in each of the three zones during January 16th.

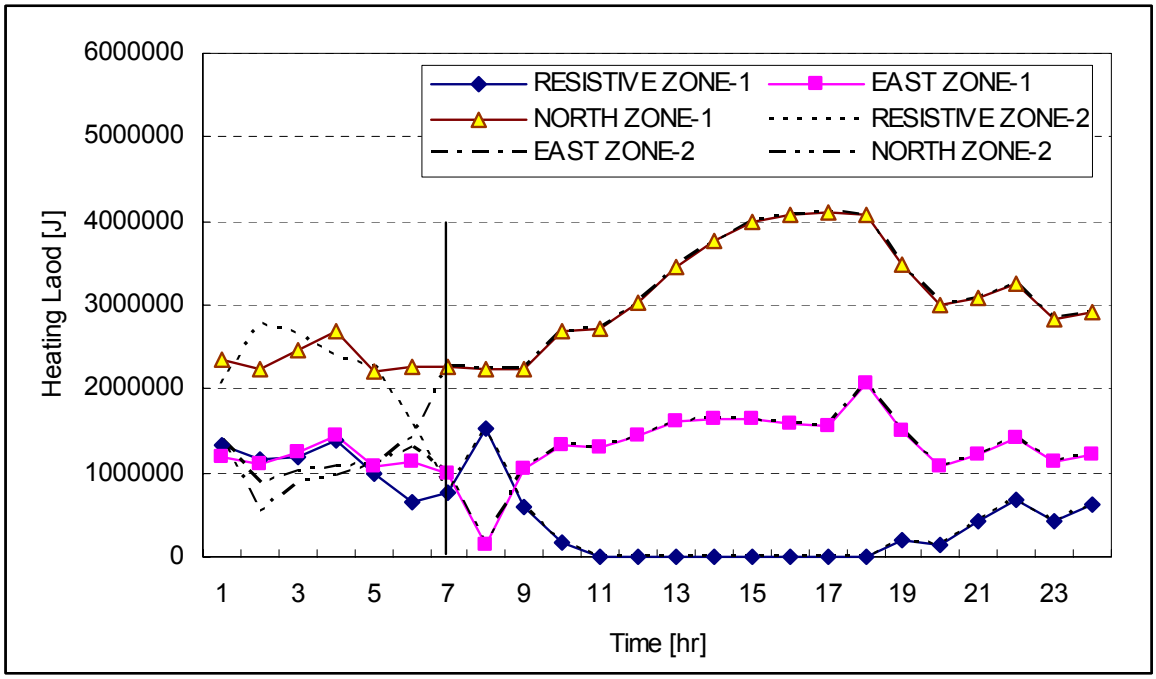

Figure 25: Total heating load for the three-zone building during January 16th.

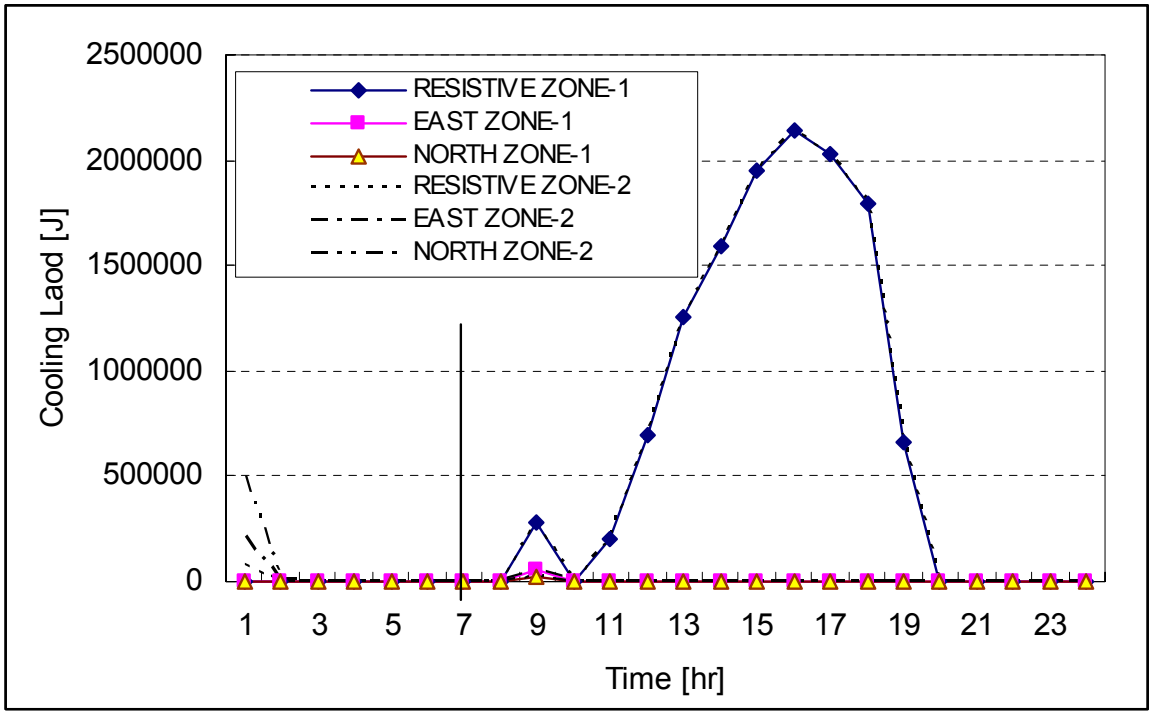

Figure 26: Total cooling load for the three-zone building during January 16th.

2.8.6 Integration of Predictive Optimal Control into EnergyPlus

2.8.6.1 Background and Purpose

In order to study predictive optimal control of building thermal storage inventories (active and passive storage), a building simulation program is necessary to simulate building heating, cooling, ventilation and other energy flows. EnergyPlus as the most advanced building energy simulation program was selected as the basis in this study.

Like other simulation programs, EnergyPlus simulates building energy flows based on an input file in which descriptions of building construction, HVAC equipment, system, plant and their controls are provided. EnergyPlus source code contains models of different HVAC equipment, systems and plants as well as algorithms calculating building heating/cooling load based on building construction and occupancy schedules, system/plant types and controls. Therefore, given the input file, EnergyPlus can simulate the corresponding building, HVAC equipment, system and plant energy flows.

EnergyPlus can carry out normal simulations where the input file must provide fixed HVAC system/plant control information. It is however not able to conduct optimization simulations where optimization algorithms can be used to find an optimal control strategy which is unknown by the input file provider. Therefore, given EnergyPlus as the simulation tool, it had to be modified to be able to do predictive optimization simulations to serve the purposes of our project.

2.8.6.2 Introduction of Optimization Subroutines and Their Application

There are many optimization routines available as encapsulated subroutines that can be used as "black-box" optimizers. All that users of these optimization routines need to do is to provide the required input data related to the control variable(s) that need to be optimized. Then, the encapsulated subroutines return optimized control variable(s). Although the algorithms that these optimization "black-boxes" use to find the optimal value may vary, what needs to be provided by users is similar. These inputs usually include control variable(s) and their bounds/constrains, some kinds of step sizes, and tolerances, etc. Due to this similarity of optimization routines on inputs and outputs, the optimization routine using the Nelder-Mead simplex method (BCPOL) in IMSL library is taken as the sample optimization routine to illustrate the integration method in this document.

The BCPOL routine requires 8 inputs and provides 2 outputs. It has the form of the following.

```
CALL DBCPOL(FCN, NumVariables, Guess, IBTYPE,  &
    LowerLimit, UpperLimit, Tolerance, MaxRunningNum, &
                                OptimumX, OptimumValue)
```

2.8.6.3 Introduction to EnergyPlus

It is necessary to understand how *Normal-EnergyPlus* (The released EnergyPlus without an optimization function is referred as *Normal-EnergyPlus* in this document.) simulates the controls of HVAC zones, systems and plants as well as how Normal-EnergyPlus is constructed in order to integrate optimization routines into *Normal-EnergyPlus* and thus turn *Normal-EnergyPlus* into *Optimization-EnergyPlus* (referring to Normal-EnergyPlus after being integrated with optimization functions)

How does EnergyPlus Run?

When EnergyPlus starts to run, the input file is first processed by calling *ProcessInput* subroutine where the input file is checked and read and values are stored in global arrays that can be accessed easily by subroutines that are designed to retrieve data from them. Then follows the core line of the program block of EnergyPlus, i.e., calling *ManageSimulation* subroutine in *SimulationManager*. Here, an initialization is first carried out and then 'loop-in-loop' simulation is started and finished.

After the initialization, EnergyPlus calculates from outside to inside the *environment loop*, *day loop*, *hour loop*, and *timestep loop*. The term "environment" in EnergyPlus can be simply understood as a thermal history concatenated running period. For example, if in the input file, running period is July 20 to Nov 20,

there is one environment. If in the input file, one running period is July 20 to Aug 30 and another running period is from September 1st to December 5th, there are two environments. By calling *GetNextEnvironment* subroutine in *WeatherManager* file, environment loop counts the environments needed to be simulated and initializes the next available environment to be simulated by the *day loop*. Each environment contains one or more days. These days are simulated one by one in the *day loop*. In each day, 24 hours are simulated from 1 to 24 in *hour loop*. In each hour, a *timestep loop* of up to six timesteps is allowed. The core calculation of EnergyPlus is performed each timestep. In each timestep, routines inside EnergyPlus read building, system and plant schedules, as well as other input information of that timestep, then calculate building heat transfer, zone load, system load, plant load and eventually energy consumption of that timestep, then report outputs if requested. This core calculation is repeated until the last timestep of the last hour of the last day of the last environment is completed.

In *Normal-EnergyPlus*, these control schedules must be provided as fixed values and will not be changed by EnergyPlus. In *Optimization-EnergyPlus*, these schedule values should be able to be changed by the optimization "routine, then fed back to EnergyPlus calculations to produce the cost function values for each optimization iteration.

How does EnergyPlus simulate controls?

EnergyPlus simulates the control of HVAC zones, systems and plants through schedules. In the input file, schedules of control variables need to be provided. Each schedule is made of sub-schedules, i.e. schedules are made of *week schedules*, *week schedules* are made of *day schedules*, and *day schedules* contain 24 hourly values. For simulations with timesteps less than one hour, the schedule values are interpolated between hours. At the start of the first timestep of the first hour of the first day of the first environment, subroutine *ProcessScheduleInput* is called. This subroutine collects all the schedules in the input file and stores them in a global array, i.e., *Schedule*. Then, at each timestep simulation, whenever a schedule value of that time step is needed, subroutine *GetCurrentScheduleValue* is called. Inputting a schedule index that relates to the sequence number of that schedule stored in the *Schedule* array, the schedule value of that timestep can be returned. Knowing the name of the schedule, the schedule index number of a schedule can be retrieved by calling subroutine *GetScheduleIndex* that takes the schedule name as an input and returns the schedule index in the *Schedule* array where all the schedules are stored. The existences of these schedule handling subroutines make it very convenient to get any schedule value at that timestep just by knowing the name of the schedule.

An Example of EnergyPlus Inputs and Outputs

In the following example, a 3-story, 15-zone office building is simulated on July 20, Phoenix, AZ. The following figure shows the simulated zone air temperature and plant chiller power consumption under conventional nighttime setback control.

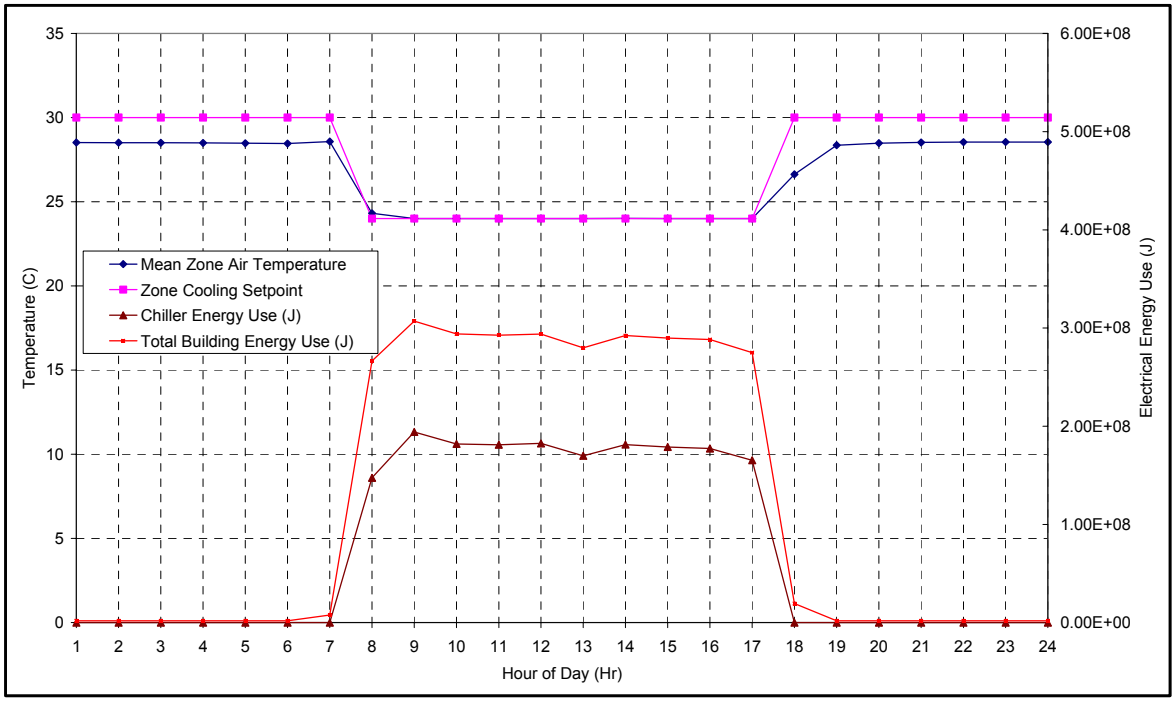

Figure 27: Simulation of a night setback control of an office building using EnergyPlus

From Figure 27 it can be observed that, in nighttime setback control, the zone air temperature floats during the night unless it goes higher than the cooling setpoint, i.e. 30°C. During occupied time, the cooling setpoint is 24°C. The total chiller power consumption is 489 kWh with a peak at 9:00 of 53.9 kW; the building total electrical consumption is 813 kWh with a peak at 9:00 of 85.3 kW. If the electrical rate is 0.20 $/kWh and 10$/kW from 9:00-18:00 (On-Peak period) and 0.05 $/kWh and 0 $/kW during the rest of the day (Off-Peak period), the owner of the building is paying $178.8 in total for electricity.

2.8.6.4 Integration of a Standard Optimization Subroutine into EnergyPlus

Integrating optimization subroutines into EnergyPlus starts by modifying the construction of Energy-Plus, after understanding how EnergyPlus is constructed and how the zones, systems and plants are controlled by schedules.

The *ManageSimulation* subroutine

The integration of optimization function(s) starts by modifying the *ManageSimulation* subroutine. First, the initialization part needs to be separated from repeated calculations. The initialization part ends at line *BeginFullSimFlag = .True.*, which means initialization is done and the full simulation begins. The code following this line in the *ManageSimulation* subroutine is moved into a separate subroutine *EnvironSimulation* where the *environment loop* simulation starts. Also, in order to keep the flexibility of choosing between *Normal-EnergyPlus* and *Optimization-EnergyPlus*, a new field choosing between optimization or no optimization is added into the *Run Control* section in the input file. The *Run Control* section as well as the *TimeStep In Hour* section in the input file are read by calling *GetProjectData* in the initialization part, since the information contained in these sections guides the simulation.

If the input value of the do-optimization-or-not field of the Run control section is 'YES', then the newly created global flag *DoOptmization* is set to 'true', otherwise, it is set to 'false'. Then, in *ManageSimulation* subroutine, instead of starting an environment simulation directly by calling *EnvironSimulation*, the simulation is branched into two newly added subroutines, i.e. *ManageNormalEnergyPlus* and *ManageStdOptimEnergyPlus*, by the value of *DoOptimization*. If *DoOptimization* is 'false', *ManageNormalEnergyPlus* is called, where EnvironSimulation is called directly. Otherwise, *ManageStdOptimEnergyPlus* is called, where another initialization subroutine for optimization purpose, i.e. *ProcessOptimizationInput*, is first called to prepare the inputs needed by the optimization subroutine (BCPOL), then the BCPOL subroutine

is called and EnergyPlus with optimization is run here. In the latter case, the *EnvironSimulation* subroutine serves as the cost function calculator. In the BCPOL 'black-box', more than one iteration are run until the optimal values of control variables are found. In each iteration, BCPOL modifies the value of control variables and calculates and compares the cost of that set of values by calling *EnvironSimulation* subroutine (indirectly). After BCPOL returns the optimal control variable values, *EnvironSimulation* subroutine is called one more time and the outputs are reported.

Handling of inputs for optimization subroutine

The BCPOL routine requires eight inputs and provides two outputs. It has the following format:

```
CALL DBCPOL(FCN, NumVariables, Guess, IBTYPE,  &
    LowerLimit, UpperLimit, Tolerance, MaxRunningNum, &
    OptimumX, OptimumValue)
```

These inputs are prepared by calling *ProcessOptimizationInput* subroutine in *ScheduleManager* file. In order for the BCPOL to know which control variables need to be optimized, new sections named *Optimization:Schedule* are created in the input file, which has the format showed below.

```
OPTIMIZATION:SCHEDULE,
    A1, \field OptimizationScheduleName
    \Required-field
    \Type alpha
    A2, \field Guess Schedule
    \Required-field
    \Type object-list
    \Object-list ScheduleNames
    A3, \field Lower Limit Schedule
    \Required-field
    \Type object-list
    \Object-list ScheduleNames
    A4;     \field Upper Limit Schedule
    \Required-field
    \Type object-list
    \Object-list ScheduleNames
```

Each control variable that needs to be optimized must have a corresponding *Optimization:Schedule* section in the input file. A2, A3, A4 are schedules provided in input file. A2 is the name of the schedule providing the initial values of the control variable. A3 and A4 are the names of the schedules providing the lower bounds and upper bounds of the control variable, respectively. A1 is the name of the controlled variable schedule, which needs to be used in every corresponding place in the system/plant part of the input file. The construction of this section corresponds to the *OptimizationScheduleData* data type defined in a newly added global data file *DataOptimization*. In the newly added *ProcessOptimizationInput* subroutine, the schedule indices of these schedules in the *Optimization:Schedule* sections are stored in array *OptimizationSchedule* that is defined in a *OptimizationScheduleData* data type. Since EnergyPlus already has routines that can retrieve the schedule value by the schedule index, it is straightforward to get each value of each schedule of the *OptimizationSchedule* array.

Thus, as explained above, once the schedule names of the control variables are read into *Optimization-Schedule*, it is easy to get their values and store them into arrays that serve as inputs for optimization routines by using subroutines like *GetScheduleIndex* and *GetCurrentScheduleValue*. Therefore, in the *ProcessOptimizationInput* subroutine, the *Guess, LowerLimit, UpperLimit, OptimumX* arrays are allocated according to the number of control variables that need to be optimized. And the schedule values of these control variables are also stored in *Guess, LowerLimit*, and *UpperLimit* sequentially.

Other inputs of BCPOL, i.e., *NumOfVariables, Tolerance, IBTYPE, MaxRunningNum* are also assigned values in calling *ProcessOptimizationInput*. Now, all that the BCPOL routine needs is a subroutine that calculates cost functions, i.e., *FCN*. Therefore, a new external subroutine FCN is added located in the *SimulationManagerFile*. It has the following format.

SUBROUTINE FCN (N, X, F)

The optimization subroutine manipulates the *Guess* array values and feeds those into the dummy variable *X* of *FCN* and then get the cost function value returned by *FCN*. The core line of subroutine *FCN* is calling *EnvironSimulation*. The newly added economic module allows for the costs of energy, i.e. electrical energy cost, electrical demand cost and total electrical cost, being calculated for each calling of *EnvironSimulation*. Thus, after calling *EnvironSimulation* in *FCN*, one of these costs is selected as the cost function value to be returned to the optimizer and serves for the evaluation of optimality. The following section is added to keep the flexibility of allowing to choose from using energy cost, demand cost or total cost to be returned as cost function value in FCN.

OPTIMIZATION:COST,
\Memo Optimization Cost 1: Energy (Energy based Optimization)
\Memo Optimization Cost 2: Demand (Demand based Optimization)
\Memo Optimization Cost 3: Both (Energy and Demand based Optimization)
N1; \field Optimization Cost
\Type choice
\Key 1
\Key 2
\Key 3

This section is processed in *ProcessOptimizationInput* and the value is stored in variable *OptimizationCost* that is defined in *DataOptimization*. Then, *GetCurrentScheduleValue* subroutine in *ScheduleManager* file is modified. As explained before, the function of this subroutine is to retrieve the schedule value of the inputted schedule index at this timestep. In *Normal-Energyplus*, this subroutine traces the values stored in the *Schedule* array that stores all the schedule values in the input file. In *Optimization-EnergyPlus*, if the schedule is not the optimization schedule, its value is traced in the *Schedule* array. Otherwise, its value is traced in the *XguessSort* array that is just another form of Guess array and its values are changed by the optimization routine in each optimization iteration.

The optimization routine returns the optimal values of control variables in array *OptimX* that is defined in *DataOptimization*. Then, *EnvironSimulation* is called one more time with *XGuess* equals *OptimX* to get the final optimal outputs and report them.

Output control

There are modifications related to output reporting. Unlike *Normal-EnergyPlus* where there is only one iteration for each environment simulation, *Optimization-EnergyPlus* requires more than one iteration to find the optimal value. Without changing the report handling, outputs for each iteration are reported. If these intermediate outputs are not wanted, modifications related to output reporting are needed. In *DataOptimization*, a variable *EndOptimizationFlag* is defined. This variable is set to false until the optimization is done. Only before the final simulation run, *EndOptimizationFlag* is set to "true". The outputs reporting of *Normal-EnergyPlus* is controlled by *DoOutputReporting* variable solely. In *Optimization-EnergyPlus*, all that needs to be modified is that instead of being solely controlled by *DoOutputReporting*, the reporting has to be controlled by the *EndOptimizationFlag*, too.

Handling Thermal History

Up to now, *Normal-EnergyPlus* has been modified so that the value of control variables can be modified by the optimizer while the *EnvironSimulation* subroutine is separated to be used by the optimizer as the cost function calculator. In order for the optimizer to call *EnvironSimulation* in each iteration for many iterations, other modifications related to the handling of environments and thermal history are necessary.

First, *EnvironSimulation* uses *GetNextEnvironment* subroutine to judge if there is another environment available for simulation and initialize the new available environment if there is any. The total numbers of environments are counted from the input file at the initialization stage of EnergyPlus, i.e., before calling *EnvironSimulation*. There is an internal counter that stores the number of *GetNextEnvironment* being called. It increases by one each time this subroutine is called. When the counter counts the same number as the total number of environments, in its next call, it will return the next environment as 'unavailable' to the *EnvironSimulation* subroutine. Then the *EnvironSimulation* subroutine exits. In order for the optimizer to call *EnvironSimulation* as many times as needed, this environment counter in *GetNextEnvironment* subroutine is reset to zero in each iteration after *EnvironSimulation* exits.

Second, when calling *EnvironSimulation*, before starting to simulate this environment, EnergyPlus runs a "warming-up" period to initialize the thermal history of the building construction, HVAC system/plant. This warming-up period is realized by starting from an arbitrary set of values of thermal history related variables. Then, by repeatedly running the first day of that environment until these thermal history related variables converge, the warming up period is finished and the thermal history at the start of the first timestep of the first hour of the first day of that environment is found. Then, based on this starting thermal history, the actual "simulation" begins.

Without modifying the warming-up period input, the warming-up period always uses the same input as the first day of that environment. In our optimization scenario, this is incorrect. Since the optimizer is trying different control variables of that environment in each iteration, the warming-up period of that iteration is changed according to the control variable values at that iteration. This again is incorrect. The real thermal history at the start of that environment should not be changed by the later operation of the system/plant and should be a sole result of the operations that has already happened. Thus, the warming-up period should be separated from the real simulation. In the warming-up period, instead of using the "first day" inputs of that environment as inputs, the operation of "yesterday" should be the inputs of the warming-up period. After the warming-up period is done, the thermal history at the start of the first timestep of the first hour of the first day of the environment should be recorded and should be locked in. The calculation of cost function values in each iteration of the optimizer should be based on this same starting thermal history.

To be able to record thermal history at the end of the warming-up period and upload the thermal history at the start of the real simulation, variables that store building, system, and plant thermal histories need to be found and subroutines that record and update thermal history value are needed. Since in the released EnergyPlus document, there is no content explaining which variables store thermal history, the identifcation of these thermal history related variables was carried out by trial-and-error. The file *ThermalHistoryManager* is added to EnergyPlus, which includes public subroutines that record and update thermal histories, i.e. *RecHistoryValues* and *UpdateHistoryValues*.

Then, since in EnergyPlus, there is already a logical variable, i.e. *WarmUpFlag* marking the starting and ending of the warming-up period, it is easy to record thermal history after the warming-up period is finished and upload recorded thermal history at the start of the first timestep. Lines of code for recording and updating thermal histories are added in the timestep loop of EnvrionSimulation.

Handling Environment

Next, subroutines related to initializing new environments need to be modified so that during the warming-up period, the warming-up is based on yesterday's data, i.e., building schedule, weather data, etc. This is done by modifying subroutines in *WeatherManager*. Unlike other inputs to EnergyPlus, the weather data is read day by day instead of timestep by timestep. Before the beginning of each day, the weather data is read into a global variable *Tomorrow* by calling *ReadWeatherForDay* subroutine. At the beginning of that day, global variable *Today* is updated by *Tomorrow* by calling *UpdateWeatherForDay* subroutine. This process is done in the *InitializeWeather* subroutine in *WeatherManager*. Both *Today* and *Tomorrow* are of weather data type which stores weather data like outside dry bulb/dew point temperatures, pressure, solar radiation, wind speed/direction, illumination data, etc. In *Normal-EnergyPlus*, the warming-up period reads the weather information of the first day of the environment. Here, this is changed to reading weather information of one day before the first day of the environment. Also, the date is changed to one day before the first day so that the building schedules are yesterday's.

With these modifications, *Normal-EnergyPlus* has become *Optimization-EnergyPlus*, which has the flexibility of choosing between normal EnergyPlus simulations and optimization EnergyPlus simulations and choosing among using energy cost, demand cost and total cost as the optimization objective function.

An Example of Optimization Control

Figure 28 shows results of optimal control on zone temperature setpoints for the example 15-zone office building. Zone cooling setpoints, average zone air temperatures and the chiller power consumption is provided.

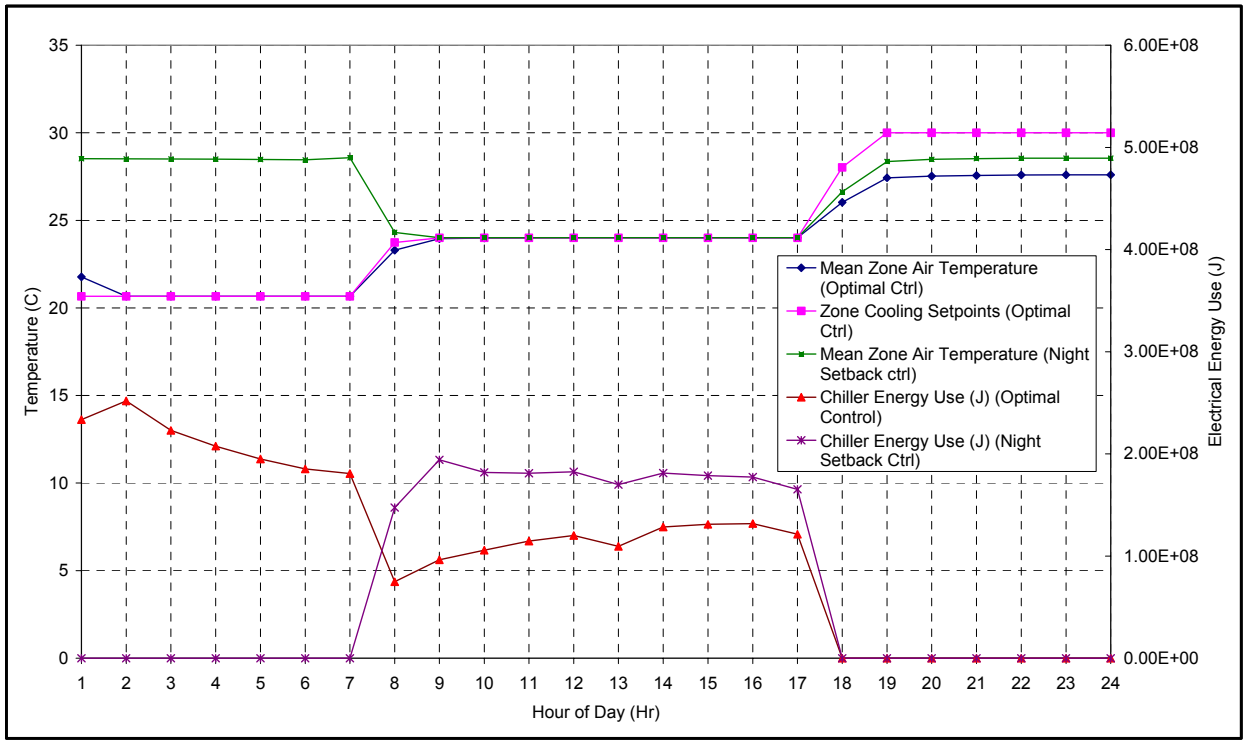

Figure 28: Optimal control of passive thermal storage inventory of a 15-zone office building using EnergyPlus

From Figure 28, it can be observed that instead of setting up temperature during the night, it decides to precool the building. During the day, the release of cooling energy stored in building envelope helps to bring down the chiller electrical demand. Under this optimal control, the total chiller power consumption is 725.3 kWh with a peak of 2:00 at 70 kW. The building total electrical consumption is 1234.7 kWh with a peak of 2:00 at 105 kW. Under the same utility rate structure mentioned before, the total electrical bill is $146.2 with a savings of 18%.

2.8.6.5 Integration of Closed-Loop Optimization (Moving Window) into EnergyPlus

EnergyPlus has been modified to allow for the optimization of control variables. In real operation, optimization has to be carried out based on predicted weather conditions because the true weather conditions are not known until they have occurred. Therefore, the accuracy of optimal control is affected by the accuracy of weather prediction.

There are many forecasting methods available. Usually, the error increases as the time horizon from "now" increases. For example, it is likely that the weather prediction made five hours ahead at the start of the day may be a lot less accurate than the weather prediction made one hour ahead. Predictive optimal control technique, i.e., certainty-equivalent closed-loop optimization, as illustrated in Figure 18 aims at minimizing the impact of inaccuracy of optimization of control variables caused by the inaccuracy of weather prediction.

Here, two new terms are introduced, the optimization window length *WL* and moving length *ML*. The term window length refers to the time horizon for weather prediction. The term moving length refers to the frequency of updating weather prediction. Given *WL* = 24 hours and *ML* = 2 hours, the moving window optimization operates as follows:

Before the first hour of the day on which optimal operation commences, weather is predicted once for the time horizon *WL*. Optimization of control variables over the time of *WL* is conducted based on this prediction. The time consumed by doing optimization is called time cost of optimization *TCO*. Then, starting from hour one of the day, the plant is operated according the optimal control given by the first optimization run for *ML* = 2 hours. Towards the end of the second hour, the true weather for nearly the first two hours of the day has already been obtained. The second weather prediction is now carried out over the next *WL* hours, i.e. from hour three of today to hour 2 of tomorrow. The second optimization is then carried out and finished by the end of hour 2. The control of the plant from hour three is modified according to the second optimization for the next 2 hours. This process is repeated indefinitely.

Adapting Moving Window Optimization Concept into EnergyPlus

Theoretically speaking, *WL* and *ML* can be chosen arbitrarily as long as *WL* is not less than *ML*. However, given the structure of EnergyPlus, the moving length cannot be adapted with such flexibility.

EnergyPlus simulation can be called a "one day" simulation, meaning not only the simulation must be at least 24 hours or an integer multiple of 24 hours, but also it has to start from hour one of the day and end at hour twenty four of the day, i.e. the simulation cannot start from hour 3 of the day and end at hour 2 of the next day which is also a 24 hour span. Therefore, the example above, which has a *ML* = 2 hours and the optimization of the second move requires simulation as well as optimization starting at hour 3 of today and ending at hour 2 of tomorrow, is impossible for the current EnergyPlus to carry out. The moving window concept has to be adapted indirectly into EnergyPlus by a two-day-simulation approach.

Using the two-day-simulation technique, each day of the running period is a group sequence of two days. For example, a runtime period of July 20 to July 25 is finished in 6 runs, i.e. 7/20-7/21, 7/21-7/22, 7/22-7/23, 7/23-7/24, 7/24-7/25, and 7/25-7/26. Given 24 hour is the fixed *WL*, those moves that do not start from hour one of the day, can be carried out by picking the corresponding time span in the two-day-simulation instead of "run" the time span directly. For example, if a runtime period of July 20 to July 21 is required and if *ML* = 6 hours, the closed-loop optimization is going to be carried out in eight two-day runs as follows:

Move #1: Running 7/20-7/21, optimizing hours 1-24, collecting hours 1-6.

- Predicting weather of hour 1-24 of 7/20 (Weather prediction of 7/21 is necessary for the run but will not affect the results).
- Optimization based on minimizing total cost of hour 1 of 7/20 to hour 24 of 7/20, collecting optimal control from hour 1 to 6.
- Starting from hour 1 of 7/20, operating the plant according to the optimal control output of the optimization until hour 6.
- At the end of hour 6, updating weather of hours 1-6 of 7/20 with true weather in EnergyPlus.
- At the end of hour 6, recording the true thermal history at the end of hour 6 by running EnergyPlus one more time while the weather of first 6 hours being updated with true weather.

Move #2: Running 7/20-7/21, optimizing hour 7-30, collecting hours 7-12.

- Predicting weather from hour 7 of 7/20 to hour 6 of 7/21.
- Optimization based on minimizing total cost of hour 7 of 7/20 to hour 6 of 7/21. In this optimization runs, the simulation of hour 7 of 7/20 is started based on uploading the recorded true thermal history at the end of hour 6. Collecting optimal control from hour 7 to 12.
- Then starting at 7:00 of 7/20, operating the plant according to the optimal control output of the optimization for hours 7 to 12.
- At the end of hour 12, updating weather of hours 7-12 with true weather in EnergyPlus.
- At the end of hour 12, recording the true thermal history at the end of hour 12 by running EnergyPlus one more time while the weather of the second 6 hours being updated with true weather.

Move #3: Running 7/20-7/21, optimizing hour 13-36, collecting hour 13-18.

- Predicting weather form hour 12 of 7/20 to hour 12 of 7/21.
- Optimization based on minimizing total cost of hour 13-36. In every run of this optimization, the simulation of hour 13 starts from uploading the thermal history recorded at the end of hour 12. Collecting optimal control from hour 13 to 18.
- Then starting at 13:00 of 7/20, operating the plant according to the optimal control collected.
- At the end of hour 18, updating weather of hours 13-18 with true weather in EnergyPlus.
- At the end of hour 18, recording the true thermal history by running EnergyPlus one more time with the weather of the third 6 hours being updated with true weather.

Move #4: Running 7/20-7/21, optimizing hour 19-42, collecting hour 19~24.

- Predicting weather form hour 19 of 7/20 to hour 18 of 7/21.
- Optimization based on minimizing total cost of hour 19-42. In every run of this optimization, the simulation of hour 13 starts from uploading the thermal history recorded at the end of hour 12. Collecting optimal control from hour 19 to 24.
- Then starting at 19:00 of 7/20, operating the plant according to the optimal control collected.
- At the end of hour 24, updating weather of hour 19-24 with true weather in EnergyPlus.
- At the end of hour 24, recording the true thermal history at the end of hour 24 by running Energy-Plus one more time while the weather of the fourth 6 hours being updated with true weather.

Move #5 to Move #8: Similar to Move #1 to Move#4, with run period 7/21-7/22.

From the above example, it can be observed that for each move a two-day simulation is carried out. The second day is just to help gather data of that move. During each move, the process of weather prediction, optimization with uploading of thermal history when necessary, operating, updating weather, and recording thermal history is repeated. The next section describes in detail how this adaptation is realized in the source code.

Realizing the Moving Window Optimization Concept in EnergyPlus

The variables DoSTDOptim and DoMoveWinOptim

In order to keep the flexibility of choosing between standard optimization (without weather prediction) and optimization, two new flags are added in *DataOptimization*: *DoSTDOptim* and *DoMoveWinOptim*. In the input file, a new section, i.e. *OPTIMIZATION:STYLE*, is created. The form of this section is as follows:

```
OPTIMIZATION: STYLE,
                \memo 1: Standard Optimization
                \memo 2: Moving Window Optimization
    N1;         \field Optimization Style
                \type choice
                \key 1
                \key 2
```

This section allows the user to choose between standard optimization (key value = 1) and moving window closed-loop optimization (key value = 2). This section is processed after processing the *RunControl* section in *GetProjectData* subroutine. As stated above, the *GetProjectData* subroutine reads information in "Run Control" and "Time Step in Hour" sections of the input file, then assigns 'true' or 'false' to the flag *DoOptimization*. If *DoOptimization* is 'true'; lines are added to handle *Optimization:Style* section in input file. If the key value is 1, *DoSTDOptim* is assigned 'true' and *DoMoveWinOptim* is assigned 'false'. If the key value is 2, *DoSTDOptim* is assigned 'false' and *DoMoveWinOptim* is assigned 'true'.

The variable MoveLength

Another modification of the input file is to add a *MoveLength* section as follows

MoveLength,
\Memo For Moving Window Optimization, it is MoveLengh of shifting.
\Memo Window Size is always 24-hour period.
\Memo It should be 1 <= MoveLength <=24 from choice.
N1; \field Move Length
\Type choice
\Key 1
\Key 2
\Key 3
\Key 4
\Key 6
\Key 8
\Key 12
\Key 24

Since the *WL* is fixed at 24 hours, the ML can only be numbers listed in the key value list. This section of input file is processed in calling *ProcessOptimizationInput*, which needs to be called before starting the optimization.

The variable WholeRunPeriod

An additional variable *WholeRunPeriod* is incorporated into EnergyPlus in *DataOptimization*. The value of this variable is assigned the first time when collecting environment information, i.e., during the first call of *GetNextEnvironment*. *GetNextEnvrironment* is called before starting the simulation of each environment. In the first call of *GetNextEnvironment*, the environment information is read and the variable *Environment* is assigned values when calling *GetUserWeatherInput*. The variable *Environment* stores information such as the start and end date of each environment. Here, lines are added in *GetUserWeatherInput* that calls a newly added subroutine *CalcMoveOptimRunPeriod*. In this subroutine, the value of *RunPeriod* when conducting moving window optimization is calculated. As shown in the example above, when conducting moving window optimization for July 20-July 21 with *ML* = 6, the number of runtime periods is eight instead of one for the case of standard (consecutive time block) optimization or the normal EnergyPlus scenario. For EnergyPlus, this change increases the number of environments so that EnergyPlus will not exit after finishing the first move but continues with the next move which may or may not have the same run period. In this newly added *CalcMoveOptimRunPeriod* subroutine, the number of total environments for the moving window optimization is calculated according the two-day simulation rule and the value of *ML*. The *WholeRunPeriod* variable is initialized and assigned values here. The purpose of the *WholeRunPeriod* is to store the environment information for all of the moves. Then, instead of reading information for variable *Environment* from the input file, the variable reads information from this *WholeRunPeriod* variable.

The subroutine GetNextEnvironment

Another important change is to add lines of code to count the number of environments correctly under different scenarios. Source code is added to assign correct values to the environment integer counter variable *Envrn* and the logical variable *Available* so that when running normal EnergyPlus or standard EnergyPlus, the *Envrn* increases by one at each calling of *GetNextEnvironment* and *Available* is 'True' when *Envrn* is less or equal to the total number of *Environment*. When carrying out moving window optimization, *Envrn* increases by one at the start of each new move and keeps the same value within that move, and *Available* is 'true' when *Envrn* is less or equal to the total number of environment. Also, these added lines have to separate the optimization runs from the "last run" that is used to record thermal history after each move.

The subroutine ManageMoveWinOptimEnergyPlus

In *SimulationManager*, a new branch is added in the branch *DoOptimization* equals 'True'. If *DoSTDOptim* is 'true', the program branches into calling *ManageSTDOptimEnergyPlus* that is *ManageOptimization*. If *DoMoveWinOptim* is 'true, the program branches into calling the newly added subroutine *ManageMoveWinOptimEnergyPlus*. All this subroutine does is to put the content of *ManageSTDOptimEnergyPlus* into loops of moves. Therefore, instead of exiting after finishing one optimization, it starts another optimization for the next move until all the moves are finished.

In the closed-loop optimization, before the optimization of a move starts, weather data for the next 24 hours is first predicted. After the optimization is done for that move, there is a "last run" at the end of each move after the optimization, where the weather file is updated with true weather data up to the end of the collection hour of that move and the thermal history at the end of the collecting hour of that move is recorded for use in the next move. By controlling the value of the newly added logical variable, i.e., *BeginEachRunMoveWinOptimFlag*, in *DataOptimization* at each move, the correct environment to be used in that move can be controlled in conjunction with *BeginEachRunMoveWinOptimFlag*.

The subroutine EnvironSimulation

In the *EnvironSimulation* subroutine, flags that mark the environment information are added before each environment simulation. Whenever *BeginEnvrnFlag* is set to 'true', the thermal history has to be cleared and a warming-up period is necessary to get the thermal history at the beginning of that environment. For closed-loop optimization, this flag has to be controlled so that the thermal history recorded from the previous move can be used in the consecutive move. This is done by modifying the initializing of these control flags at the beginning of each environment and before the start of day-loop in the *EnvironSimulation*.

Lines that record thermal history at the end of the collecting hour and update thermal history at the start of the collecting hour of each move is added inside the hour loop. Since the environment information like the collecting hours of each move has already been stored in the *WholeRunPeriod*, it is straightforward to control the thermal history recording and updating.

With these changes, the major program structure that enables moving window optimization is complete.

An Example of Predictive Optimal Control

Using the same sample building, if the weather predictor that is available to predict the weather 24 hours ahead is to use yesterday's weather, Figure 29 shows the comparison of optimal control results with and without weather prediction updating.

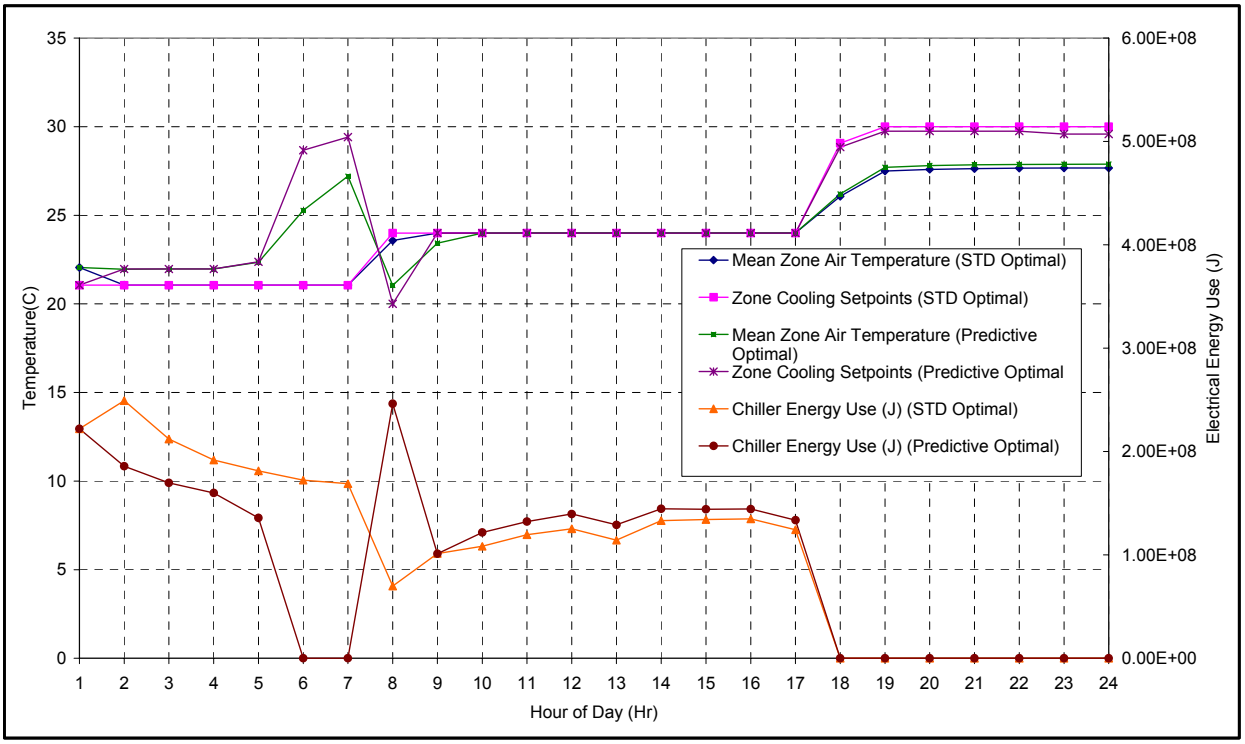

Figure 29: Comparison of optimal control of a 15-zone office building with and without weather updating

Average zone air temperature, zone setpoints and chiller electrical consumption are shown. From Figure 29, it can be observed that without using weather predictor, the optimal control chooses to precool the building to 21°C from 1:00 to 7:00, which when updating the weather file proves to be too much precooling. In predictive optimal control, the optimizer changes its strategy according to the newly updated weather information. As a result, predictive (closed-loop) optimization cost is $143.6 dollars and saves 3 more dollars than standard optimization (continuous time block).

2.8.6.6 Integration of Weather Predictor into EnergyPlus

The purpose of the weather predictor is to provide predicted weather for the optimization of each move.

As stated above, the weather information is read daily instead of per timestep as is done with other input information. The weather data of the simulated day is recorded in variable *Today*, which is read and updated in subroutine *InitializeWeather*. In subroutine *InitializeWeather*, the *BeginDayFlag* that is set to 'true' before the first timestep simulation of each day and set to 'false' after the first timestep simulation of each day. In subroutine *InitializeWeather*, whenever BeginDayFlag is 'true', variable *Today* is updated by reading the 24 hours weather data from the weather data file.

To integrate the weather predictor, a new variable *PredictedWeatherData* is introduced which stores all the weather information of 24 hours in the weather data file. When a new environment or a new move begins, the weather of the first day is loaded into variable *Tomorrow* and then at the beginning of a day, the data in Tomorrow is loaded into Today, and variable Tomorrow is updated by reading the next 24 lines in the weather data file. Thus, to realize weather prediction and update true weather data is a matter of manipulating weather data file at appropriate times.

Once a weather prediction routine predicted the weather for the next 24 hours, it is stored in variable *PredictedWeatherData*. A new subroutine *UpdateWeatherFileWithPredictedWeather* is controlled to be called at the start of each move to write the data in *PredictedWeatherData* into the weather file. Also, at the end of each move, the collected true weather data of this move is written into the weather file to replace the data predicted by calling new subroutine *UpdateWeatherFileWithTrueWeather*.

Index of Modified Source Codes

- Added *DataOptimization* file, which declares all the variables related to the optimization.
- In *SimulationManager* file
  - Added:
    - *ManageNormalEnergyPlus*
    - *ManageSTDOptimizationEnergyplus*
    - *EnvironSimulation*
    - *FCN*
  - Modified: *ManageSimulation*
- In *ScheduleManager* file
  - Added: *ProcessOptimizationInput*
  - Modified: *GetCurrentScheduleValue*
- In *WeatherManager* file
  - Added:
    - *UpdateWeatherFileWithPredictedWeather*
    - *UpdateWeatherFileWithTrueWeather*
    - *WeatherPredictor*
  - Modified:
    - *GetNextEnvironment*
    - *InitializeWeather*
    - *ReadEPlusWeatherForDay*

2.9 Task 7: Optimization System Design

Task Purpose: Based on Task 6, a functional design of the predictive optimal controller will be developed, which will provide functional descriptions of all components of the design, methods for forecasting electricity price and non-cooling electricity demand, suitable models for cooling loads and building energy systems, communication requirements between optimizer and building automation system (BAS), and method(s) to incorporate optimization control variables into the BAS software.

Some of the key optimization system design decisions will be identified and prioritized. Examples include:

- What is a suitable real-time system identification method to adequately mirror the actual building energy systems behavior as well as building dynamic response and to adjust model parameters?
- How can electrical demand charges be incorporated into the optimization so that traditional time-of-use rates may also be accounted for?
- How can real-time electricity prices be most accurately predicted?
- What forecasting techniques are suitable for this application, and what are their limitations?

Task Summary: Based on the closed-loop approach to the predictive optimal control of active and passive building thermal storage inventory, a calibration procedure for the building model and a methodology to account for monthly demand charges have been developed and investigated. Further, several forecasting models are currently under investigation, from simple same-as-yesterday predictors to more advanced seasonal autoregressive integrated moving average (SARIMA) models. The results will be reported as they are produced.

2.9.1 System Identification and Model Calibration

2.9.1.1 Problem Description

After setting up the model for the commercial building under investigation and its building energy systems, the thermal response of the building and behavior of the building energy systems can be predicted within the simulation and optimization environment. However, these simulated results will not accurately represent the actual response of the real building. At the same time, information from the building automation system is available which can be considered a reliable source of data of the actual building given proper sensor calibration. Therefore, an efficient method is needed to refine the simulation models using the real-time data from the BAS. This procedure can be considered a system identification or model calibration process. System identification can be deemed as an investigation process generating a mathematical model of a given system based on experimental data, measurements, and observations. Figure 30 shows the system identification loop (modified from [99]).

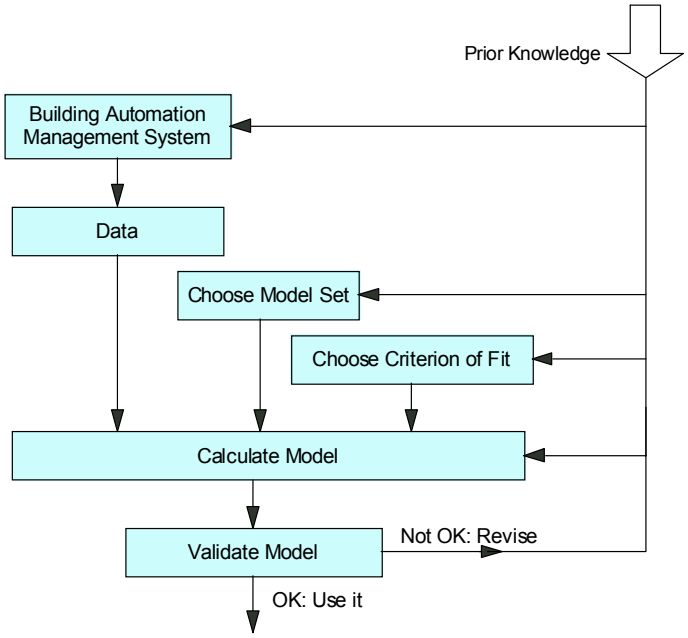

Figure 30: System Identification Loop

System identification problem can be formulated as follows [100]: We have observed inputs, $u(t)$ and outputs $y(t)$ from a dynamic system:

$$u^t = [u(1), u(2), ..., u(t)]$$

$$y^t = [y(1), y(2), ..., y(t)]$$

We are looking for a relationship between past observations $[u^{t-1}, y^{t-1}]$ and future outputs $y(t)$:

$$y(t) = g(u^{t-1}, y^{t-1}) + v(t)$$

The additive term $v(t)$ arises from the fact that the next output $y(t)$ cannot be the exact function of the past data.

Inverse modeling is known as the process when system identification is based entirely on measured data or experiment results. Many endeavors have been undertaken into the building simulation analysis involving a variety of the approaches and algorithms, such as autoregressive moving average (ARMA) models, artificial neural network model, etc. [102] indicate that these approaches are efficient, although they may lead to results which do not respect the physical properties of the real systems. Braun and Chaturvedi proposed a so-called "gray box" model in [102]. In this approach, the thermal response of the building

structure is modeled after the transfer function method, and the parameters of the transfer function are constrained within specified feasible ranges. A global search method and nonlinear regression algorithm are applied to identify the optimal parameters of the transfer function which generate best thermal response to "fit" the data of simulation result of TRNSYS.

In the given case, EnergyPlus provides a fully detailed simulation environment in which the building can be modeled with a high degree of accuracy. Information from the building automation system is available that reflects the thermal response of the actual building. This provides an opportunity to train the model of EnergyPlus to make it better. The goal of the system identification process is to develop a program or environment to calibrate the existing model using the information from the BAS to make it represent the building as close as possible.

2.9.1.2 Methodology

Objective function

A modern building automation system provides a wealth of information available either directly from measured data by the sensors or indirectly generated by post-processing measured data. In the following descriptions, we assume that the total building sensible cooling load is monitored by the building automation system, a set of data $RL(t)$ is recorded which represents the hourly sensible cooling load profile.

$$RL(t) = [RL_1, RL_2, ...RL_{T-1}, RL_T]$$

Each element of the vector represents the hourly building real cooling load, t is the index of the time series, and the T is the number of hours of the monitoring period, which is equal to the total calibration hours. On the other hand, the predicted hourly cooling load profile $SL(t)$ is generated by the simulation program.

$$SL(t) = [SL_1, SL_2, ...SL_{T-1}, SL_T]$$

Then a set of error data is generated:

$$\begin{aligned} Er(t) &= [Er_1, Er_2, ...Er_{T-1}, Er_T] \\ &= [\ |RL_1 - SL_1|,\ |RL_2 - SL_2|, ...|RL_{T-1} - SL_{T-1}|,\ |RL_T - SL_T|] \end{aligned}$$

Then the root-mean-square error (RMSE) can be defined as:

$$RMSE = \sqrt{\frac{\sum_{i=1}^{T} (Er_i)^2}{T-1}}$$

In our system identification process, we are trying to calibrate the parameters of the building simulation model to minimize the root-mean-square error *RMSE*.

Calibration parameters

Three categories of parameters are under consideration.

Table 12: Candidate parameters for calibration

Building construction	Internal heat gain	Energy system
✓ Geometry and scale of the building, layout of the zones. ✓ Thermal properties of construction materials (thermal conductance, specific heat, etc).	✓ Schedule of occupancy, light, and equipment ✓ Power density lighting and equipment, ✓ Number of people.	✓ Capacity of the energy system components. ✓ Operating performance parameters of the components (COP, PLR, etc)

As Table 12 indicates, there is a variety of factors affecting the simulation model. It is impossible and unwise to take all of them into consideration. An information collection procedure must precede the setup of the simulation model for a building. Some of the parameters in Table 12 can be obtained accurately during this procedure. For example, the geometry and scale of the building, fenestration area and the layout of zones can be attained from architectural drawings of the building. A checklist is proposed to make this procedure as accurate as possible. This can be considered a pre-processing step to calibrate the simulation model. Table 13 gives a draft of the checklist; the detailed list of items depends on the conditions of the specific building we are trying to control.

Table 13: Summary of Checklist of pre-process and calibration information

Category	Information from pre-processing	Information needed to calibrate
Building construction	✓ Orientation (azimuth) of the building ✓ Detailed scale of the building ✓ Layout of the zones ✓ Information on fenestration of the building ✓ Detailed scale of the construction	➢ Material properties — thermal conductance — specific heat — density
Internal heat gain	✓ Detailed schedule of the occupancy ✓ Detailed schedule of the lighting control ✓ Detailed schedule of the equipment control	➢ Power density of the light (LPD) ➢ Power density of the equipment (EPD)
Energy system	✓ Organization of the system (including layout of the air distribution system and water system) ✓ Capacity of the components of the system	➢ Operating parameters — Coefficient-of-performance (COP) — Part-load performance

Calibration environment

A calibration environment is developed to find the optimal values of the parameters which are hard to obtain by pre-processing. Two approaches are considered to fulfill this task. One is to use the GenOpt to cooperate with EnergyPlus (Figure 31); the other approach is to use optimization routines from the IMSL Math Library or other optimization tools (Matlab optimization tool box) integrated with EnergyPlus modules (Figure 32).

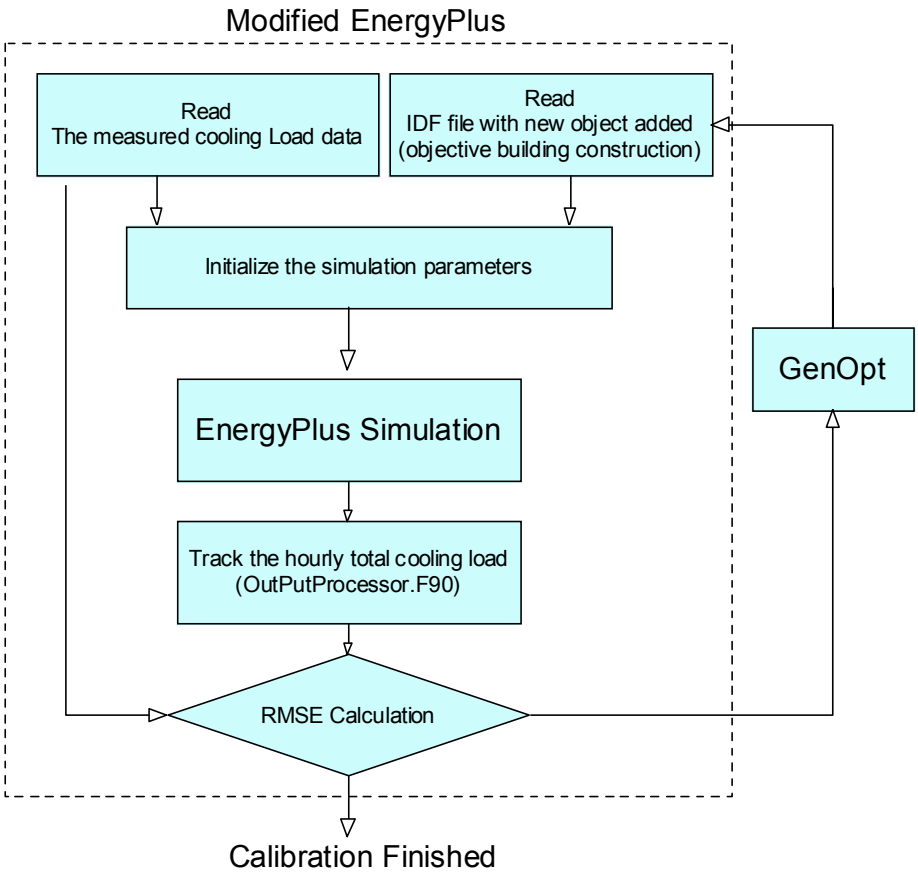

Figure 31: Calibration environment with GenOpt

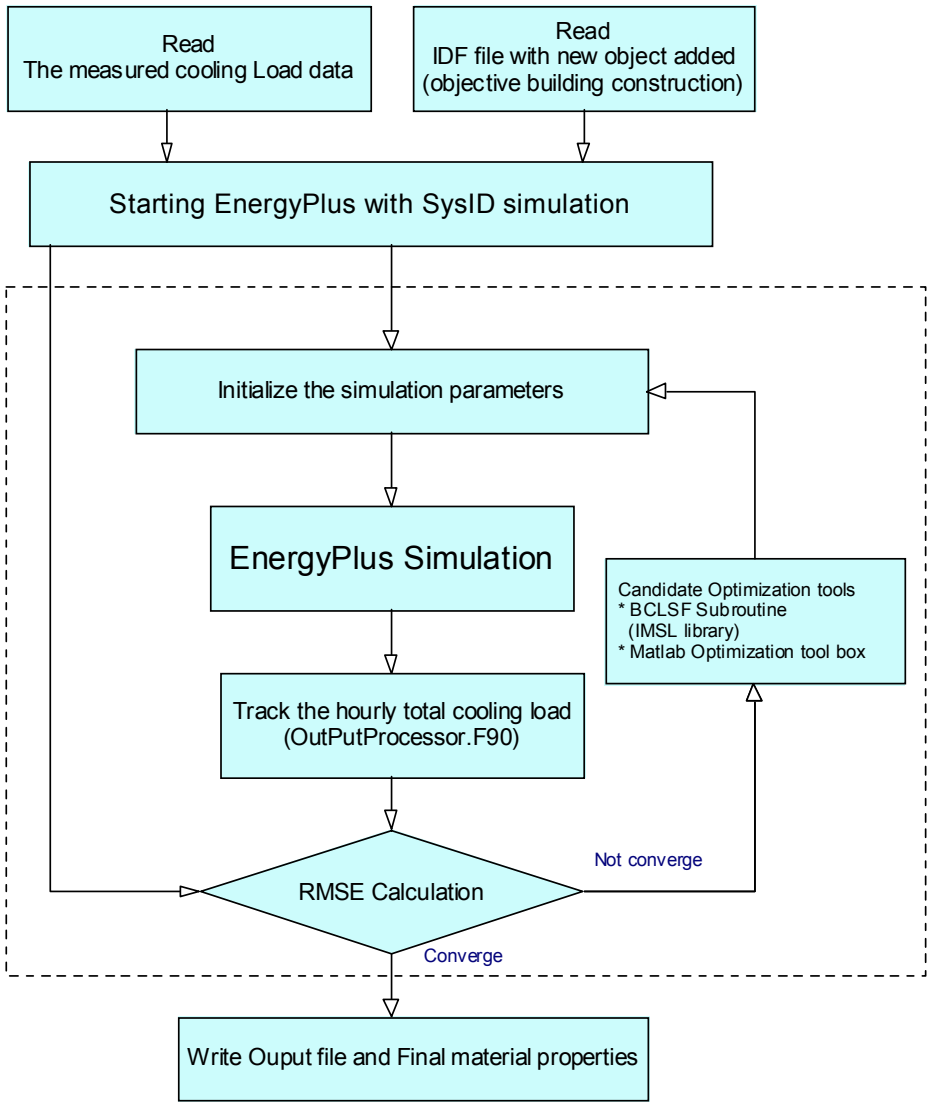

Figure 32: Calibration environment with optimization tools integrated with EnergyPlus

Results

As a test of these approaches above, a series of calibration simulations was completed and the results are presented below. A three-zone building is used as the sample building we are trying to control. Due to the lack of actual information coming from a building automation system, the results of a basecase run is selected and assumed to be the actual building information as fed back from the building automation system. The specific heat of the materials, lighting power density and equipment power density of each zone are selected as the calibration parameters. Construction is simplified to one layer to reduce the dimensionality of the optimization problem. Table 14 gives the settings of the basecase and selected optimization cases, and Table 15 summarizes the results by GenOpt.

Table 14: Parameters settings for the base case and optimization cases

Calibration parameters	**Specific heat [J/kg*K]**		**Lighting power [W]**			**Equipment power [W]**		
Component of EP	External wall	Roof	East zone	North zone	Resis-tive zone	East zone	North zone	Resistive zone
Basecase	1750	1350	1500	2500	1500	3000	1500	3000
Initial values of the optimiza-tion cases	836	836	1200	2100	1300	2700	1300	2700
Optimization Case 1	√	√						
Optimization Case 2			√	√	√	√	√	√
Optimization Case 3	√		√	√	√			
Optimization Case 4	√					√	√	√
Optimization Case 5	√	√	√	√	√	√	√	√

Table 15: Summary of results for the optimization cases by GenOpt

(All the simulation and optimizations is finished on a P4 1.4GHz and 256M ram computer with Windows 2000 platform)

Optimization Cases	**Time [min]**	**Number of runs**	**Algorithm**	**Remarks**
Optimization Case 1	2-3	32-37	Nelder-Mead Hooke-Jeeves	
Optimization Case 2	3-4	51-61	Nelder-Mead Hooke-Jeeves	Hooke-Jeeve attained much bet-ter optimal values
Optimization Case 3	3-4	54	Hooke-Jeeves	
	4-5	76	Nelder-Mead	
Optimization Case 4	7	63	Hooke-Jeeves	
	3	48	Nelder-Mead	
Optimization Case 5	23	404	Hooke-Jeeves	Nelder-Mead converged faster than Hooke-Jeeve
	10	158	Nelder-Mead	

Table 16: Summary of results for the optimization cases by GenOpt

('NM' denotes the algorithm is Nelder-Mead, 'HJ' denotes Hooke-Jeeves)

Calibration parameter		**Base case value**	**Optimal values**									
			Case 1		**Case 2**		**Case 3**		**Case 4**		**Case 5**	
Specific heat	External wall	1750	NM	HJ			NM	HJ	NM	HJ	NM	HJ
			1737	1741			1750	1736	1740	1736	1818	1736
	Roof	1350	1336	1356							1339	1361
Lighting power density	East zone	1500			NM	HJ	1492	1275			1636	1275
					1687	1500						
	North zone	2500			2255	2400	2467	2500			2030	2475
	Resistive zone	1500			1511	1600	1560	1700			1621	1775
Equipment power density	East zone	3000			3177	3000			3197	2975	3100	2925
	North zone	1500			1698	1600			1611	1500	1551	1575
	Resistive zone	3000			2641	2900			2704	3000	3116	2975
Root-mean-square error			0.07	0.009	0.014	0.0001	0.007	0.015	0.017	0.014	0.305	0.027

Table 16 lists the optimal values found by GenOpt. The results show that in all five calibration cases, the minimization routine can find optimal values which lead to a thermal response that is very close to the actual response of the basecase. The root-mean-square errors in all five optimal cases are small, sufficient for building energy system simulation. Figures 33 to 36 give the cooling load profile of the base case which represents the real value from the building management system, including the initial profile and the profile with the optimal values found by the optimizer. All four figures indicate that the optimal profile is almost the same as the basecase. Comparing the results of root-mean-square error in the five cases, it seems that the optimization time and the magnitude of the error increases when the dimensionality of the *RMSE* minimization problem increases.

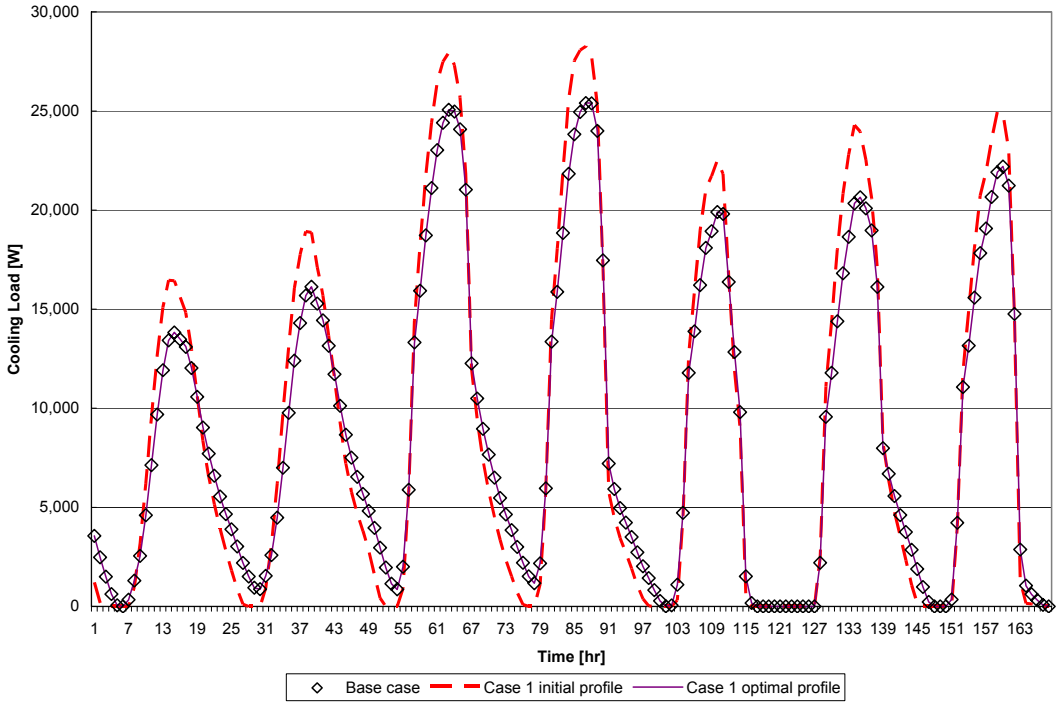

Figure 33: Cooling load profiles of basecase and Case 1 with initial and optimal values

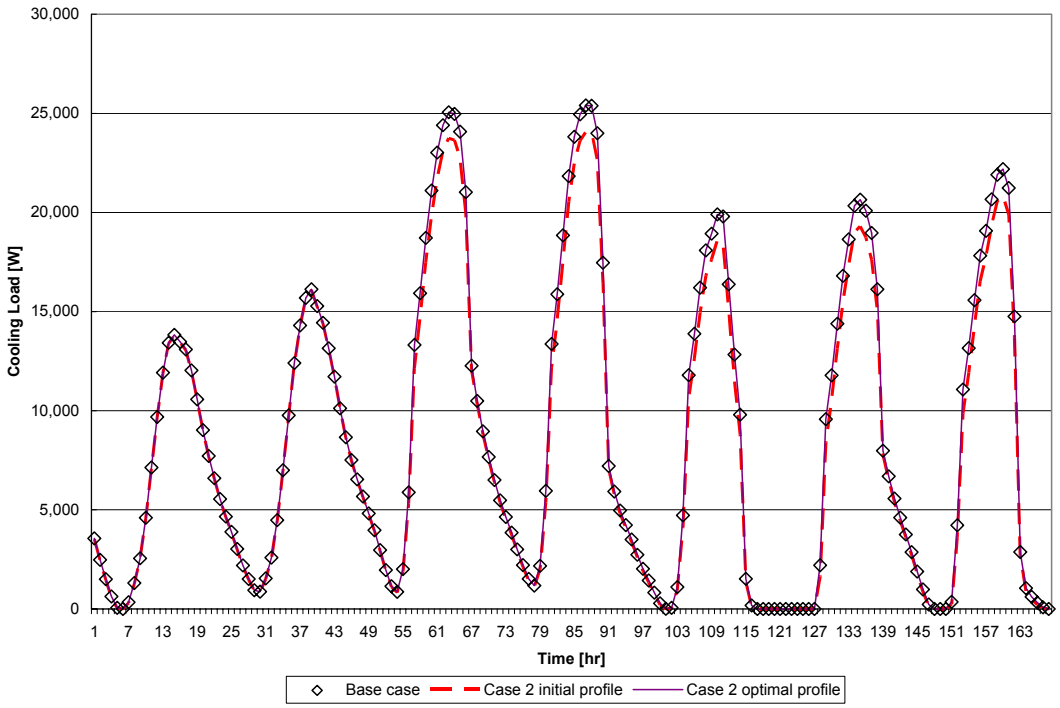

Figure 34: Cooling load profiles of basecase and Case 2 with initial and optimal values

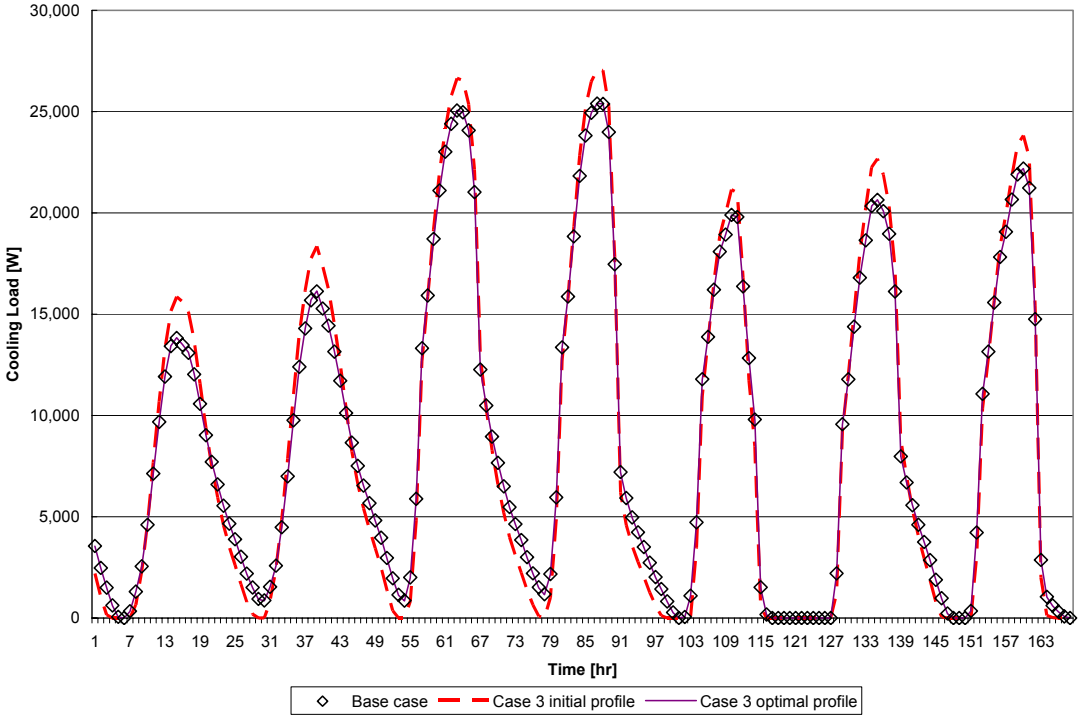

Figure 35: Cooling load profiles of basecase and Case 3 with initial and optimal values

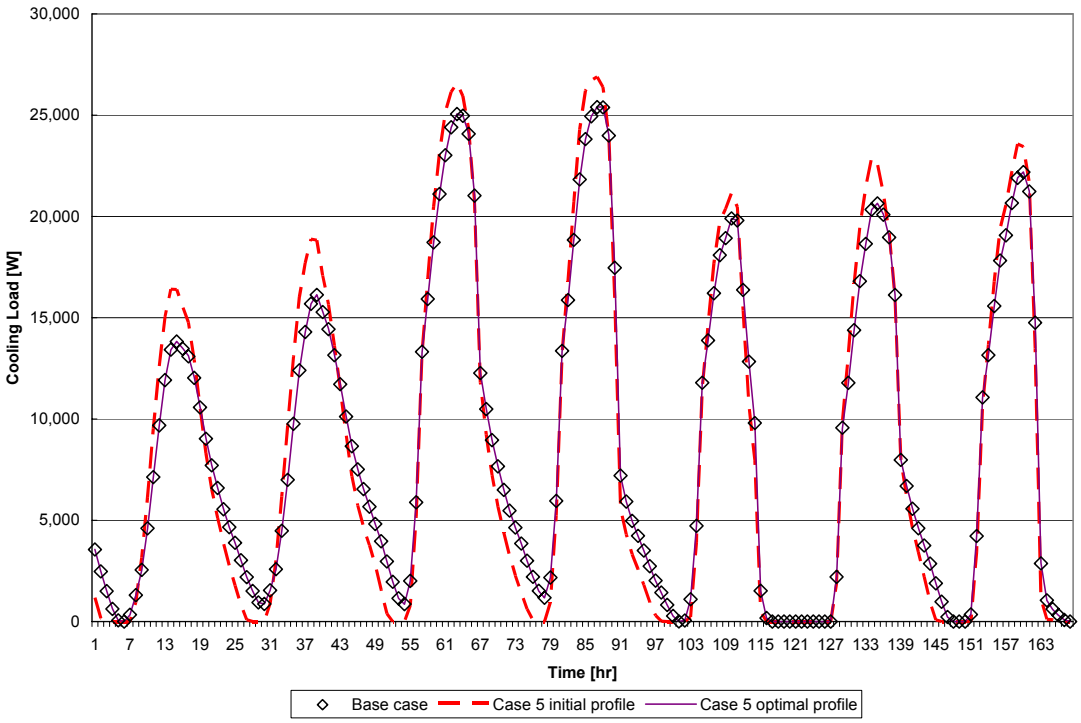

Figure 36: Cooling load profiles of basecase and Case 5 with initial and optimal values

Conclusions

From the results above, the methodology of the calibration environment can be expected to satisfy the system identification requirements. This process is not only supposed to be carried out before the predictive optimal control procedure begins, but also to be repeated periodically (e.g., once a month) to ascertain that the building simulation models adequately represent the real building.

The alternative approach of the calibration environment which integrates the *RMSE* minimization routines into EnergyPlus is under development. This approach is expected to provide greater flexibility for the user to manipulate the parameters of the building simulation models in order to decrease the dimensionality of the optimization problem and shorten the optimization time. An update of the results of this approach is expected to be finished in the near future.

Recommended Procedure

System identification is a calibration procedure, which harnesses available information from the building automation system to calibrate the building simulation model to better represent the actual building, which is a prerequisite for the predictive optimal control strategy to qualify as actually being optimal. In addition to the general calibration process described above, a specific sequence of calibration steps is recommended

a) The **preprocessing** step will be carried out before the building simulation model is placed into the calibration environment. It is recommended to make sure that all the items in the **checklist** have been accounted with utmost care.
b) It is advised to calibrate the **internal heat gain** parameters first and if possible to keep the number of parameters to be fit low in order for the **dimensionality** of the *RMSE* minimization problem to be as low as possible.
c) The **material properties** are crucial factors affecting the building thermal response; it is suggested to calibrate these factors when all of the other parameters have been properly tuned.
d) The calibration of **operating parameters** of the energy system of the building can be done separately from the other parameters mentioned above. The same methodology can be applied.

3 Results and Discussion

3.1 Introduction

This chapter contains a parametric analysis of predictive optimal control of building thermal storage inventories. Different parameters, e.g. building thermal mass, electrical utility rate, season, plant size, are considered. Also, the effects of different prediction periods are compared and their results are analyzed.

3.2 Keywords

Some of the keywords frequently referred to in this chapter are

- *Standard Optimization* is the optimization of building setpoints based on true weather data; therefore, there is no prediction of weather involved.
- *Building Modes* is to group building zone temperature setpoints according to the building's operational status. Usually, building can be operated in four modes, i.e. Unoccupied-Offpeak, Unoccupied-Onpeak, Occupied-Offpeak, and Occupied-Onpeak, indicating whether the building is occupied (and therefore, thermal comfort need to be maintained) and whether electricity is expensive (during on-peak period).
- *Sequential Optimization* means to optimize zone temperature setpoints (passive storage) first, and then based on the optimized setpoints to optimize active storage charging/discharging rates.
- *Predictive Optimization* is synonymous with closed-loop moving window optimization (CLO) in this document. Predictive optimization is an optimization technique that attempts to compensate for the inaccuracies of standard optimization by adjusting weather prediction and thus repeat the op-

timization periodically based on updated weather and new prediction. The time span of one prediction is called *window length* and the period between two predictions is called *moving length*.

- Continuous time block optimization (CTBO) has *WL* = *ML* = 24 hours, i.e., a policy is planned over the next WL = 24 hours and executed for the same *ML* = 24 hours. Update forecasts are therefore not utilized.

3.3 Building Models, Weather Files and Basecase Scenario

This section describes the building models that are used to run the parametric analysis and the base cases that the parametric analysis is compared to.

3.3.1 Building Models

To simulate a typical office building, a three-story fifteen-zone building as shown in Figure 37 is modeled.

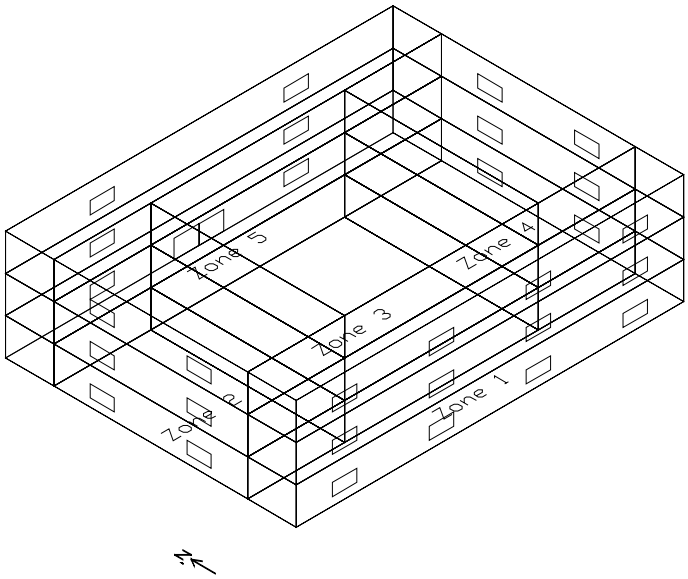

Figure 37: Isometric view of 15-zone office building

Building floor area is 48 by 36 square meters. Each floor is divided into five zones, i.e. North-Zone, South-Zone, East-Zone, West-Zone and Center-Zone. Figure 38 shows the zone dimensions of each floor. The dimensions of each zone are: North-Zone: 48m by 6m South-Zone: 48m by 6m, West-Zone: 24m by 12m, East-Zone: 24m by 12m.

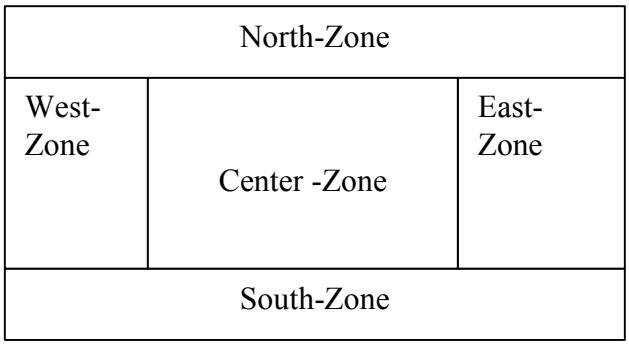

Figure 37: Floor dimensions

Table 17 describes the wall constructions of exterior walls, interior partitions, ceilings and floors for a super heavy mass case. This construction gives a building mass of 203.5 lbm/ft2.

Table 17: Construction of a very heavy mass building

CONSTRUCTION	d (m)	k (W/m-K)	Rho (kg/m3)	Cp (J/kg-K)	R (m2 K /W)
EXTWALL-mass-in					
A1 - 1 IN STUCCO	0.0250	0.691831	1858.14	836.8	0.03614
b6	0.0500	0.043000	91.00	840.0	1.16279
E2 - 1 / 2 IN SLAG OR STONE	0.0120	1.435549	881.02	1673.6	0.00836
C4 - 4 IN COMMON BRICK	0.1000	0.726422	1922.22	836.8	0.13766
E1 - 3 / 4 IN PLASTER OR GYP BOARD	0.0200	0.726422	1922.22	836.8	0.02753
InternalWall					
E1 - 3 / 4 IN PLASTER OR GYP BOARD	0.0200	0.726422	1922.22	836.8	0.02753
C4 - 4 IN COMMON BRICK	0.1000	0.726422	1922.22	836.8	0.13766
E1 - 3 / 4 IN PLASTER OR GYP BOARD;	0.0200	0.726422	1922.22	836.8	0.02753
ceiling					
E1 - 3 / 4 IN PLASTER OR GYP BOARD	0.0200	0.726422	1922.22	836.8	0.02753
C10 - 8 IN HW CONCRETE	0.2000	1.729577	2242.59	836.8	0.11564
E1 - 3 / 4 IN PLASTER OR GYP BOARD;	0.0200	0.726422	1922.22	836.8	0.02753
ROOF-mass-in					
C12 - 2 IN HW CONCRETE	0.0500	1.729577	2242.59	836.8	0.02891
E2 - 1 / 2 IN SLAG OR STONE	0.0120	1.435549	881.02	1673.6	0.00836
E3 - 3 / 8 IN FELT AND MEMBRANE	0.0100	0.190254	1121.29	1673.6	0.05256
B12	0.0760	0.043000	91.00	840.0	1.76744
c13	0.1500	1.731000	2243.00	840.0	0.08666
FLOOR SLAB 8 IN					
DIRT 12 IN	0.3048	0.172958	1041.20	836.8	1.76228
C10 - 8 IN HW CONCRETE;	0.2000	1.729577	2242.59	836.8	0.11564

In this parametric analysis, three different mass levels are studied, i.e., heavy-mass, medium-mass and light-mass. These mass levels are modeled based on the construction in Table 17. By varying the density of the material in constructions in Table 17, three different mass levels are achieved. The heavy mass building has a mass level of 130 lbm/ft^2. The medium mass building has a mass level of 81 lbm/ft^2. The light mass building has a mass level of 37.5 lbm/ft^2.

The building is occupied from 8:00-19:00 and unoccupied for the rest of the day. There are 0.08 person/m^2. The equipment and lightings are modeled in the same schedule that gives 31.25 W/m^2. Table 18 summarizes the internal load schedules.

Table 18: Internal load schedules

Time	1	2	3	4	5	6	7	8	9	10	11	12	13	14	15	16	17	18	19	20	21	22	23	24
Lighting WeekDay	0.05	0.05	0.05	0.05	0.05	0.05	0.2	1	1	1	1	1	1	1	1	1	1	0.5	0.05	0.05	0.05	0.05	0.05	0.05
People WeekDay	0	0	0	0	0	0	0	0.5	1	1	1	1	0.5	1	1	1	1	0.5	0.1	0	0	0	0	0

Three electrical rate structures are studied: strong-incentive rate, weak-incentive rate, and no-incentive rate. Table 19 summarizes these rates.

Table 19: Electrical rate structures

Time	1	2	3	4	5	6	7	8	9	10	11	12	13	14	15	16	17	18	19	20	21	22	23	24
Stong Incentive Elec. Rate Structure																								
Energy Rate ($/KWH)	0.05	0.05	0.05	0.05	0.05	0.05	0.05	0.05	0.2	0.2	0.2	0.2	0.2	0.2	0.2	0.2	0.2	0.2	0.05	0.05	0.05	0.05	0.05	0.05
Demand Rate ($/KW)	0	0	0	0	0	0	0	0	10	10	10	10	10	10	10	10	10	10	0	0	0	0	0	0
Weak Incentive Elec. Rate Structure																								
Energy Rate ($/KWH)	0.2	0.2	0.2	0.2	0.2	0.2	0.2	0.2	0.2	0.2	0.2	0.2	0.2	0.2	0.2	0.2	0.2	0.2	0.2	0.2	0.2	0.2	0.2	0.2
Demand Rate ($/KW)	5	5	5	5	5	5	5	5	10	10	10	10	10	10	10	10	10	10	5	5	5	5	5	5
NO Incentive Elec. Rate Structure																								
Energy Rate ($/KWH)	0.2	0.2	0.2	0.2	0.2	0.2	0.2	0.2	0.2	0.2	0.2	0.2	0.2	0.2	0.2	0.2	0.2	0.2	0.2	0.2	0.2	0.2	0.2	0.2
Demand Rate ($/KW)	10	10	10	10	10	10	10	10	10	10	10	10	10	10	10	10	10	10	10	10	10	10	10	10

From above information, it can be deduced that the building is operated under the following five unique building modes.

Unoccupied-Offpeak-1: 1:00-6:00

Occupied-Offpeak-1: 7:00-8:00

Occupied-Onpeak: 9:00-18:00

Occupied-Offpeak-2: 19:00
Unoccupied-Offpeak-2: 20:00-24:00

3.3.2 System and Plant Models

3.3.2.1 Secondary HVAC System Model

A VAV reheat system with dual setpoints with deadband zone control is used. Table 20 shows the zone setpoints and minimal fresh air schedule for conventional nighttime setback control and the zone set-points upper and lower bounds for zone control setpoint optimization.

Table 20: Night-Setback control schedules

Time	1	2	3	4	5	6	7	8	9	10	11	12	13	14	15	16	17	18	19	20	21	22	23	24
Cooling Setpoint	45	45	45	45	45	45	24	24	24	24	24	24	24	24	24	24	24	24	24	45	45	45	45	45
Heating Setpoint	12	12	12	12	12	12	18	18	18	18	18	18	18	18	18	18	18	18	18	12	12	12	12	12
Minimal OA Fraction	0	0	0	0	0	0	0.15	0.15	0.15	0.15	0.15	0.15	0.15	0.15	0.15	0.15	0.15	0.15	0.15	0	0	0	0	0

The outdoor air flow rate is controlled by a temperature based economizer that adjusts the outdoor air fraction from 0% to 100% by comparing the temperature of return air and outdoor air. At the same time, the outdoor air fraction must meet the schedule of minimal outdoor air fraction.

3.3.2.2 Primary Plant Model

- Big Chiller: Cooling is provided by a constant-COP electrical chiller with a nominal capacity of 500 kW and a COP (coefficient-of-performance) of 4.5.
- TES Model: The constant-COP TES model is used. This model includes an ice tank and its dedicated constant COP chiller (small chiller) and tower. The ice tank size is 1,500 kWh. The small chiller nominal capacity is 250 KW with a constant COP of 3.0.

3.3.3 Weather File and Simple Weather Predictor

In this document, the location for all the simulations is Phoenix, AZ.

3.3.3.1 Summer, Spring and Winter TMY2 Weather

Figure 38 shows the dry bulb temperature of a typical day in summer, spring and winter, i.e. July-20th, April-2nd, January-17th. Table 21 summarizes the dry bulb temperature information of the three typical days.

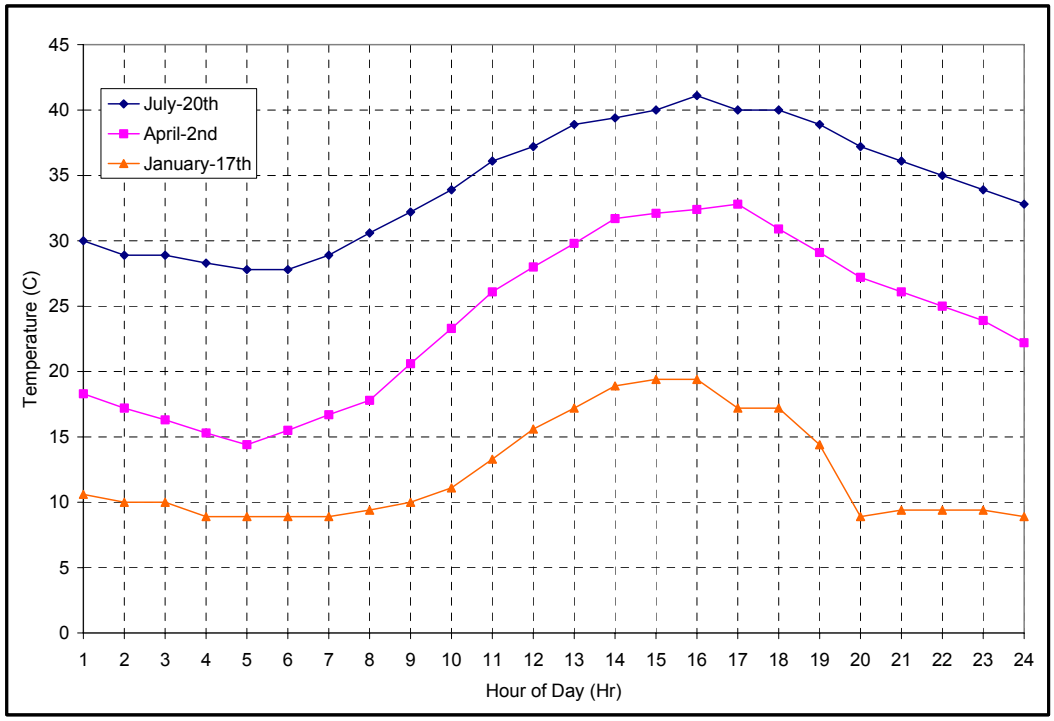

Figure 38: Outdoor dry-bulb temperature of typical days of summer, spring, and winter in Phoenix, AZ

Table 21: Summary of outdoor dry bulb temperatures of typical days in summer, spring and winter

(unit: degree C)	20-Jul	2-Apr	17-Jan
Average	34.3	23.9	12.3
Minimal	27.8	14.4	8.9
Maximal	41.1	32.8	19.4
Day-Night Swing	13.3	18.4	10.5

3.3.3.2 A Simple Weather Predictor

A simple weather predictor that predicts a 24-hour weather profile based on the previous 24-hours of weather is used. This weather predictor makes the first prediction at hour one of the day by using the weather of last 24 hours. Then at every hour requiring an update, the prediction is adjusted by calculating the error of the prediction one hour before the updating hour and then shifting the last prediction upwards or downwards by the same absolute deviation. Figure 39 shows an example of the results of this predictor by using this predictor to update prediction every *ML* = 6 hours for July-20th.

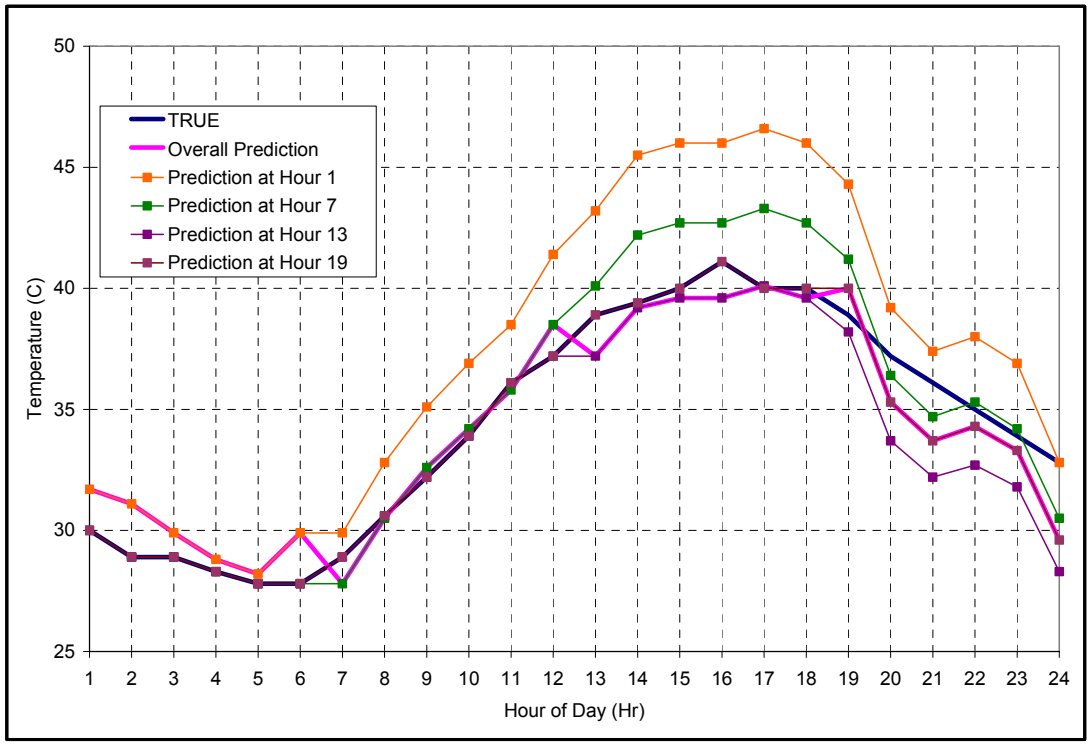

Figure 39: Prediction of weather of July-20 using a simple predictor and updating every 6 hours

Figure 39 illustrates the true weather data and the weather prediction at each move, i.e. at hour 1,7,13, and 19. Also shown is the overall weather prediction. The average errors of predictions at each move are 3, 0.7, -1.76 and -1.28 °C respectively.

3.3.4 Basecases

The optimal control of passive and active building thermal storage inventories is compared with two base-cases. In basecase-1, the ice tank is not used, and the plant/system operation is nighttime setback control. In basecase-2, the plant/system control is a nighttime setback control but an ice tank is used to try to shift part of the on-peak load to off-peak. In this base case, chiller-priority control is used: the ice tank is charged to 100% during the night when the electrical rate is off-peak and during the hours that the cooling load is nonzero, the cooling load is met by the big chiller up to its capacity and the ice tank is going to melt as much ice as it is necessary to meet the fraction of cooling load that cannot met by the big chiller. Since the ice tank control is not optimized, chiller-priority control may actually cost more than without ice tank. Table 22 shows the comparison of the two base cases, i.e. base case with ice tank dormant and base case with chiller-priority control. Different mass levels *L* (light), *M* (medium), and *H* (heavy), different electrical rate structure 0 (no incentive), 1 (weak incentive) and 2 (strong incentive), and different seasons are compared.

Table 22: Comparison of TES dormant and Chiller priority controlled TES plant

	L-0	L-1	L-2	M-0	M-1	M-2	H-0	H-1	H-2
SUMMER									
Base case -1: TES Dormant	294.5	294.5	263.3	292.0	292.0	260.4	288.8	288.8	257.5
Base case -1:Chiller Priority	327.9	327.9	221.6	325.4	325.4	218.8	322.1	322.1	215.8
Comparing with Base case-1	10.2%	10.2%	-18.8%	10.2%	10.2%	-19.0%	10.3%	10.3%	-19.3%
SPRING									
Base case -1: TES Dormant	223.8	223.8	200.4	218.8	218.8	195.4	216.0	216.0	192.8
Base case -1:Chiller Priority	266.3	250.0	135.4	266.2	250.0	135.4	266.0	249.7	135.3
Comparing with Base case-1	16.0%	10.5%	-48.0%	17.8%	12.5%	-44.3%	18.8%	13.5%	-42.5%
WINTER									
Base case -1: TES Dormant	149.3	149.3	131.1	148.3	148.3	130.1	147.9	147.9	129.6
Base case -1:Chiller Priority	260.7	243.8	133.7	260.7	243.8	133.7	260.7	243.8	133.7
Comparing with Base case-1	42.7%	38.8%	1.9%	43.1%	39.2%	2.7%	43.3%	39.3%	3.0%

From Table 22, it can be observed that when the electrical rate structure offers no incentive or only a weak incentive, operation of the ice tank cost more money. With a strong incentive electrical rate, chiller-priority control of ice tank can save some money in the summer and spring but not in the winter. This is because in summer and spring, the cooling load is substantial. The strong incentive electrical rate can be taken advantage of by shifting a large amount of cooling load from on-peak to off-peak. In the winter, the cooling load is small. Even under strong-incentive electrical rates, less money can be saved by shifting the load from on-peak to off-peak and since the COP of the small chiller is significantly lower than the big chiller's, the saving from shifting the load is not sufficient to compensate for the inefficiency of the small chiller.

It can be concluded from Table 22 that, without appropriate control, not only does the TES system possibly not save money, but it may actually cost more money than a system without active storage.

3.4 Assumptions

3.4.1 Building Mode and Sequential Optimization

It is necessary to use some simplifications to help the optimization routine find globally optimal solutions. In this chapter, the building mode and sequential optimization techniques are used in all of the optimization runs.

The zone air temperature setpoints are optimized using the IMSL BCPOL routine to minimize total electrical costs. After the optimal zone setpoints are found, the plant cooling load profile can be obtained by running the simulation program once more. Then this plant load profile and other non-cooling electrical loads can be transferred to the dynamic programming module to find the optimal charging discharging rates of the ice tank to yield the minimal total electrical cost.

The active storage charging/discharging rate is optimized using dynamic programming. Since dynamic programming itself can only minimize incrementally additive energy cost, a demand cost limit is added as a hard limit at each calculation of instant cost in the backward propagation process of the dynamic programming. Each time when the instantaneous cost is calculated, the demand cost is calculated and compared with the demand cost limit. When this instant demand cost is larger than the demand cost limit, a penalty value is added to the instant cost. Therefore, the backwards propagation process is forced towards a route that has a demand cost lower that the given demand limit, i.e., it observes the preset demand ceiling. Given different demand limits, different route of optimal charging/discharging rate can be found. Thus, an outer loop that provides different demand limits is added to help dynamic programming to minimize energy cost while search for lowest demand cost.

The demand limit has to be chosen appropriately. The demand cost of a nighttime setback control is chosen to be the highest demand limit. The demand cost when there is no cooling load, i.e., non-cooling electrical loads only, is chosen to be the lowest demand limit. And the demand limits used in the dynamic programming is increased from the lowest demand limit to the highest demand limit. Then a comparison of

the total electrical costs under these different demand limits is performed to find the best demand limit that gives the lowest total electrical cost. This completes the optimization of the passive and active building thermal storage inventory.

This process can be described as in the following figure and is called non-feedback sequential optimization because after the active system is optimized, the solution is not fed back to the passive system to adjust the optimization of the passive system.

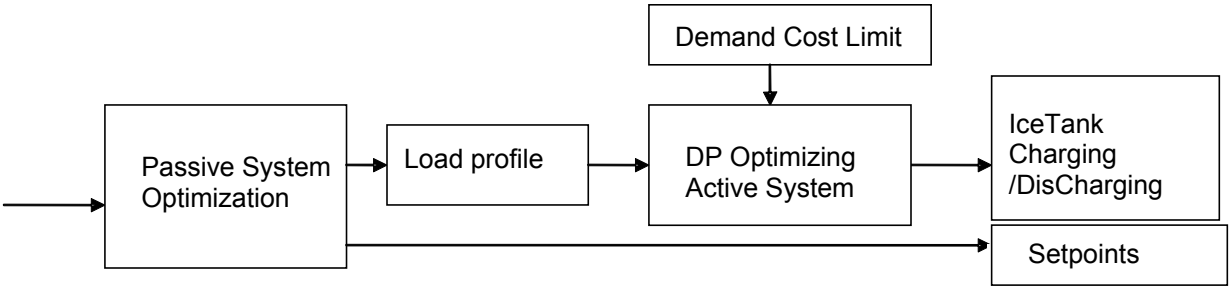

Figure 40: Non-feedback sequential optimization

A feedback sequential optimization takes the optimized active storage charge/discharge rates and feeds those back to optimize the passive system and the results are compared until convergence is reached.

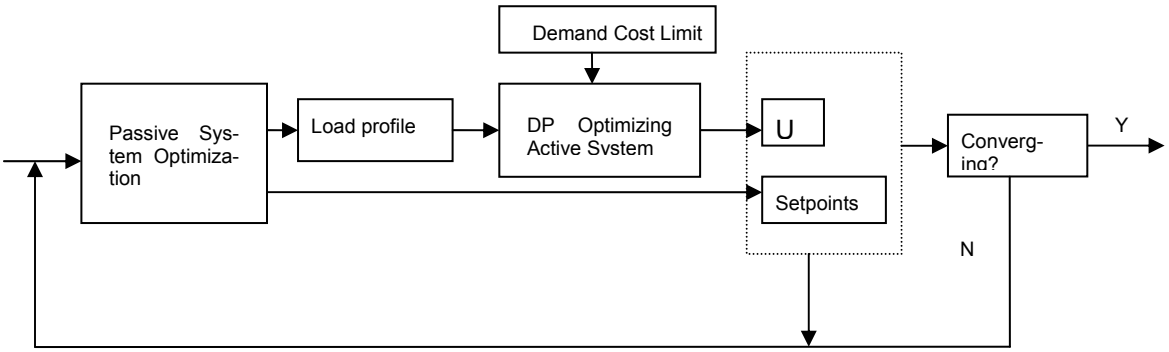

Figure 41: Sequential optimization with feedback

Table 23 compares some of the optimization results from no-feedback and from onetime feedback sequential optimization.

Table 23: Comparison of no-feedback sequential optimization and feedback sequential optimization

SUMMER				
	H-2-SUMMER	H-1-SUMMER	L-2-SUMMER	L-1-SUMMER
BASE-CASE	257.48	288.78	263.31	294.53
No-feedback	148.15	269.19	149.15	275.17
SAVING	-42.5%	-6.8%	-43.4%	-6.6%
Feedback-once	147.68	269.73	149.04	274.86
SAVING	-42.6%	-6.6%	-43.4%	-6.7%

SPRING				
	H-2-SPRING	H-1-SPRING	L-2-SPRING	L-1-SPRING
BASE-CASE	192.78	215.97	200.37	223.78
No-feedback	129.01	210.1	130.75	218.09
SAVING	-33.1%	-2.7%	-34.7%	-2.5%
Feedback-once	127.58	210.02	130.85	213.44
SAVING	-33.8%	-2.8%	-34.7%	-4.6%

It can be seen that the difference of savings between no-feedback sequential optimization and onetime feedback sequential optimization ranges from 0.0-2.5%. Therefore, no-feedback sequential optimization is sufficiently accurate for the project. The optimization results in this document are therefore conducted with no-feedback sequential optimization.

3.4.2 Typical Day Optimization

The way the building thermal mass level affects the optimal zone air setpoints varies according to the thermal history of the thermal mass. Optimization based on different initial thermal histories may lead to completely opposite results, e.g. first-day optimization and typical-day optimization. In a first day optimization, the day that will be optimized is the first day after past conventional controls, i.e., yesterday was still conventional control and today is going to be optimized. In a typical-day optimization, the day that needs to be optimized is a day following an optimized day, i.e., today is going to be optimized and yesterday was optimized. Table 24 compares the total electrical costs of optimizing zone air setpoints of a heavy-mass building and a light-mass building under first day optimization. Figure 42 and Figure 43 shows the indoor air temperatures and big chiller electrical use.

Table 24: Light-mass and heavy-mass building under first day optimization

	Heavy Mass	Light Mass
Night Setback Control Total Elec. Cost ($)	221.6	263.0
Optimal Control Total Elec. Cost ($)	183.6	205.5
Savings	-17.1%	-21.9%

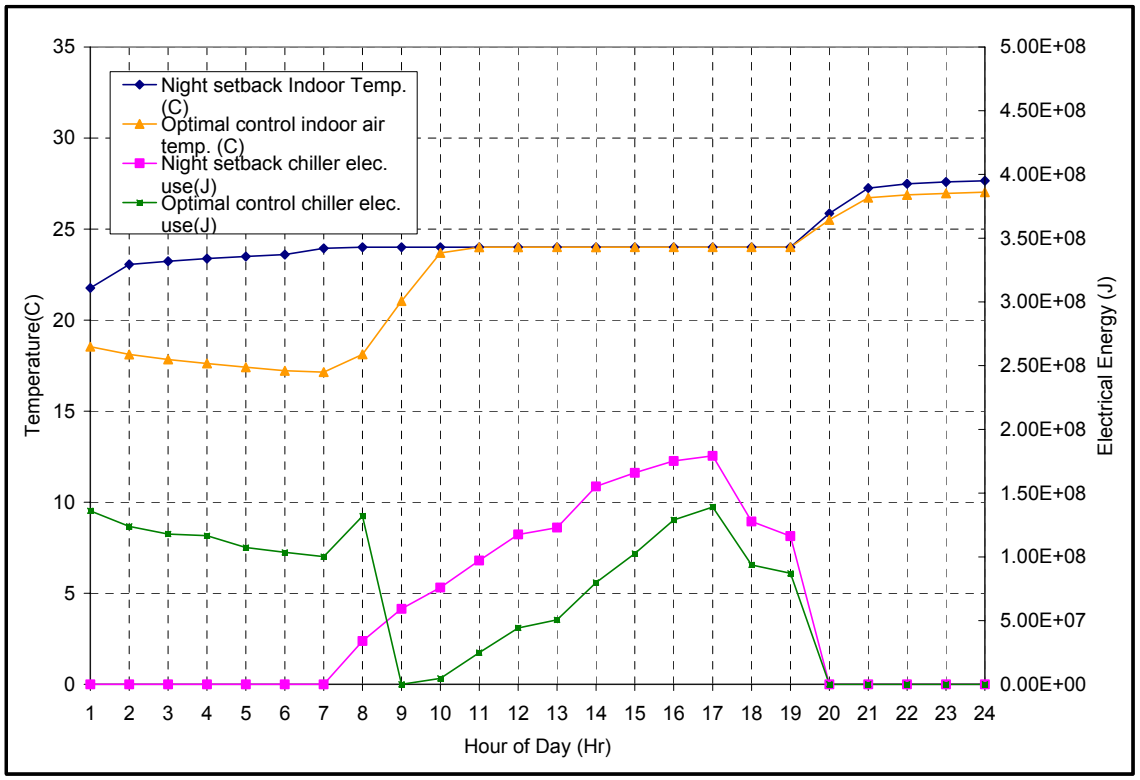

Figure 12: Optimizing zone setpoints of a light mass building under first day optimization

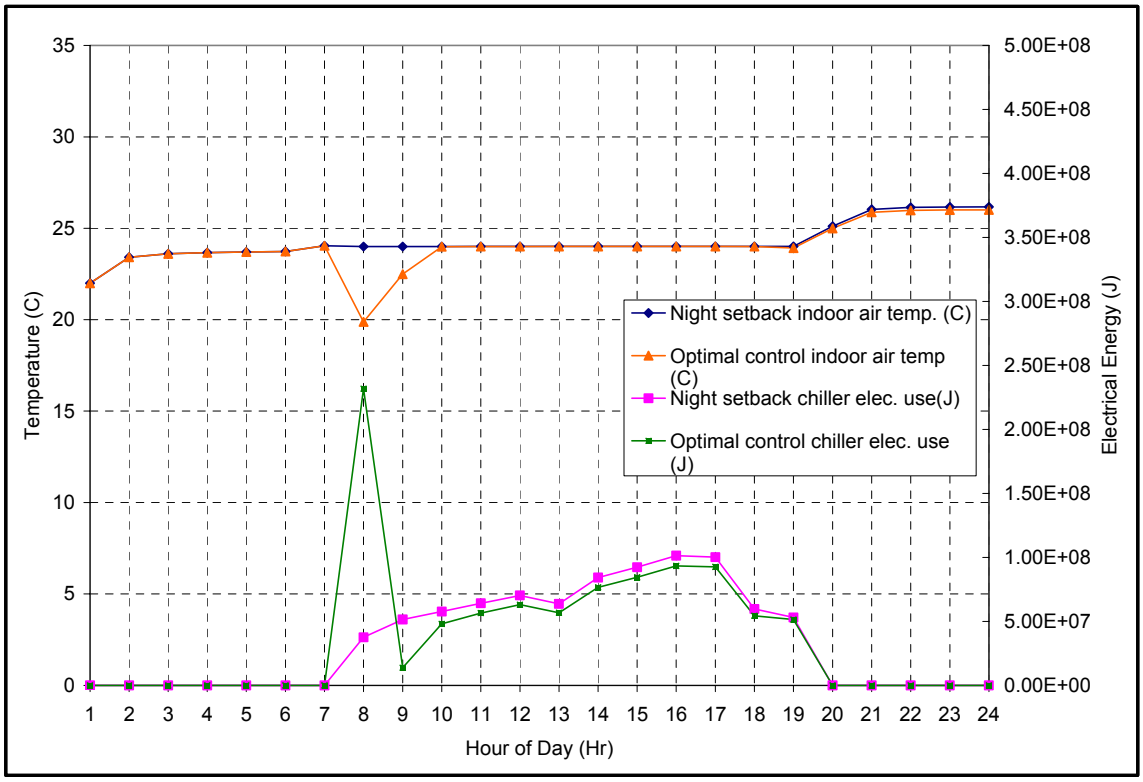

Figure 43: Optimizing zone set points of a heavy mass building under first day optimization

From Table 24, it can be observed that the light-mass building saves more than the heavy-mass building does when the passive thermal inventory is optimized. As shown in Figure 42 and Figure 43, the light-

mass building exhibits more precooling than the heavy mass building does. This is because under first-day optimization yesterday was still under nighttime setback control. The indoor air temperature during the night is high. Heavy mass buildings stores more heat in the building mass than light-mass buildings. Therefore, the next morning, it will take more chiller power in the heavy-mass building to cool this thermal mass down. Balancing the advantage of precooling and the disadvantage of precooling a heated heavy mass, the optimization routine chooses not to precool the heavy-mass building as much as it does to the light-mass building. Therefore, it appears that the light mass building offers a greater potential for savings than the heavy-mass building does. This is not correct.

It is the typical day performance that is of greater interested in this report. Therefore, the results of the simulations in this report are all based on a typical day instead of a non-typical day such as the first day. Since indoor air temperature is a more direct reflection of the results of the control than the setpoints, it is shown in the figures instead of the setpoints in this report.

3.5 Continuous Time Block Optimization with Moving Length ML = 24 hours

In this section, we want to study the effects of building mass, electrical utility rate, season, plant size and thermal comfort on optimization. In order to focus on these parameters only, results of predictive optimization with moving length *ML* = 24 hours are presented, also known as continuous time block optimization (CTBO). This way, all the optimizations are done to minimize the electrical cost of hour one to hour 24 of the optimized day and there is no extra cost from the next day involved, which will at times affect the conclusions on the effects of the parameters that are studied in this section. In reality, closed-loop predictive optimal control with moving length *ML* < 24 hours are more appropriate and but also more complicated to analysis. Results of predictive optimization with moving length less than 24 hours are discussed below.

3.5.1 Effect of Building Mass

Three building mass levels are considered, i.e. light-mass, heavy-mass and medium-mass. Table 25 summarizes the results of optimization the passive thermal inventory for different building mass levels under different rate structures and seasons.

Table 25: Summary of passive thermal storage optimization

	NO INCENTIVE RATE			WEAK INCENTIVE RATE			STRONG INCENTVIE RATE		
SUMMER									
	LIGHT	MEDIUM	HEAVY	LIGHT	MEDIUM	HEAVY	LIGHT	MEDIUM	HEAVY
NIGHT-SETBACK CTRL.	355.2	352.1	348.1	355.2	352.1	348.1	317.4	313.9	310.3
OPTIMAL CTRL.	354.8	351.8	347.6	332.2	329.5	326.9	229.1	219.9	216.9
SAVINGS	-0.1%	-0.1%	-0.2%	-6.5%	-6.4%	-6.1%	-27.8%	-29.9%	-30.1%
SPRING									
	LIGHT	MEDIUM	HEAVY	LIGHT	MEDIUM	HEAVY	LIGHT	MEDIUM	HEAVY
NIGHT-SETBACK CTRL.	276.7	270.9	267.6	276.7	270.9	267.6	247.7	242.0	238.9
OPTIMAL CTRL.	272.7	266.8	264.6	260.0	249.1	251.4	189.4	182.9	182.4
SAVINGS	-1.4%	-1.5%	-1.1%	-6.0%	-8.1%	-6.1%	-23.5%	-24.4%	-23.7%
WINTER									
	LIGHT	MEDIUM	HEAVY	LIGHT	MEDIUM	HEAVY	LIGHT	MEDIUM	HEAVY
NIGHT-SETBACK CTRL.	187.2	186.1	186.2	187.2	186.1	186.2	166.5	164.6	164.3
OPTIMAL CTRL.	181.5	183.7	176.1	181.5	176.8	169.9	122.9	127.5	127.6
SAVINGS	-3.0%	-1.3%	-5.4%	-3.0%	-5.0%	-8.7%	-26.2%	-22.6%	-22.3%

As it can be observed in Table 25, the savings potential of light-mass, medium-mass and heavy-mass buildings are similar. The heavy-mass building does not have prominent advantage in terms of optimal control of passive storages. This is due to many reasons and should be analyzed on a case-by-case basis. For example, one reason is that in the summer with high incentive electrical rates, the cooling energy is less than 50% percent of the total energy used. The cooling energy savings coming from optimal control of passive thermal storage can only be partially reflected in total energy use. Figure 44 shows the indoor air temperature and cooling energy use of optimal controlled passive storage of a light-mass building and a heavy-mass building.

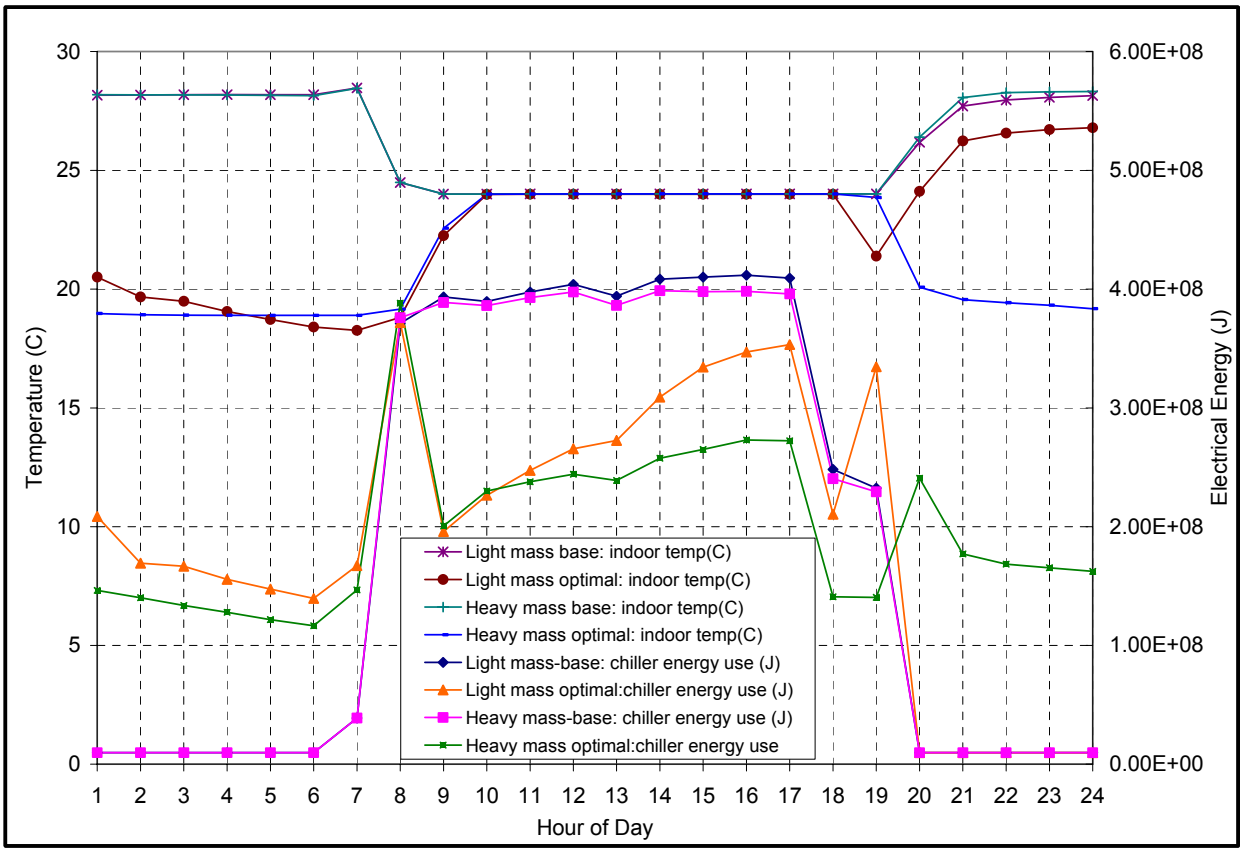

Figure 44: Comparison of optimal control of passive thermal storage of a light mass and heavy mass building

From Figure 44, it can be observed that the heavy-mass building shifts more on-peak cooling energy use to off-peak than the light mass building does. Actually, in the nighttime setback controls, the light-mass building total cooling costs is $137 and the heavy mass building total cooling costs is $131. In the optimal control, the light mass building total cooling costs is $71.3 and the heavy mass building total cooling costs is $55.4. Therefore, considering cooling costs savings only, the light-mass building saves 47.9% and the heavy-mass building saves 57.5%. The difference of mass level can be therefore clearly observed.

It can also be observed that instead of letting the indoor air temperature float, both optimal controls continue to cool the building down after on-peak hours. The light-mass building cools for one hour in 19:00 and the heavy mass building cools continuously to about 19°C starting from 20:00. The reason for cooling during this period is due to the typical-day optimization. The optimization is done in a way that it thinks the day is a typical-day. Therefore, it keeps control zone air temperature during the night so the thermal history for the precooling of the morning is controlled not to be too warm to start precooling. This difference between typical-day optimization and non-typical day optimization can be seen clearly by comparing Figure 43 with Figure 44, i.e., optimization of zone temperature setpoints of a heavy-mass building using first-day simulation.

3.5.2 Effect of Economizer

Due to the availability of a temperature economizer, which adjust fresh air flow rate by comparing the outdoor air temperature and return air temperature, night ventilation can be used to increase the effect of passive thermal storage. Figure 45 shows indoor air temperature and outdoor air fraction of optimal control with or without economizer. Figure 46 shows the electrical energy use of the big chiller.

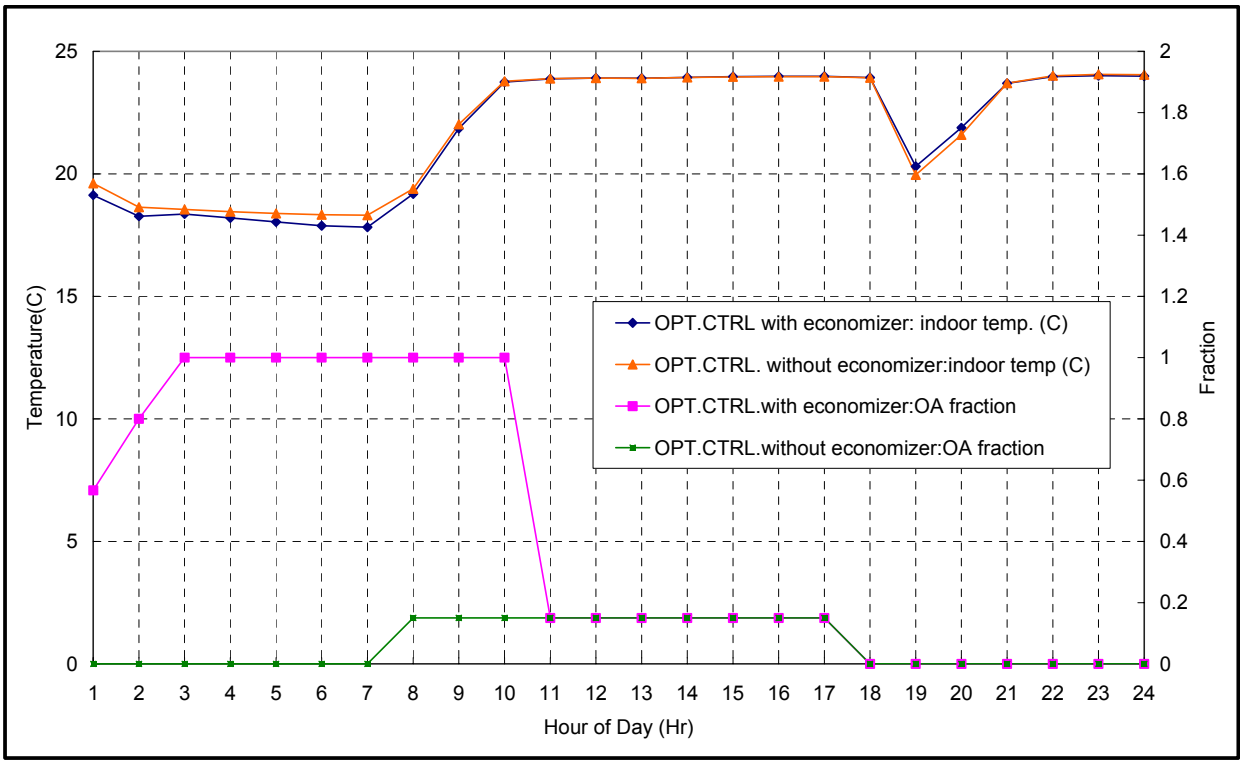

Figure 45: Indoor air temperature and OA fraction of optimal control with or without economizer

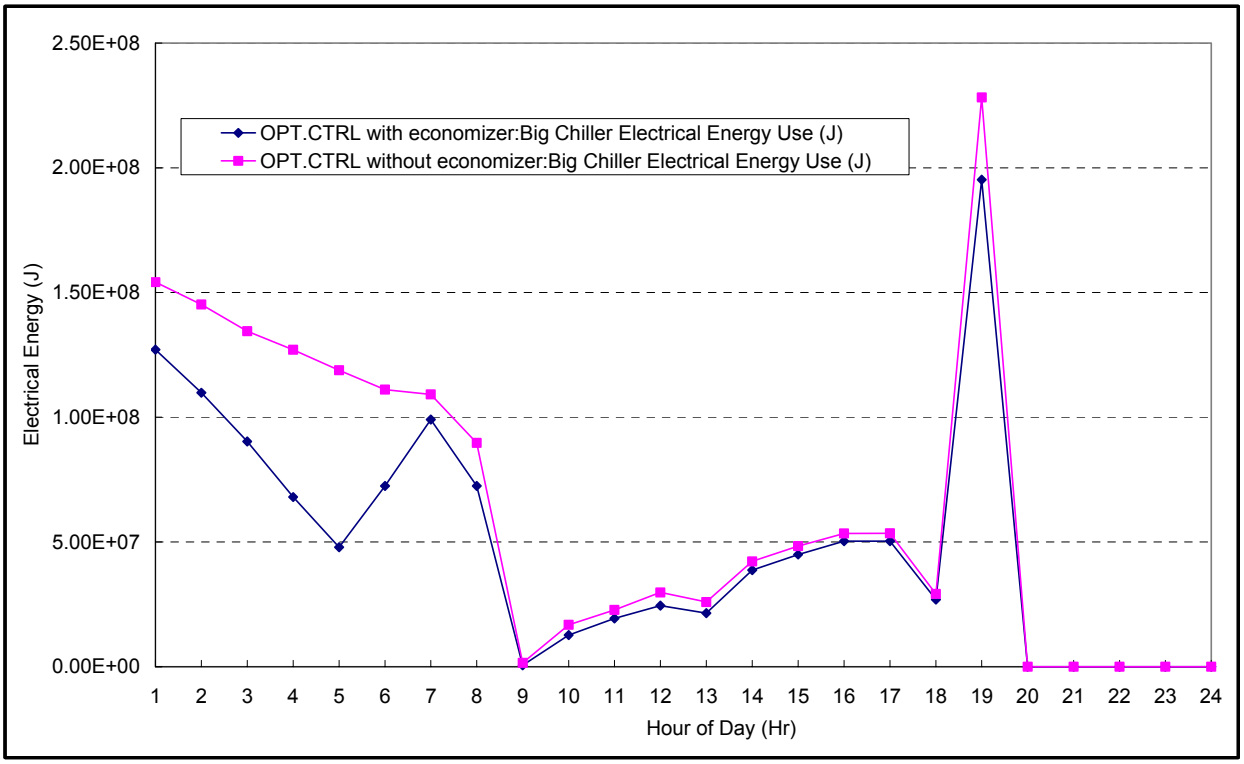

Figure 46: Chiller electrical energy use of optimial control with or without economizer

From the figures, it can be observed that in spring and winter, the economizer can take advantage of cool night air to accomplish part of the precooling. Cooling energy is saved. Table 26 summarizes the comparison of optimal control with or without economizer.

Table 26: Comparison of optimal control with or without economizer

SPRING			
	L-2	M-2	H-2
NIGHT SETBACK CTRL:TOTAL COST ($)	247.70	241.95	238.91
OPT. CTRL with ECONOMIZER	189.45	182.89	182.40
SAVINGS	-23.5%	-24.4%	-23.7%
OPT. CTRL without ECONOMIZER	195.83	189.53	187.73
SAVINGS	-20.9%	-21.7%	-21.4%

WINTER			
	L-2	M-2	H-2
NIGHT SETBACK CTRL:TOTAL COST ($)	166.47	164.62	164.31
OPT. CTRL with ECONOMIZER	122.90	127.46	127.64
SAVINGS	-26.2%	-22.6%	-22.3%
OPT. CTRL without ECONOMIZER	137.81	134.43	137.77
SAVINGS	-17.2%	-18.3%	-16.2%

3.5.3 Effect of Electrical Rate

Three electrical rate structures are considered, i.e. no-incentive, weak-incentive and strong-incentive. Figure 47 shows the indoor air temperature, ice level of optimal control under strong-incentive and weak-incentive rates. Figure 48 shows the total electrical energy use of optimal control under strong and weak incentive rates. Also shown is the indoor air temperature and total electrical energy use of night setback control.

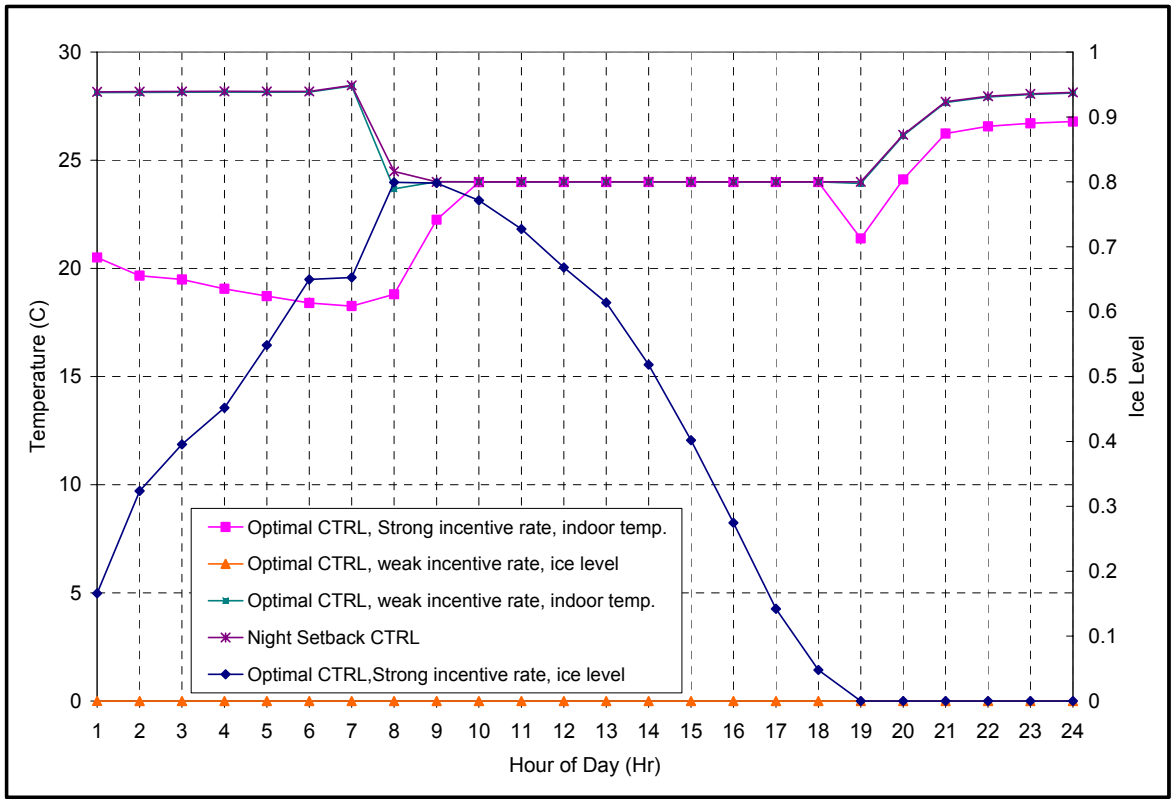

Figure 47: Optimal control variables under strong and weak electrical rate

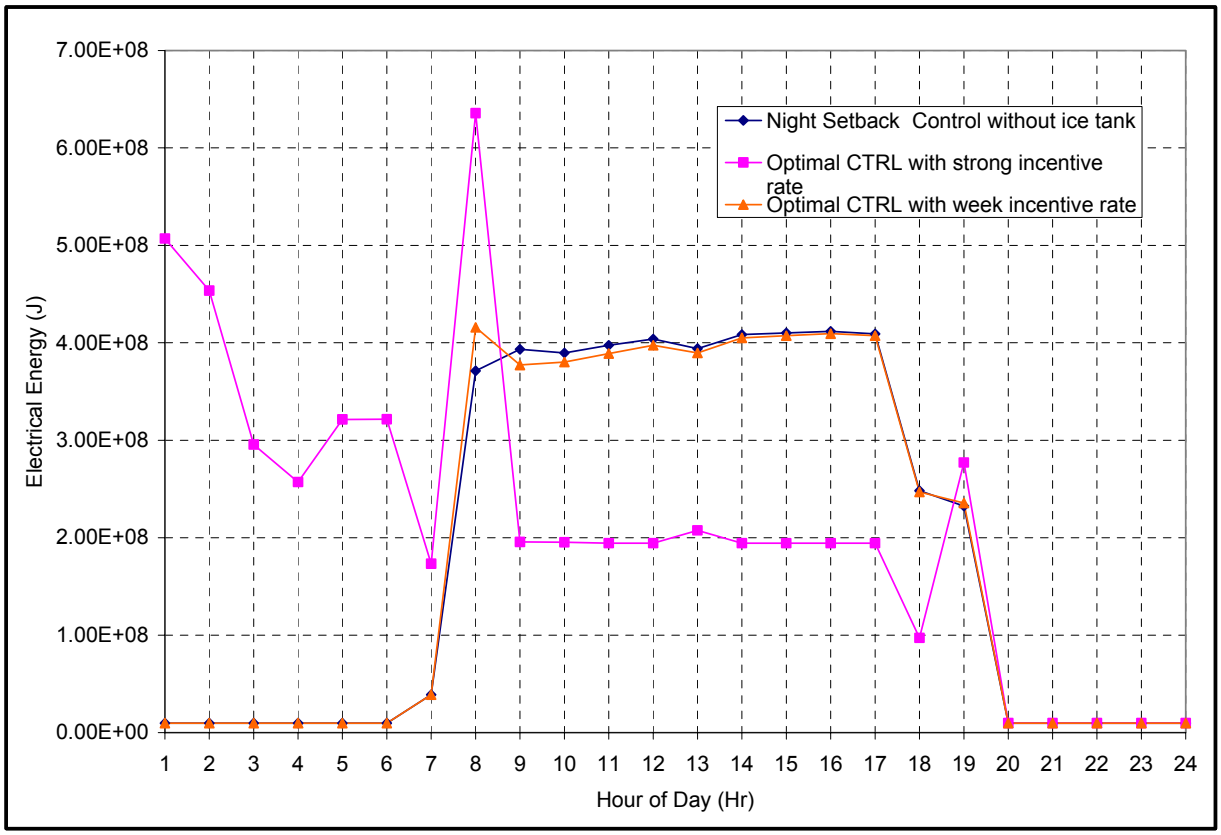

Figure 48: Optimal control total electrical energy use under strong and weak electrical rate

It can be observed that under strong electrical rate incentives, both passive and active thermal storage are made use of substantially. Before the building is occupied at 8:00, zone temperature is precooled to 18-20°C during the night and the ice tank is charged full. When building begins to be occupied and electrical rate becomes on-peak, zone air temperatures are kept at the highest limit of 24°C. The ice tank is not discharged immediately but is discharged during the whole on-peak period. Therefore, a big portion of on-peak energy is shifted to off-peak time. And the daily peak demand appears at 8:00 when off-peak demand rate is used.

Under the weak electrical rate, since the energy cost rate is flat throughout the day and the demand rate is 5$/kW off-peak and 10$/kW on-peak, there is not much the ice tank can do to shift the load due to the lower COP of the ice tank dedicated chiller. Only one hour before the on-peak rate started, i.e., at 8:00, the passive storage is precooled. The purpose of this one-hour precooling is to shift the peak demand from 14:00 during the on-peak period to 8:00 in the off-peak period. Cost saving is achieved by this peak demand shifting.

Table 27 summarized the results of optimization both the passive and active thermal inventory for different electrical rate structures. Comparing the optimally controlled TES system with a TES-less system under night time setback control (base-1), it can be observed that the higher incentive the rate structure is, the more savings can be obtained by shifting on-peak load to off-peak period by using both passive and active thermal inventories. Comparing an optimally controlled TES system with a chiller-priority controlled TES system; it can also be observed that optimal control saves more than chiller-priority control does. When using chiller-priority control, there are numerous cases that it cost more than without ice tank system. However, using optimal control can always achieve savings or at least will not cost more than no ice tank system.

Table 27: Summary of effect of electrical rate structure

SUMMER									
	L-0	L-1	L-2	M-0	M-1	M-2	H-0	H-1	H-2
base - 1	294.5	294.5	263.3	292.0	292.0	260.4	288.8	288.8	257.5
Optimal CTRL Savings	0.0%	-6.7%	-43.4%	0.0%	-6.8%	-42.4%	0.0%	-6.8%	-42.5%
base - 2	327.9	327.9	221.6	325.4	325.4	218.8	322.1	322.1	215.8
Optimal CTRL Savings	-10.2%	-16.2%	-32.7%	-10.2%	-16.4%	-31.4%	-10.3%	-16.4%	-31.3%

SPRING									
SPRING	L-0	L-1	L-2	M-0	M-1	M-2	H-0	H-1	H-2
base - 1	223.8	223.8	200.4	218.8	218.8	195.4	216.0	216.0	192.8
Optimal CTRL Savings	-1.0%	-4.2%	-34.7%	-1.7%	-6.3%	-33.8%	-1.3%	-2.7%	-33.1%
base - 2	266.3	250.0	135.4	266.2	250.0	135.4	266.0	249.7	135.3
Optimal CTRL Savings	-16.8%	-14.2%	-3.4%	-19.2%	-18.0%	-4.5%	-19.8%	-15.9%	-4.7%

WINTER									
WINTER	L-0	L-1	L-2	M-0	M-1	M-2	H-0	H-1	H-2
base - 1	149.3	149.3	131.1	148.3	148.3	130.1	147.9	147.9	129.6
Optimal CTRL Savings	-0.6%	-6.6%	-17.1%	-1.9%	-8.4%	-16.4%	0.0%	-6.5%	-16.2%
base - 2	260.7	243.8	133.7	260.7	243.8	133.7	260.7	243.8	133.7
Optimal CTRL Savings	-43.1%	-42.8%	-18.7%	-44.2%	-44.3%	-18.7%	-43.3%	-43.3%	-18.7%

3.5.4 Effect of Season

Three seasons are considered, i.e. summer, spring, winter. Figure 49 shows the indoor air temperature, ice inventory level of optimal control in summer and spring. Figure 50 shows the total electrical energy use of optimal control in summer and spring. Also shown is the indoor air temperature and total electrical energy use of nighttime setback control.

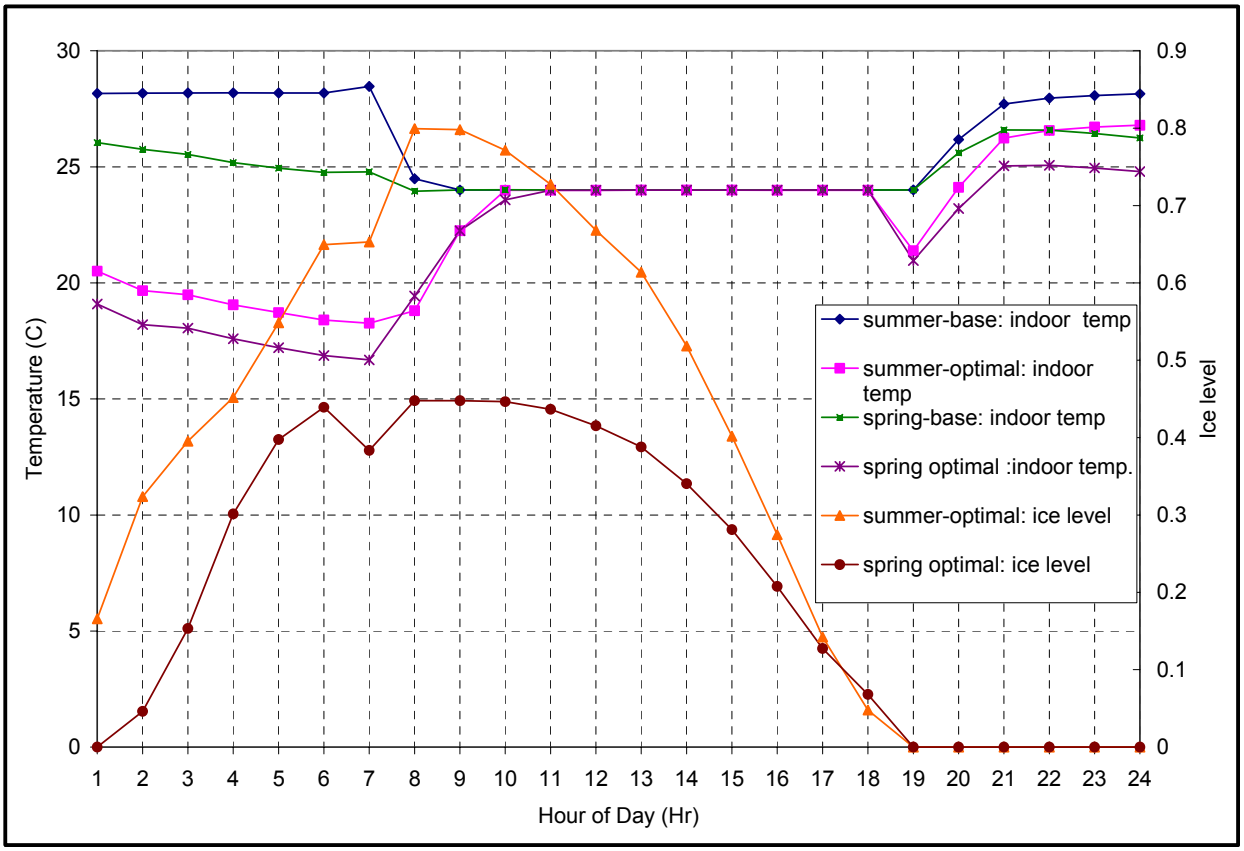

Figure 49: Indoor temperature and ice level of optimal control in summer and spring

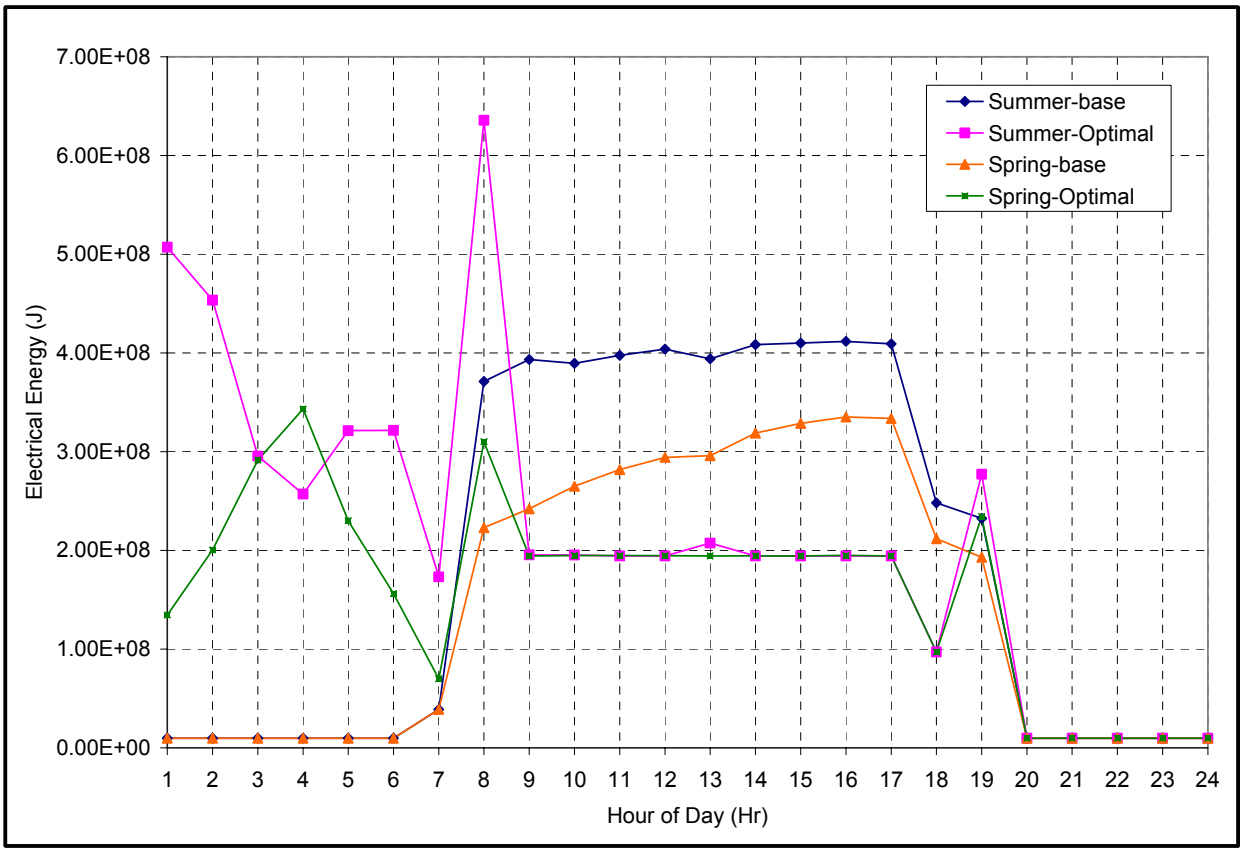

Figure 50: Total energy use of optimal control in summer and spring

It can be observed that in summer and spring, both passive and active storage are optimized so that almost all of the cooling-related electrical energy of the total electrical energy is shifted to off-peak hours. In the summer, cooling electrical energy is about 50% of total electrical energy used. In spring, cooling electrical energy is about 34% of total electrical energy used. Under strong-incentive rate, there is more energy shifted to off-peak hours in summer than in spring or winter. If the plant size is large enough, a large amount of savings can be achieve in summer than in spring or winter. The seasonal effect can also be observed in Table 27.

3.5.5 Effect of Plant Size

Figure 51 shows the indoor air temperature and ice storage inventory level of two plants of different sizes. Plant 1 has big chiller capacity of 200 kW and ice tank size of 300 kWh. Plant 2 has big chiller capacity of 300 kW and ice tank size of 300 kWh. Figure 52 shows the total electrical energy uses. Summary of results from different plant sizes is included in Table 28.

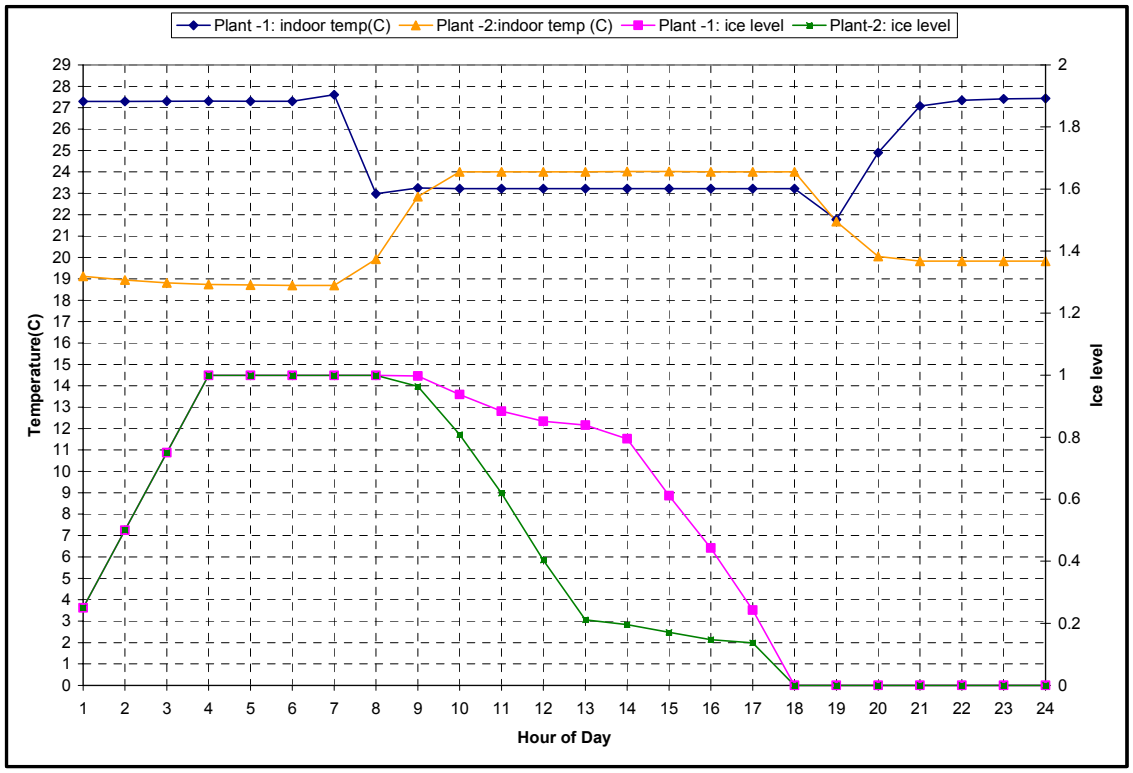

Figure 51: Indoor temp and ice level of optimal control of two plants

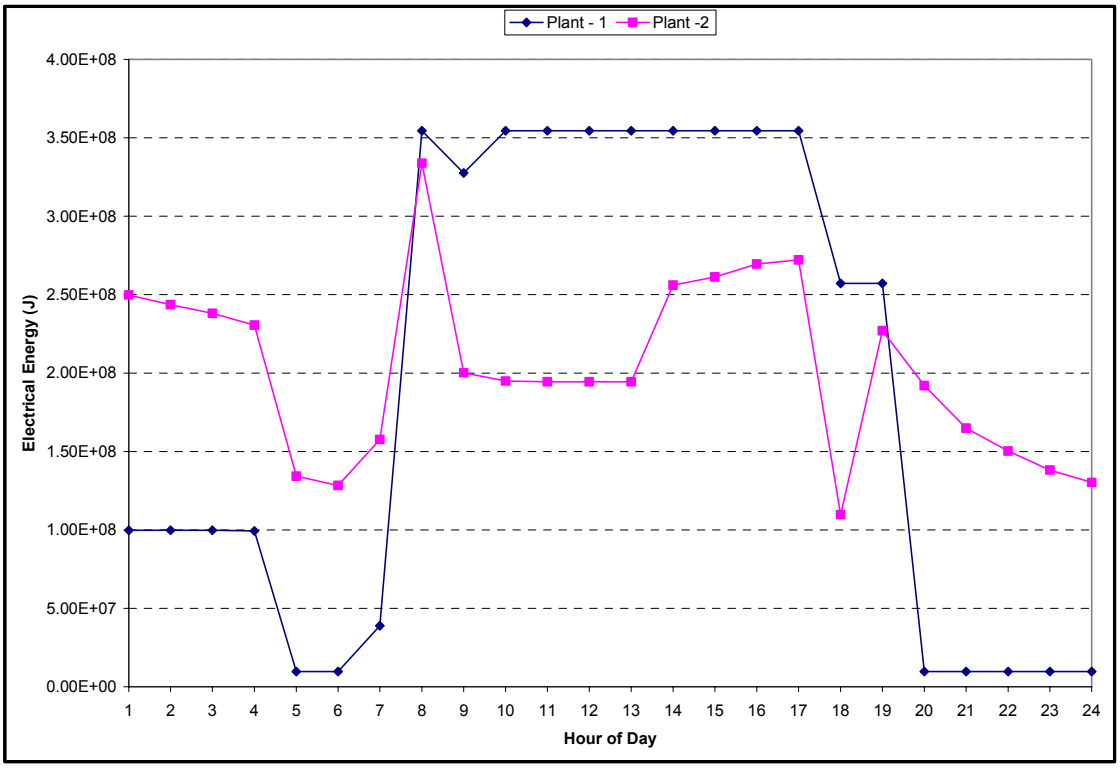

Figure 52: Total electrical energy use of optimal control of two plants

Table 28: Summary of optimal control costs and savings of different plants

	Chiller 500 KW, Tank 1500 KWH
BASE	257.48
OPTIMAL	148.15
SAVING	-42.5%
	CHILLER 200 KW, TANK 1500 KWH
BASE	235
OPTIMAL	230
SAVING	-2.1%
	CHILLER 200 KW, TANK 300 KWH
BASE	235
OPTIMAL	206
SAVING	-12.3%
	CHILLER 300 KW, TANK 300 KWH
BASE	235
OPTIMAL	157
SAVING	-33.2%
	CHILLER 300 KW, TANK150 KWH
BASE	235
OPTIMAL	161
SAVING	-31.5%
	CHILLER 300 KW, TANK400 KWH
BASE	235
OPTIMAL	154
SAVING	-34.5%
	CHILLER 300 KW, TANK400 KWH
BASE	235
OPTIMAL	163
SAVING	-30.6%

It can be observed that as the big chiller sizes down, it has less capability to do precooling, i.e., to make use of the passive thermal inventory. As the ice tank is sized down, it has less capacity to make use of the active thermal inventory.

3.5.6 Effect of Thermal Comfort Penalty

When thermal comfort is considered, the cost function of the optimization routine becomes:

$$CostFunctionValue = TotalElectricalCost(1 + ThermalComfortPenalty)$$

The thermal comfort penalty coefficient is calculated as follows:

At hour *t*, the Fanger PMV value of the building is the PMV value of the most uncomfortable zone, i.e.,

$$PMV_t = \max\left(\left|PMV_j\right|\right) \text{ for } j = 1,\ldots,\text{number of zones}$$

The hourly thermal comfort penalty coefficient at hour t is,

$R_t = 0$ if $PMV_t \le 0.5$ or if the building is unoccupied

$R_t = 1$ if $PMV_t > 2.0$ and the building is occupied

$R_t = \left[\frac{PMV_t - 0.5}{1.5}\right]^2$ if $0.5 < PMV_t \le 2.0$ and the building is occupied

And the total thermal comfort penalty coefficient is the sum of hourly thermal comfort penalty coefficient over the optimizing period, i.e.,

$$ThermalComfortPenalty = \sum_t PMV_t$$

Figure 53 shows the *PMV* value of each zone at each hour under optimized indoor air temperature *without* thermal comfort penalty. Figure 54 shows the PMV value of each zone at each hour under optimized indoor air temperature *with* thermal comfort penalty.

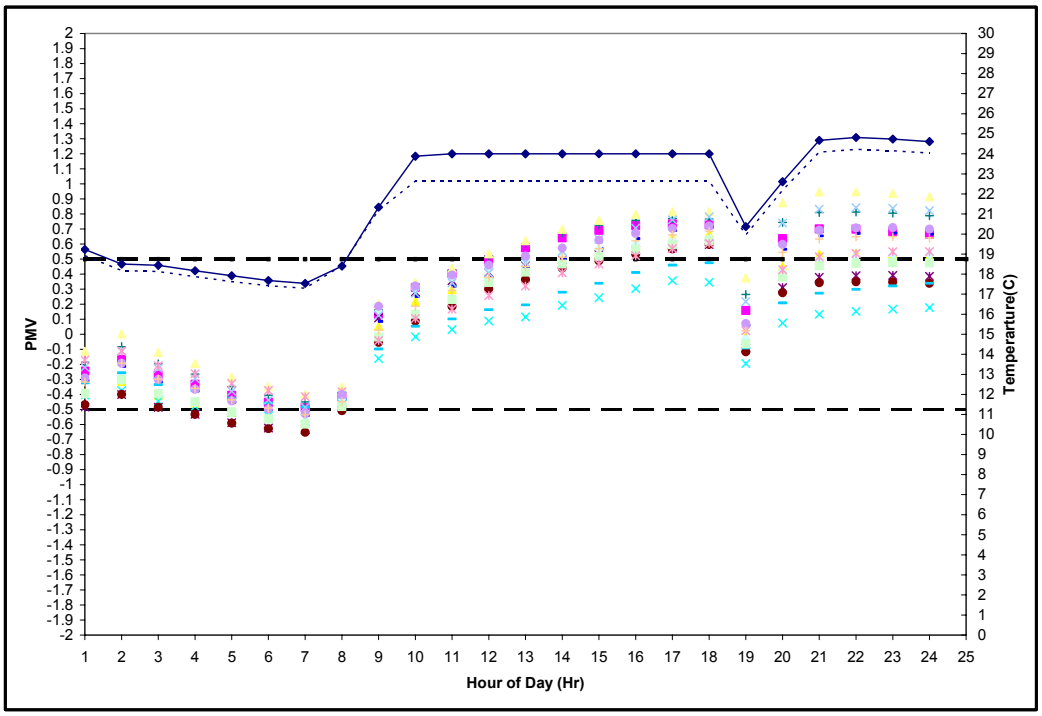

Figure 53: Indoor temperature and PMV value of optimal control without thermal comfort penalty

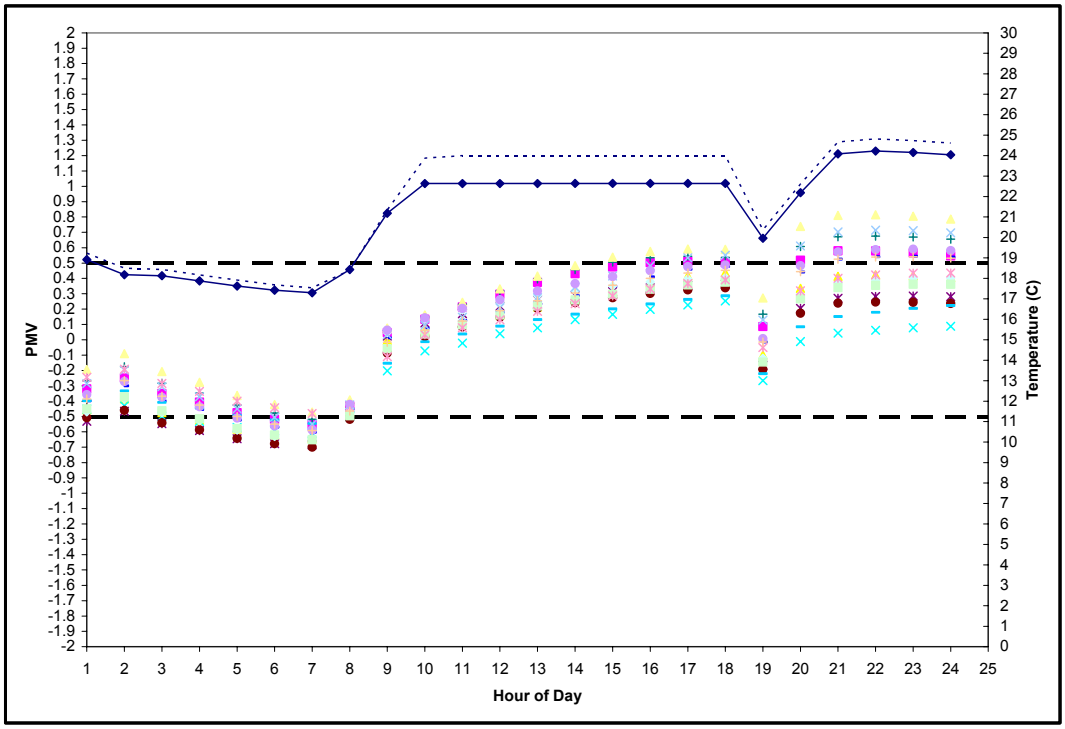

Figure 54: Indoor temperature and PMV value of optimal control with thermal comfort penalty

It can be observed from the above figures that without thermal comfort penalty, indoor temperature during occupied period (8:00-19:00) is kept at 24°C. In the afternoon (after 13:00) most of the zones are too warm. Thermal comfort penalty coefficient is 0.182. With thermal comfort penalty, indoor temperature during occupied period is kept at 22.8°C. Almost all of the zones are in comfort area (-0.5 ≤ PMV ≤ 0.5). The thermal comfort penalty coefficient is reduced to 0.0106. Table 29 summarizes some optimal control comparisons with or without thermal comfort penalty.

Table 29: Comparison of optimal control with or without thermal comfort penalty

SPRING			
	L-2	M-2	H-2
Night Setback Control:Total Cost ($)	200	195	193
Thermal CMFT penalty	1.07	0.82	0.733
Optimization Without Thermal Comfort Penalty:Total Cost ($)	130.8	129.3	129.0
Thermal CMFT penalty	0.456	0.182	0.117
Total Cost Savings compared with night setback control	-34.6%	-33.7%	-33.2%
Cost function with Thermal CMFT penalty	139.1	131.1	130.2
Thermal CMFT penalty	0.008	0.011	0.012
Total Cost Savings compared with night setback control	-30.5%	-32.8%	-32.6%

SUMMER			
	L-2	M-2	H-2
Night Setback Control:Total Cost ($)	263	260	257
Thermal CMFT penalty	1.86	1.63	1.53
Optimization Without Thermal Comfort Penalty:Total Cost ($)	149.2	150.1	148.2
Thermal CMFT penalty	0.673	0.245	0.209
Total Cost Savings compared with night setback control	-43.3%	-42.3%	-42.4%
Cost function with Thermal CMFT penalty	157.1	152.5	150.5
Thermal CMFT penalty	0.020	0.013	0.015
Total Cost Savings compared with night setback control	-40.3%	-41.4%	-41.4%

Without thermal comfort penalty, total electrical costs for optimal control are slightly lower than with thermal comfort penalty. The thermal comfort penalty coefficient is high in the case of nighttime setback control.

Observing the thermal comfort penalty coefficient in Table 29, it can be found that when conducting optimization without thermal comfort penalty, the light-mass building has a higher penalty than the heavy-mass building when both indoor air temperatures are about 24°C. This is because the mean radiant temperature of the heavy-mass building is less than that of the light-mass building. Therefore, when thermal comfort penalty is introduced in optimization, the light-mass building tends to lose more savings than the heavy-mass building does.

3.5.7 Comparison of Passive Thermal Inventory and Active Thermal Inventory

Table 30 lists a comparison of optimal control of passive storage only, active storage only and sequential optimization of passive and active system.

Table 30: Comparison of optimal control of passive and active system

SUMMER									
	L-0	**L-1**	**L-2**	**M-0**	**M-1**	**M-2**	**H-0**	**H-1**	**H-2**
BASE	295.00	294.53	263.31	292.04	292.04	260.43	288.78	288.78	257.48
ZS	294.14	275.17	179.95	291.67	272.16	166.78	288.16	287.13	164.10
SAVING	-0.3%	-6.6%	-31.7%	-0.1%	-6.8%	-36.0%	-0.2%	-0.6%	-36.3%
TES(NS)	295.00	285.43	183.56	292.04	285.89	181.38	288.78	281.11	178.95
SAVING	0.0%	-3.1%	-30.3%	0.0%	-2.1%	-30.4%	0.0%	-2.7%	-30.5%
TES(ZS)	294.14	275.17	149.15	291.67	272.16	150.12	288.16	273.27	148.15
SAVING	-0.3%	-6.6%	-43.4%	-0.1%	-6.8%	-42.4%	-0.2%	-5.4%	-42.5%

SPRING									
	L-0	**L-1**	**L-2**	**M-0**	**M-1**	**M-2**	**H-0**	**H-1**	**H-2**
BASE	223.78	223.78	200.37	218.77	218.77	195.40	215.97	215.97	192.78
ZS	220.08	223.78	145.43	215.07	217.66	138.22	213.16	215.87	137.04
SAVING	-1.7%	0.0%	-27.4%	-1.7%	-0.5%	-29.3%	-1.3%	0.0%	-28.9%
TES(NS)	223.78	212.45	133.25	218.77	212.47	131.99	215.97	210.92	131.70
SAVING	0.0%	-5.1%	-33.5%	0.0%	-2.9%	-32.5%	0.0%	-2.3%	-31.7%
TES(ZS)	220.08	212.45	130.75	215.07	209.57	129.28	213.16	210.10	129.01
SAVING	-1.7%	-5.1%	-34.7%	-1.7%	-4.2%	-33.8%	-1.3%	-2.7%	-33.1%

It can be observed from Table 30 that optimization of passive system only can achieve savings even when there is no incentive in the electrical rate. This is because beside the electrical rate incentive, the passive system can also take advantage of the cooler outdoor environment during the night. On the other hand, the active system cannot achieve savings when there is no incentive in the electrical utility rate. This is due to the lower COP of the dedicated chiller of the active system: the cooling provided by discharging of the ice is less cost-effective than the cooling provided by the big chiller with higher COP directly. If there is no incentive in the electrical rate, it is better to simply employ the big chiller.

3.6 Closed-Loop Optimization with Moving Length ML = 1 hour

The utility rate selected for this analysis is $0.20/kWh on-peak and $0.05/kWh off-peak, no demand charge is levied. The on-peak period is weekdays from 9 AM to 6 PM, off-peak all remaining hours. The building is occupied from 7 AM to 5 PM.

The viewgraphs in this section are created on the basis of simulation in which July 21 in Phoenix, AZ is repeated over and over again until steady-state conditions are attained after about 7 identical days. The outdoor ambient temperature swings from about 16°C early in the morning to over 38°C at 6 PM. Table 31 lists the nominal capacities of the base chiller and the active storage and chiller capacities for the five investigated cases.

Case 1 represents the basecase in which cooling loads have to be met without any storage available. Case 2 makes use active thermal storage as governed by chiller-priority control, i.e., the downsized base chiller meets the cooling loads up to its capacity $CCAP_{base}$, thereafter the active storage contributes the remainder. The dedicated active storage chiller requires SCAP/$CCAP_{tes}$ = 10 hours to recharge an empty storage tank. Case 3 optimizes the passive storage capacity by properly precooling the building structure using a fully sized base chiller. In Case 4, the active storage is now optimized instead of governed by a simple rule such as chiller-priority. Finally, Case 5 optimizes both active and passive storage media is represents the focus of this research.

Case 5 is solved in two ways: First, we employ the closed-loop optimization (CLO) described above using a moving time window of *WL* = 24 hours length and hourly updates *ML* = 1 hour. Second, we optimize each 24 hour interval sequentially, i.e. as a series of consecutive time blocks (CTBO) of *ML* = 24 hours length each. The CTBO method does not allow for the consideration of newly available new information as it becomes available. However, it represents a reference scenario for comparison as we assume perfect prediction for this study. Both, CLO and CTBO should produce similar results.

Table 31: System Sizing for Investigated Control Strategies

Case No.	Optimization	Units	Sizing
1	**Basecase WITHOUT Active Storage**		
	CCAPbase	kW	500
	CCAPtes	kW	0
	SCAP	kWh	0
			Base chiller fully sized, no active storage; night setup.
2	**Basecase WITH Active Storage**		
	CCAPbase	kW	250
	CCAPtes	kW	250
	SCAP	kWh	2,500
			Base chiller downsized; chiller-priority active storage control; night setup.
3	**Passive Only**		
	CCAPbase	kW	500
	CCAPtes	kW	0
	SCAP	kWh	0
			Base chiller fully sized, no active storage; zone setpoints optimized.
4	**Active Only**		
	CCAPbase	kW	500
	CCAPtes	kW	250
	SCAP	kWh	2,500
			Base chiller fully sized; optimal active storage control; night setup.
5	**Active and Passive**		
	CCAPbase	kW	500
	CCAPtes	kW	250
	SCAP	kWh	2,500
			Base chiller fully sized; optimal active storage control; zone setpoints optimized.

The blue lines in Figure 55 represent the upper and lower temperature bounds for the operation of the office building. It can be seen how passive only decides on substantial nighttime precooling down to about 21°C zone temperature averaged over all 15 zones. When the temperatures are allowed to float, the average zone temperature rises beyond 28°C during unoccupied times. The combined utilization of active and passive storage leads to less precooling than in the passive only case. All strategies involving passive storage allow for the temperatures to float from the end of occupancy at 5 PM to 6 PM because electricity prices are still high during this time. After 6 PM, electricity prices are low and the building is unoccupied. The consecutive time block optimization (CTBO) of the combined case is much smoother and precooling is stronger than for the closed-loop optimization case.

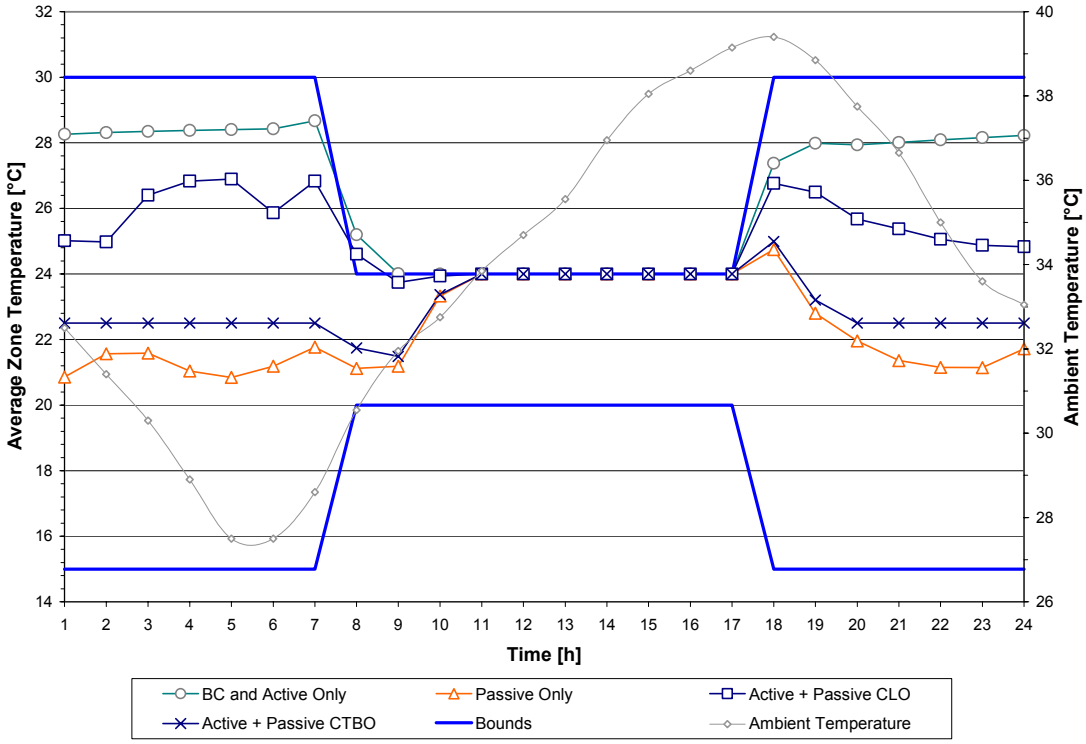

Figure 55: Average Zone Temperature Profiles

The inventory of state-of-charge of the active storage is shown in Figure 56 from midnight to midnight for those strategies involving active storage. For the basecase with active storage under chiller-priority control, the storage is fully charged during off-peak hours and discharged by about 50% during the day. The active only optimization discharges fast as of 8 AM, but slows down during the early afternoon hours to end up empty by the end of occupancy. The closed-loop optimization of the combined storage discharges a full storage evenly to end up empty by 5 PM already. The CTBO approach makes less use of the active storage. Thus, there appears to be a trade-off between active and passive storage utilization that has little overall cost function impact.

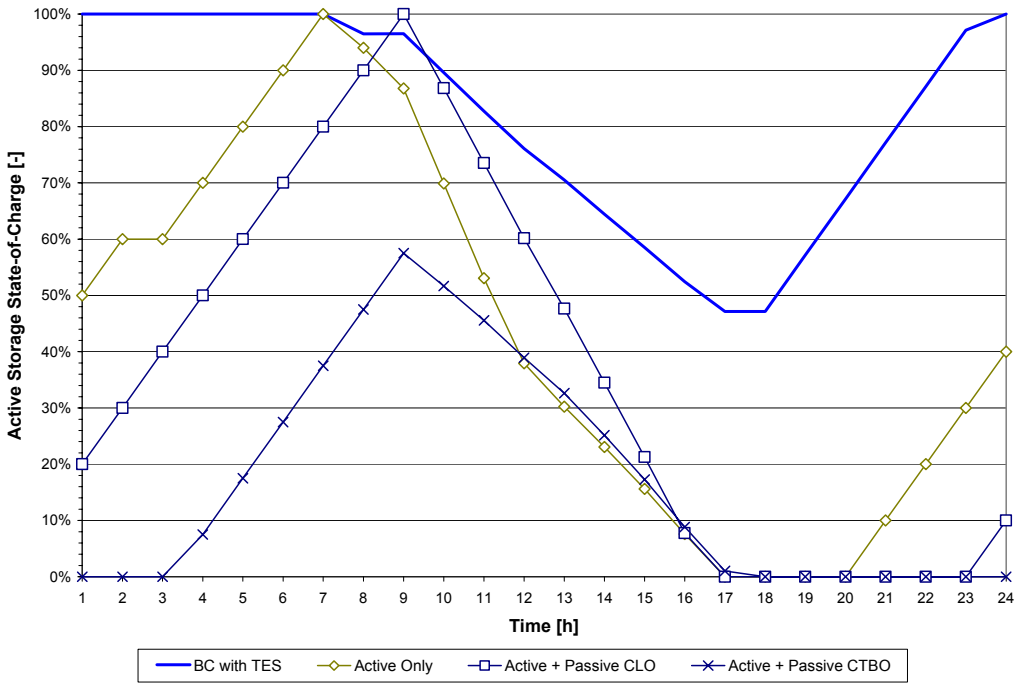

Figure 56: Active Storage State-of-Charge Profiles

Figure 40 illustrates the effect of precooling on the daytime cooling load profile and shows how the building cooling load is shifted away from the expensive on-peak period to the off-peak period for all cases involving passive storage utilization. The passive only approach leads to the lowest on-peak cooling loads, next comes the CTBO approach to the combined case and finally the CLO approach.

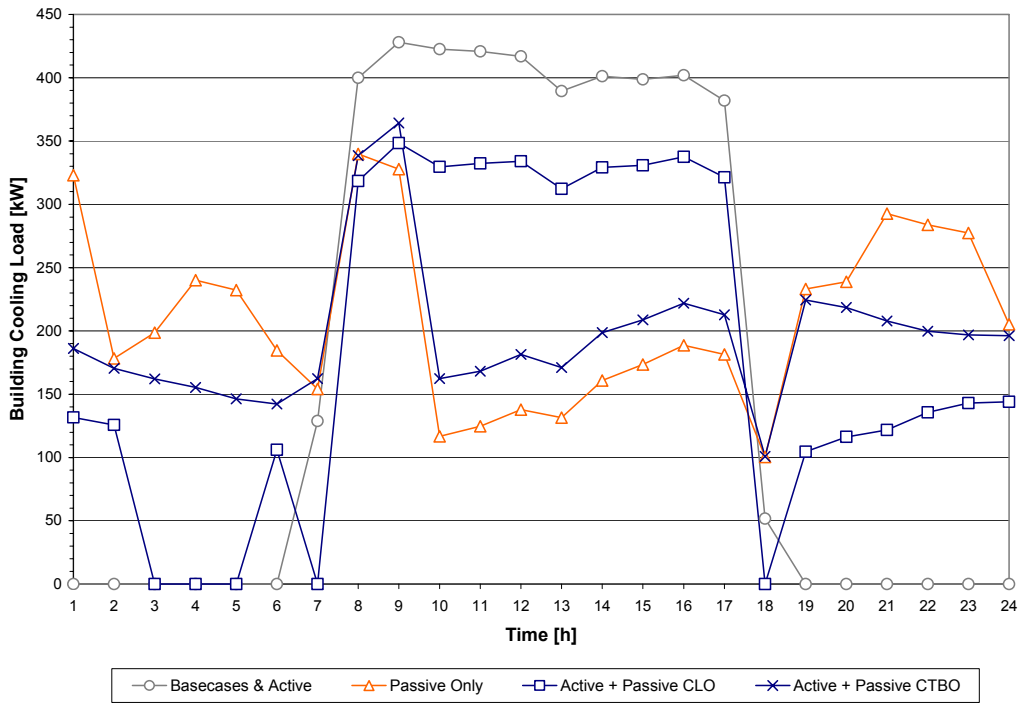

Figure 57: Building Cooling Load Profiles

Reducing on-peak electrical demand is a side effect of shifting expensive on-peak cooling loads to off-peak periods as can be see in Figure 58. While the basecase with active storage under chiller-priority control already reduces the demand by 20%, the combined optimization cuts the overall demand nearly in half. For CLO of the combined case at the end of occupancy, the demand is raised from its lowest value since the active storage is depleted and the base chiller has to pick up the remainder of the load. Since demand charges are not imposed in this example, the combined optimization is valid in spite of the apparent demand violation at 5 PM. Active only and passive only are both superior to the basecase with active storage, but inferior to the combined case solved by either CLO or CTBO.

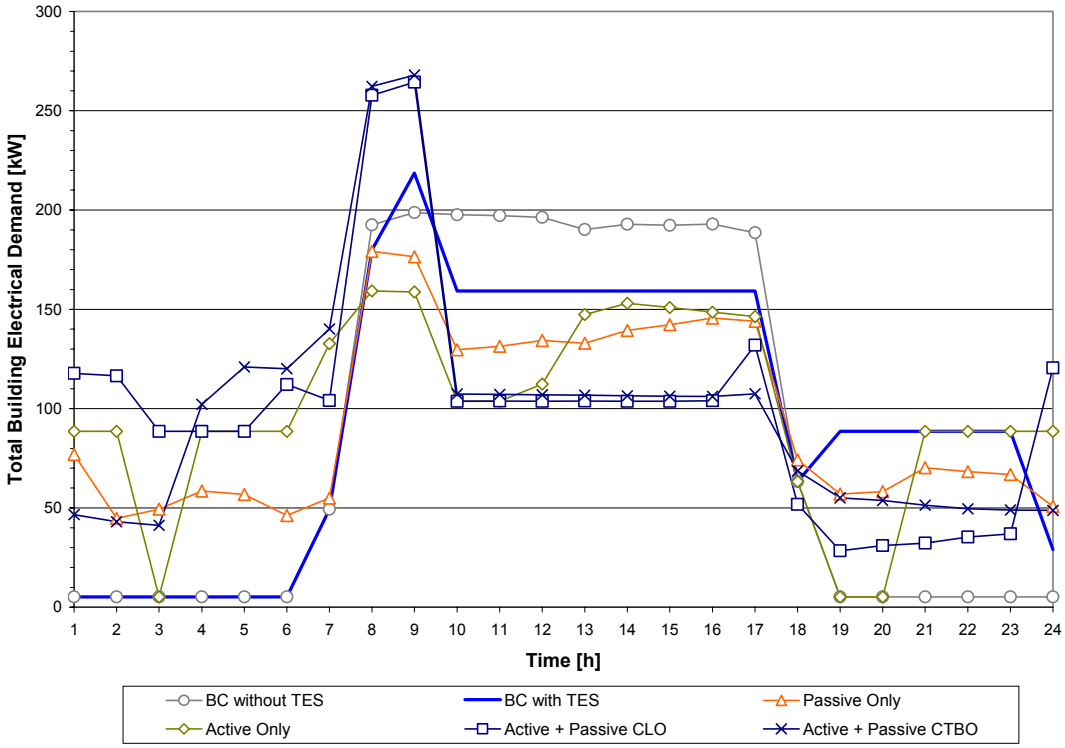

Figure 58: Total Building Electrical Demand Profiles

For a utility rate without demand charges, we can plot daily profiles of utility cost. The total building hourly operating cost including non-cooling cost is shown in Figure 59. The areas under each curve represent the total daily operating cost. It is obvious that on-peak cost savings are traded off against nighttime expenses for recharging active and/or passive storage inventories.

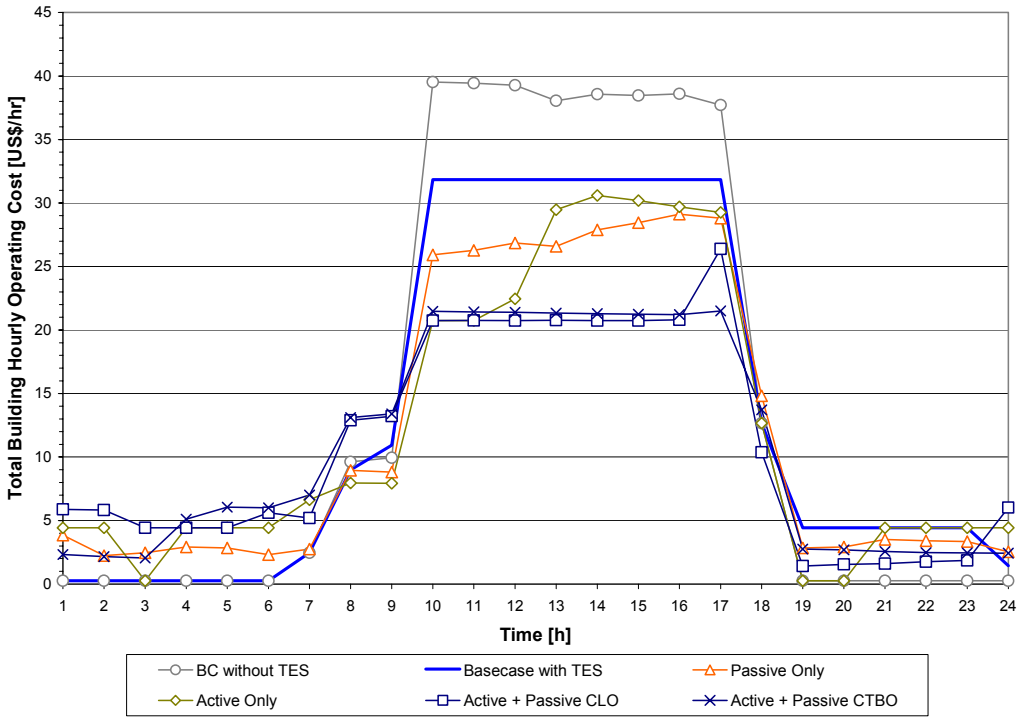

Figure 59: Total Building Hourly Operating Cost Profiles

Figure 60 illustrates how the cooling related costs are effectively shifted to nighttime periods. In fact, the combined storage cases lead to near-zero cooling costs during the on-peak period, except for the hour of 5 PM for the CLO case, when the base chiller has to be brought online prematurely.

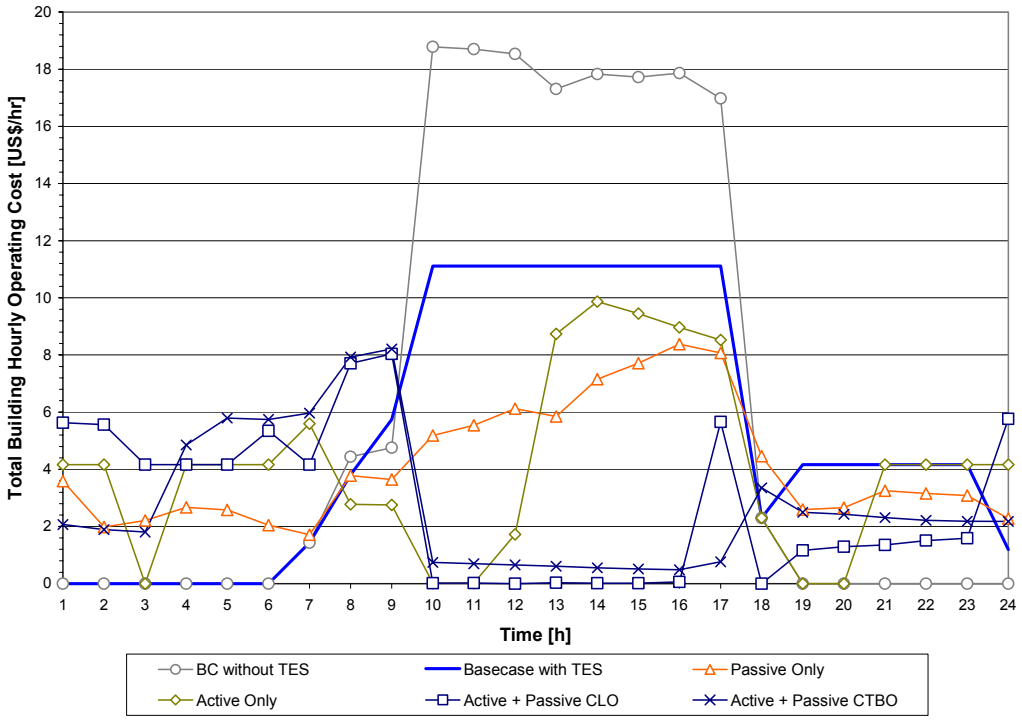

Figure 60: HVAC Hourly Operating Cost Profiles

Finally, Table 32 provides an overview of the daily cost savings achieved for this prototypical day in Phoenix, AZ. Based on total utility cost, savings of about 16% can be achieved for either passive or active only storage, and about 26% for the combined case when compared to the basecase without storage. Compared to the basecase with active storage under chiller-priority control, savings of about 8% can be achieved for either passive or active only storage and about 18% for the combined case. Based on cooling related utility cost only, savings of about 37% can be achieved for either passive or active only storage, and about 57% for the combined case when compared to the basecase without storage. Compared to the basecase with active storage under chiller-priority control, savings of about 20% can be achieved for either passive or active only storage and about 46% for the combined case. These results show that given strong load-shifting incentives, the benefits of the proposed optimization system may be substantial.

Table 32: Summary of Daily Operating Costs

Total Building Hourly Operating Cost

Basecase without TES	Basecase with TES	Passive Only	Active Only	Active + Passive CLO	Active + Passive CTBO
$ 347.42	$ 314.97	$ 290.46	$ 289.00	$ 258.20	$ 257.22
Savings	BC without TES:	16.4%	16.8%	25.7%	26.0%
	BC with TES:	7.8%	8.2%	18.0%	18.3%

HVAC Hourly Operating Cost

Basecase without TES	Basecase with TES	Passive Only	Active Only	Active + Passive CLO	Active + Passive CTBO
$ 156.65	$ 124.20	$ 99.69	$ 98.23	$ 67.42	$ 66.45
Savings	BC without TES:	36.4%	37.3%	57.0%	57.6%
	BC with TES:	19.7%	20.9%	45.7%	46.5%

3.7 Summary

In this chapter, predictive optimal control of building passive and active thermal inventory was studied. The optimal control of building TES varies depends on many factors including building mass level, electrical rate structure, season, plant/system characteristics etc. Optimal control for a specific case needs to be calculated by optimization routines.

The introduction of thermal comfort penalty in the objective value calculation in optimizing helps to improve the thermal comfort level of the building while maintains cost savings.

Due to the uncertainty of future weather data, predictive optimal control needs to be updated and the optimal control of the building needs to be adjusted. The accuracy of optimal control is determined by factors like the weather prediction accuracy, updating frequency, etc.

On average, predictive optimal control of building passive and active thermal inventory can achieve savings of 5-45% of total electrical costs.

4 Conclusion

Cooling of commercial buildings contributes significantly to the peak demand placed on an electrical utility grid. Time-of-use electricity rates encourage shifting of electrical loads to off-peak periods at night and weekends. Buildings can respond to these pricing signals by shifting cooling-related thermal loads either by precooling the building's massive structure or the use of active thermal energy storage systems such as ice storage. While these two thermal batteries have been engaged separately in the past, this project investigated the merits of harnessing both storage media concurrently in the context of predictive optimal control.

The research results presented in this topical report covers the first of three project phases. Based on the dynamic building simulation program EnergyPlus, we added a utility rate module, two thermal energy storage models, and incorporated a sequential optimization approach to the cost minimization problem using direct search, gradient-based, and dynamic programming methods. The objective function is the total utility bill including the cost of heating and a time-of-use electricity rate with demand charges. The evaluation of the combined optimal control assumes perfect weather prediction and match between the building model and the actual building counterpart.

The analysis shows that the combined utilization leads to cost savings that is significantly greater than either storage but less than the sum of the individual savings. The findings reveal that the cooling-related on-peak electrical demand of commercial buildings can be drastically reduced and justify the development of a predictive optimal controller that accounts for uncertainty in predicted variables and modeling mismatch in real time.

5 References

1. Energy Information Administration (EIA/DOE) (2000) *Annual Energy Review 1999*. U.S. Department of Energy. URL: http://www.eia.doe.gov/emeu/aer/enduse.html. June 2000.
2. Arthur D. Little, Inc. (1999) *Guide for Evaluation of Energy Savings Potential*. Prepared for the Office of Building Technology, State and Community Programs (BTS), U.S. Department of Energy.
3. American Refrigeration Institute (ARI) (1999) *Statistical Profile of the Air-Conditioning, Refrigeration, and Heating Industry*. Page 28. 4301 North Fairfax Drive, Arlington, VA. 1999.
4. American Standard, Inc. (1999) *EarthWise Today*, Vol. 24, p. 3. LaCrosse, Wisconsin.
5. National Energy Technology Laboratory (NETL/DOE) (2000) *Federal Assistance Solicitation for Energy Efficient Building Equipment and Envelope Technologies Round II*. PS No. DE-PS26-00NT40781. Page 4. U.S. Department of Energy.
6. Kaya, A., C.S. Chen, S. Raina, and S.J. Alexander (1982) "Optimum control policies to minimize energy use in HVAC systems." *ASHRAE Transactions*, Vol. 88, pt. 2, American Society of Heating, Refrigerating, and Air-Conditioning Engineers, Atlanta, Georgia.
7. Braun, J.E., S.A. Klein, W.A. Beckman, and J.W. Mitchell (1989) "Methodologies for optimal control of chilled water systems without storage." *ASHRAE Transactions*, Vol. 95, pt. 1, American Society of Heating, Refrigerating, and Air-Conditioning Engineers, Atlanta, Georgia.
8. House, J.M., T.F. Smith, J.S. Arora (1991) "Optimal Control of a thermal system." *ASHRAE Transactions*, Vol. 97, pt. 1, American Society of Heating, Refrigerating, and Air-Conditioning Engineers, Atlanta, Georgia.
9. Kasahara, M., T. Matsuba, Y. Hashimoto, I. Murasawa, A. Kimbara, K. Kamimura, and S. Kurosu (1998) "Optimal Preview Control for HVAC System." *ASHRAE Transactions*, Vol. 104, pt. 1, American Society of Heating, Refrigerating, and Air-Conditioning Engineers, Atlanta, Georgia.
10. Henze, G.P., M. Krarti, and M.J. Brandemuehl (1997a) "A Simulation Environment for the Analysis of Ice Storage Controls" *International Journal of HVAC&R Research*, 3/2 128–148, American Society of Heating, Refrigerating, and Air-Conditioning Engineers, Atlanta, Georgia.
11. Henze, G.P., R.H. Dodier, and M. Krarti (1997b) "Development of a Predictive Optimal Controller for Thermal Energy Storage Systems." *International Journal of HVAC&R Research*, 3/3 233–264, American Society of Heating, Refrigerating, and Air-Conditioning Engineers, Atlanta, Georgia.
12. Henze, G.P. and M. Krarti (1998) "Ice Storage System Controls for the Reduction of Operating Costs and Energy." *Journal of Solar Energy Engineering*, November 1998, American Society of Mechanical Engineers, New York, New York.
13. Henze, G.P. and M. Krarti (1999) "The Impact of Forecasting Uncertainty on the Performance of a Predictive Optimal Controller for Thermal Energy Storage Systems." *ASHRAE Transactions*, Vol. 105, pt. 1, American Society of Heating, Refrigerating, and Air-Conditioning Engineers, Atlanta, Georgia.
14. Marken, A.V. (1997) "Control of Thermal Energy Storage Systems for Cost-Effectiveness." Internal Report, University of Colorado, Boulder, CO.
15. Bell, D. (1998) "Evaluation of Optimal Controls for Ice-Based Thermal Energy Storage Systems." M.S. Thesis, University of Colorado, Boulder, CO.
16. Massie, D. (1998) "Optimal Neural Network-Based Controller for Ice Storage Systems." Ph.D. dissertation, University of Colorado, Boulder, CO.

17. Gibson, G.L. (1997) "A supervisory controller for optimization of building central cooling systems." *ASHRAE Transactions*, Vol. 103, pt. 1, American Society of Heating, Refrigerating, and Air-Conditioning Engineers, Atlanta, Georgia.
18. Drees, K.H. and J.E. Braun (1996) "Development and evaluation of a rule-based control strategy for ice storage systems" *International Journal of HVAC&R Research*, 2/4 312–336, American Society of Heating, Refrigerating, and Air-Conditioning Engineers, Atlanta, Georgia.
19. Braun, J.E. (1990) "Reducing energy costs and peak electrical demand through optimal control of building thermal mass." *ASHRAE Transactions*, Vol. 96, pt. 2, American Society of Heating, Refrigerating, and Air-Conditioning Engineers, Atlanta, Georgia.
20. Conniff, J.P. (1991) "Strategies for reducing peak air-conditioning loads by using heat storage in the building structure." *ASHRAE Transactions*, Vol. 97, pt. 1, American Society of Heating, Refrigerating, and Air-Conditioning Engineers, Atlanta, Georgia.
21. Morris, F.B., J.E. Braun, and S.J. Treado (1994) "Experimental and simulated performance of optimal control of building thermal storage." *ASHRAE Transactions*, Vol. 100, pt. 1, American Society of Heating, Refrigerating, and Air-Conditioning Engineers, Atlanta, Georgia.
22. Keeney, K.R. and J.E. Braun (1996) "A simplified method for determining optimal cooling control strategies for thermal storage in building mass." *International Journal of HVAC&R Research*, 2/1 59–78, American Society of Heating, Refrigerating, and Air-Conditioning Engineers, Atlanta, Georgia.
23. Mozer, M.C., L. Vidmar, and Robert H. Dodier (1997) "The Neurothermostat: Predictive optimal control of residential heating systems" *Advances in Neural Information Processing Systems*. MIT Press. Cambridge, MA.
24. Kintner-Meyer, M. and A.F. Emery "Optimal control of an HVAC system using cold storage and building thermal capacitance." Energy and Buildings No. 23, pp. 19–31. Elsevier Science Inc., New York, NY.
25. Krarti, M., M.J. Brandemuehl, and G.P. Henze (1995) "Final Project Report for ASHRAE 809-RP: Evaluation of Optimal Control for Ice Storage Systems." *ASHRAE Report*, American Society of Heating, Refrigerating, and Air-Conditioning Engineers, Atlanta, Georgia.
26. Krarti, M., G.P. Henze, D. Bell, J.F. Kreider, M.J. Brandemuehl, and L.K. Norford (1997) "Model Based Optimizer Systems With TES: Final Report", JCEM Technical Report TR/97/15, University of Colorado, Boulder, CO.
27. Krarti, M., G.P. Henze, and D. Bell (1999) "Planning Horizon for a Predictive Optimal Controller for Thermal Energy Storage Systems." *ASHRAE Transactions*, Vol. 105, pt. 1, American Society of Heating, Refrigerating, and Air-Conditioning Engineers, Atlanta, Georgia.
28. McCullough, J.M. (1988) "Ice Thermal Storage: System Selection and Design." *Consulting-Specifying Engineer*, pp. 70–77.
29. Tamblyn, R.T. (1985) "Control Concepts for Thermal Storage." *ASHRAE Transactions*, Vol. 91, pt. 1b, American Society of Heating, Refrigerating, and Air-Conditioning Engineers, Atlanta, Georgia.
30. Spethmann, D.H. (1989) "Optimal Control for Cool Storage." ASHRAE Transactions, Vol. 95, pt. 1 1189–1193, American Society of Heating, Refrigerating, and Air-Conditioning Engineers, Atlanta, Georgia.
31. Guven, H. and J. Flynn (1992) "Commissioning TES Systems." *Heating/Piping/Air Conditioning*, Vol. 64, pt. 1.
32. Tran, N., J.F. Kreider, and P. Brothers (1989) "Field Measurement of Chilled Water Storage Thermal Performance." *ASHRAE Transactions*, Vol. 95, pt. 1, American Society of Heating, Refrigerating, and Air-Conditioning Engineers, Atlanta, Georgia.
33. Sohn, C.W. (1991) "Field Measurement of an Ice Harvester Storage Cooling System." *ASHRAE Transactions*, Vol. 97, pt. 2, pp. 1187–1193, American Society of Heating, Refrigerating, and Air-Conditioning Engineers, Atlanta, Georgia.

34. Akbari, H. and O. Sezgen (1992) "Case Studies of Thermal Energy Systems: Evaluation and Verification of System Performance." LBL-30852, Lawrence Berkeley Laboratory, University of California, Energy and Environment Division.
35. Braun, J.E., S.A. Klein, J.W. Mitchell, and W.A. Beckman (1989) "Applications of Optimal Control to Chilled Water Systems without Storage." *ASHRAE Transactions*, Vol. 95, pt. 1, American Society of Heating, Refrigerating, and Air-Conditioning Engineers, Atlanta, Georgia.
36. Drees, K.H. and J.E. Braun (1995) "Modeling of area-constrained ice storage tanks." *International Journal of HVAC&R Research*, 1/2 pp. 143–159, American Society of Heating, Refrigerating, and Air-Conditioning Engineers, Atlanta, Georgia.
37. Kiatreungwattana, K. (1998) "Modeling of Indirect Ice Storage Tank during Partial Charging and Discharging Cycles." M.S. Thesis, University of Colorado, Boulder, CO.
38. Neto, J.H.M. and M. Krarti (1996a) "Deterministic Model for an Indirect Ice Storage Tank." *ASHRAE Transactions*, Vol. 103, pt. 1, 113–124, American Society of Heating, Refrigerating, and Air-Conditioning Engineers, Atlanta, Georgia.
39. Neto, J.H.M. and M. Krarti (1996b) "Experimental Validation of a Numerical Model for an Indirect Ice Storage Tank." *ASHRAE Transactions*, Vol. 103, pt. 1, 125–138, American Society of Heating, Refrigerating, and Air-Conditioning Engineers, Atlanta, Georgia.
40. Neto, J.H.M. and M. Krarti (1997) "Parametric Analysis of Internal-Melt Ice-on-Coil Tank." *ASHRAE Transactions*, Vol. 103, pt. 2, 322–333, American Society of Heating, Refrigerating, and Air-Conditioning Engineers, Atlanta, Georgia.
41. West, J. and J.E. Braun (1999) "Modeling partial charging and discharging of area-constrained ice storage tanks." *International Journal of HVAC&R Research*, 5/3 209–228, American Society of Heating, Refrigerating, and Air-Conditioning Engineers, Atlanta, Georgia.
42. Meckeler, G. (1989) "Cold Air Distribution Options with Ice Storage." *ASHRAE Transactions*, Vol. 95, pt. 2, 1194–1205, American Society of Heating, Refrigerating, and Air-Conditioning Engineers, Atlanta, Georgia.
43. Tamblyn, R.T. (1988) "Getting High on Low Temperature Air" *Heating/Piping/Air Conditioning*, Vol. 60 101–108.
44. Andresen, I., and M.J. Brandemuehl (1992) "Heat Storage in Building Thermal Mass: A Parametric Study." *ASHRAE Transactions*, Vol. 98, pt. 1, 910–918, American Society of Heating, Refrigerating, and Air-Conditioning Engineers, Atlanta, Georgia.
45. Rabl, A., and L.K. Norford (1991) "Peak Load Reduction by Preconditioning Buildings at Night." *International Journal of Energy Research* Vol. 15, pp. 781–798.
46. Snyder, M.E., and T.A. Newell (1990) "Cooling Cost Minimization Using Building Mass for Thermal Storage." *ASHRAE Transactions*, Vol. 96, pt. 2, 830–838, American Society of Heating, Refrigerating, and Air-Conditioning Engineers, Atlanta, Georgia.
47. Golneshan, A.A., and M.A. Yaghoubi (1990) "Simulation of Ventilation Strategies of a Residential Building in Hot Arid Regions of Iran." *Energy and Buildings* Vol. 14, pp. 201–205.
48. Conniff, J.P. (1991) "Strategies for Reducing Peak Air-Conditioning Loads by Using Heat Storage in the Building Structure." *ASHRAE Transactions*, Vol. 97, pt. 1, 704–709, American Society of Heating, Refrigerating, and Air-Conditioning Engineers, Atlanta, Georgia.
49. Ruud, M.D., J.W. Mitchell, and S.A. Klein (1990) "Use of Building Thermal Mass to Offset Cooling Loads." *ASHRAE Transactions*, Vol. 96, pt. 2, 820–828, American Society of Heating, Refrigerating, and Air-Conditioning Engineers, Atlanta, Georgia.
50. Kammerud, R.C. and S.L. Blanc (1999) "Economic Analysis of Optimal Control." *ASHRAE Transactions*, Vol. 105, pt. 2, American Society of Heating, Refrigerating, and Air-Conditioning Engineers, Atlanta, Georgia.
51. American Society of Heating, Refrigerating, and Air-Conditioning Engineers (1997) *Handbook of Fundamentals*, pp. 30.3–30.12 Atlanta, Georgia.

52. Stephenson, D.G., and G.P. Mitalas (1971) "Calculation of Heat Conduction Transfer Functions for Multi-layer Slabs." *ASHRAE Transactions*, Vol. 77, pt. 2, 117–126. American Society of Heating, Refrigerating, and Air-Conditioning Engineers, Atlanta, Georgia.
53. Klein, S.A., et al. (2000) *TRNSYS: A Transient System Simulation Program*, 15th Edition. Solar Energy Laboratory, University of Wisconsin-Madison.
54. Ferrano, F.J., and K.V. Wong (1990) "Prediction of thermal storage loads using a neural network." *ASHRAE Transactions*, Vol. 96, pt. 2, 723–726. American Society of Heating, Refrigerating, and Air-Conditioning Engineers, Atlanta, Georgia.
55. Miller, R.C., and J.E. Seem (1991) "Comparison of artificial neural networks with traditional methods of predicting return time from night or weekend setback." *ASHRAE Transactions*, Vol. 97, pt. 1, 500–508. American Society of Heating, Refrigerating, and Air-Conditioning Engineers, Atlanta, Georgia.
56. Kreider, J.F., and J.S. Haberl (1994) "Predicting hourly building energy usage." *ASHRAE Journal*, 36 (6) pp. 72–81. American Society of Heating, Refrigerating, and Air-Conditioning Engineers, Atlanta, Georgia.
57. Haberl, J.S. and S. Thamilseran (1996) " The great energy predictor shootout II: Measuring retrofit savings – Overview and discussion of results." *ASHRAE Transactions*, Vol. 102, pt. 2, 419–435. American Society of Heating, Refrigerating, and Air-Conditioning Engineers, Atlanta, Georgia.
58. Kreider, J., Claridge, D., Curtiss, P., Dodier, R., Haberl, J., and Krarti, M. (1995) "Building Energy Use Prediction and System Identification using Recurrent Neural Networks." *Journal of Solar Energy Engineering*, 117/3, pp. 161–166. American Society of Mechanical Engineers, New York, New York.
59. King, D.J., and R.A. Potter, Jr. (1998) "Description of a steady-state cooling plant model developed for use in evaluating optimal control of ice thermal energy storage systems." *ASHRAE Transactions*, Vol. 104, pt. 1. American Society of Heating, Refrigerating, and Air-Conditioning Engineers, Atlanta, Georgia.
60. Brandemuehl, M.J. (1994) "Development of a toolkit for secondary HVAC system energy calculations." *ASHRAE Transactions*, Vol. 100, pt. 1. American Society of Heating, Refrigerating, and Air-Conditioning Engineers, Atlanta, Georgia.
61. BLAST Support Office (1995) *Building loads and system thermodynamics (BLAST) user manual and source code*. University of Illinois at Urbana-Champaign.
62. F.W. Buhl, R.B. Curtis, S.D. Gates, J.J. Hirsch, M. Lokmanhekim, S.P. Jaeger, A.H. Rosenfeld, F.C. Winkelmann, B.D. Hunn, M.A. Roschke, H.D. Ross, G.S. Leighton. (1979) "DOE-2: A new state-of-the-art computer program for energy utilization analysis of buildings." Proceedings of the Second International CIB Symposium on Energy Conservation in the Built Environment, Copenhagen, Denmark.
63. Drury B. Crawley (U.S. Department of Energy), Linda K. Lawrie (U.S. CERL), Curtis O. Pedersen (UIUC), Frederick C. Winkelmann (LBNL). (2000) "*EnergyPlus: Energy Simulation Program*". ASHRAE Journal, Vol. 42, No. 4 (April), pp. 49–56. American Society of Heating, Refrigerating, and Air-Conditioning Engineers, Atlanta, Georgia.
64. Jekel, T.B., J.W. Mitchell, and S.A. Klein (1993) "Modeling of ice storage tanks." *ASHRAE Transactions*, Vol. 99, pt. 1. American Society of Heating, Refrigerating, and Air-Conditioning Engineers, Atlanta, Georgia.
65. Knebel, D.E. (1995) "Predicting and evaluating the performance of ice harvesting thermal energy storage systems." *ASHRAE Transactions*, Vol. 101, pt. 1, pp. 1339–1344. American Society of Heating, Refrigerating, and Air-Conditioning Engineers, Atlanta, Georgia.
66. Strand, R.K., C.O. Pedersen, and G.N. Coleman (1994) "Development of direct and indirect ice-storage models for energy analysis calculations." *ASHRAE Transactions*, Vol. 100, pt. 1. American Society of Heating, Refrigerating, and Air-Conditioning Engineers, Atlanta, Georgia.
67. Bahnfleth, W.P. (1998) "Thermal performance of a full-scale stratified chilled-water thermal storage tank." *ASHRAE Transactions*, Vol. 104, pt. 2. American Society of Heating, Refrigerating, and Air-Conditioning Engineers, Atlanta, Georgia.

68. Caldwell J S., and W.P. Bahnfleth (1998) "Identification of mixing effects in stratified chilled-water storage tanks by analysis of time series temperature data." *ASHRAE Transactions*, Vol. 104, pt. 2. American Society of Heating, Refrigerating, and Air-Conditioning Engineers, Atlanta, Georgia.
69. Musser A., and W.P. Bahnfleth (1998) "Evolution of temperature distributions in a full-scale stratified chilled-water storage tank with radial diffusers." *ASHRAE Transactions*, Vol. 104, pt. 1a. American Society of Heating, Refrigerating, and Air-Conditioning Engineers, Atlanta, Georgia.
70. Fanger, P.O. (1972) *Thermal Comfort*. Danish Technical Press, Copenhagen.
71. MacArthur, J.W. (1986) "Humidity and predicted mean vote based (PMV-based) comfort control." *ASHRAE Transactions*, Vol. 92, pt. 1b. American Society of Heating, Refrigerating, and Air-Conditioning Engineers, Atlanta, Georgia.
72. Scheatzle, D.G. (1991) "The development of PMV-based control for a residence in a hot arid climate." *ASHRAE Transactions*, Vol. 97, pt. 2. American Society of Heating, Refrigerating, and Air-Conditioning Engineers, Atlanta, Georgia.
73. Henderson, H.I., K. Rengarajan, and D.B. Shirey (1992) "The impact of comfort control on air conditioner energy use in humid climates." *ASHRAE Transactions*, Vol. 98, pt. 2. American Society of Heating, Refrigerating, and Air-Conditioning Engineers, Atlanta, Georgia.
74. Simmonds, P. (1993) "Thermal comfort and optimal energy use." *ASHRAE Transactions*, Vol. 99, pt. 1. American Society of Heating, Refrigerating, and Air-Conditioning Engineers, Atlanta, Georgia.
75. Bellman, R.E. (1957) *Dynamic Programming*. Princeton University Press, Princeton, New Jersey.
76. Bertsekas, D.P. (1995) *Dynamic Programming and Optimal Control*. Volume 1. Athena Scientific, Belmont, Massachusetts.
77. Nelder, J.A. and Mead, R. (1965) "A Simplex Method for Function Minimization." *Computer Journal*, Vol. 7, pp. 308–313.
78. Clarke, D.W., C. Mohtadi, and P.S. Tuffs (1987) "Generalized predictive control – Part 1. The basic algorithm." Automatica, Vol. 23, pp. 137–148.
79. Curtiss, P.S., J.F. Kreider, and M.J. Brandemuehl (1993) "Artificial neural networks proof of concept for local and global control of commercial building HVAC systems." ASME International Solar Energy Conference, April 1993, Washington, DC.
80. Curtiss, P.S., J.F. Kreider, and M.J. Brandemuehl (1993) "Energy management in central HVAC plants using neural networks." *ASHRAE Transactions*, Vol. 99, pt. 1, American Society of Heating, Refrigerating, and Air-Conditioning Engineers, Atlanta, Georgia.
81. Curtiss, P.S. (1997) "Experimental results from a network-assisted PID controller." *ASHRAE Transactions*, Vol. 103, pt. 1, American Society of Heating, Refrigerating, and Air-Conditioning Engineers, Atlanta, Georgia.
82. Miller, W.T, R.S. Sutton, and P.J. Werbos, Eds. (1992) *Neural Networks for Control*. MIT Press, Cambridge, Massachusetts.
83. Gagge, A.P., J.A.J. Stolwijk, amd Y. Nishi (1971) "An effective temperature scale based on a simple model of human physiological regulatory response." *ASHRAE Transactions*, Vol. 77, pt. 1, pp. 247–262. American Society of Heating, Refrigerating, and Air-Conditioning Engineers, Atlanta, Georgia.
84. ASHRAE (1999) *HVAC Applications*. 40.1–40.36. American Society of Heating, Refrigerating, and Air-Conditioning Engineers, Atlanta, Georgia.
85. Daryanian, B. and L.K. Norford (1994) "Minimum-cost control of HVAC systems under real-time prices." *Proceedings of Third IEEE Conference on Control Applications,* pp. 1855 – 1860. Glasgow, UK.
86. Norford. L.K., S.L. Englander, and B.J. Wiseley (1998) "Demonstration Knowledge Base to Aid Building Operators in Responding to Real-Time Pricing Electricity Rates." *ASHRAE Transactions*, Vol. 104, pt. 1, American Society of Heating, Refrigerating, and Air-Conditioning Engineers, Atlanta, Georgia.
87. Kreider, J.F., M.J. Brandemuehl, M. Krarti, and L.K. Norford (1997) "Model Based Optimizer Systems Without TES: Final Report", JCEM Technical Report TR/97/14, University of Colorado, Boulder, CO.

88. Reindl, D.T, R.A. Gansler, and T.B. Jekel (1999) "Final Report for 991-TRP: Simulation of Source Energy Utilization and Emissions for HVAC Systems." *ASHRAE Report*, American Society of Heating, Refrigerating, and Air-Conditioning Engineers, Atlanta, Georgia.
89. Schweppe, F.C., M.C. Caramanis, R.D. Tabors and R.E. Bohn. 1988. *Spot Pricing of Electricity*. Kluwer Academic Publishers, Boston.
90. Daryianian, B., R.D. Tabors, and R.E. Bohn. 1995. "Automatic Control of Electric Thermal Storage (Heat) Under Real-Time Pricing." NYSERDA Report 95-1, New York State Energy Research and Development Authority.
91. Braithwait, S.D. and M. O'Sheasy. 2000. "Customer Response to Market Prices – How Much Can You Expect When You Need It Most?" EPRI International Energy Pricing Conference.
92. Eatkin, K. and A. Faruqui. 2000. "Pricing Retail Electricity: Making Money Selling a Commodity" in *Pricing Electricity in Competitive Markets*, edited by A. Faruqui and K. Eatkin, Kluwer Academic Publishing.
93. Braithwait, S.D. 2000. "Residential TOU Price Response in the Presence of Interactive Communication Equipment" In *Pricing Electricity in Competitive Markets*, edited by A. Faruqui and K. Eatkin, Kluwer Academic Publishing.
94. Braithwait, S. and A. Faruqui. 2001. Unpublished information. L.R. Christensen Associates and EPRI.
95. Drury B. Crawley (U.S. Department of Energy), Linda K. Lawrie (U.S. CERL), Curtis O. Pedersen (UIUC), Frederick C. Winkelmann (LBNL). (2000) "EnergyPlus: Energy Simulation Program". *ASHRAE Journal*, Vol. 42, No. 4 (April), pp. 49–56. ASHRAE, Atlanta, GA.
96. Gagge, A.P., Fobelets, A.P., Berglund, L.G. (1997) "A Standard Predictive Index of Human Response to the Thermal Environment", ASHRAE Transactions, Vol. 83, Pt 1.
97. Berglund, Larry (1978) "Mathematical Models for Predicting the Thermal Comfort Response of Building Occupants", *ASHRAE Transactions, Vol.84.*
98. King, Dion and Potter, Robert (1998) "Description of a Steady-State Cooling Plant Model Developed for Use in Evaluating Optimal Control of Ice Thermal Energy Storage Systems", *ASHRAE Transactions*, Vol. 104, Pt. 1.
99. Ljung, L (1987). *System Identification: Theory for the User*. Prentice-Hall, Englewood Cliffs, NJ.
100. J. Sjöberg, Q. Zhang, L. Ljung, A. Benveniste, B Deylon, P-Y Glorennec, H. Hjalmarsson, and A. Juditsky (1995) "Nonlinear black–box modeling in system identification: a unified overview." *Automatica*, 31:1691–1724, Dec 1995.
101. Braun, J.E., K.W. Montgomery, and N. Chaturvedi (2001) "Evaluating the performance of building thermal mass control strategies." *International Journal of Heating, Ventilating, Air–Conditioning and Refrigerating Research* 7(4):403-428
102. N. Chaturvedi and Braun, J.E. (2002) "An inverse Gray-box model for transient building load prediction." *International Journal of Heating, Ventilating, Air–Conditioning and Refrigerating Research*, January 2002.
103. Seem, J.E. (1987) *Modeling of Heat Transfer in Buildings*, Ph.D thesis, Department of Mechanical Engineering, University of Wisconsin-Madison.